Determination of photoprotective properties of flavonols against UV-radiation induced skin damage

A Thesis Submitted to the College of

Graduate Studies and Research

in Partial Fulfillment of the Requirements

for the Degree of Master of Science

in the College of Pharmacy and Nutrition

University of Saskatchewan

Saskatoon, Saskatchewan

Canada

By

Sabia Maini

PERMISSION TO USE

In presenting this thesis/dissertation in partial fulfillment of the requirements for a master degree from the University of Saskatchewan, I agree that the libraries of this University may make it freely available for inspection. I further agree that permission for copying of this thesis/dissertation in any manner, in whole or in part, for scholarly purposes may be granted by the professor or professors who supervised my thesis/dissertation work or, in their absence, by the Head of the Department or the Dean of the College in which my thesis work was done. It is understood that any copying or publication or use of this thesis/dissertation or parts thereof for financial gain shall not be allowed without my written permission. It is also understood that due recognition shall be given to me and to the University of Saskatchewan in any scholarly use which may be made of any material in my thesis/dissertation.

Requests for permission to copy or to make other uses of materials in this thesis/ dissertation in whole or part should be addressed to:

Dean of the College of Pharmacy and Nutrition
University of Saskatchewan
Saskatoon, Saskatchewan S7N 5C9
Canada

OR

Dean of the College of Graduate Studies and Research
University of Saskatchewan
107 Administration Place
Saskatoon, Saskatchewan S7N 5A2
Canada

ABSTRACT

Flavonols constitute a class of polyphenolic compounds, which are known to protect a number of plant species from UV-radiation induced damage. Flavonols have received much interest because of the beneficial role of polyphenols in chemoprevention. The overall goal of this study was to investigate the sun screening properties of flavonols. We had 5 objectives to accomplish our goal: developing an analytical method to measure UV radiation-induced damage to DNA; determining the ability of flavonols to protect against UV radiation-induced damage to an artificial skin mimic; determining the UVA and aqueous stability properties of a range of flavonols; determine the decomposition products of the stability studies; general trend of flavonol photochemistry using a prototype compound 3-hydroxyflavone.

Objective 1: To develop an analytical method to quantify direct UV radiation-induced DNA damage. The quantitative analysis of DNA lesion was achieved by validating a simple and robust analytical method based on HPLC-APCI-MS/MS technology to quantify cyclobutane pyrimidine dimers involving two thymines, the major DNA lesions produced in human skin when exposed to UV radiation.

Objective 2: To use the analytical method for thymine dimer damage to determine the ability of three flavonols (quercetin, kaempferol and galangin) to protect EpiDerm™, an artificial skin mimic, against UV radiation-induced thymine dimer formation. We found that all three flavonols (4nmol/cm^2) protected EpiDerm™ against UVB radiation-induced DNA damage. The levels of thymine dimer formation from UVA radiation were below the limit of quantification of our method.

Objective 3: To determine the stability of a series of flavonols (galangin, kaempferol, quercetin and myricetin) to UVA radiation and aqueous media. The stability of flavonols was achieved by monitoring the levels of a range of flavonols remaining over time to UVA radiation and aqueous media by using HPLC-UV detection. We determined that stability of the flavonols was inversely related to the number of hydroxyl groups on the B-ring.

Objective 4: To determine the decomposition products of the stability studies. This was accomplished by using HPLC-MS/MS and we determined that the flavonols (galangin,

kaempferol, quercetin and myricetin) mainly decomposed to depside and its hydrolysis products in both systems and produced additional aldehyde products in the UVA experiment.

Objective 5: To study the general trend of flavonol photochemistry using a prototype compound 3-hydroxyflavone. In order to identify whether there exists a general trend of photodecomposition of flavonols, we chose to investigate decomposition of 3-OH-F.

ACKNOWLEDGEMENTS

I am most grateful to my supervisor, Dr. Ed S. Krol for his guidance, encouragement and for all his input to make this project a success. I would like to thank my advisory committee, Dr. Anas El-Aneed and Dr. Ildiko Badea for their expert advice. Special thanks to the Chair of my committee, Dr. Jane Alcorn, for her exquisite attention, expert suggestions as well as keeping track of all timelines to ensure timely completion of my program.

To you Dr. Brian Fahlman, I wish to appreciate all your great suggestions and support throughout this project. Your expertise which you shared with me all the time made the whole journey easier. I am grateful to Isaac Asiamah and Dr. Jennifer Billinsky for being there for me any time I needed their help. Thank you, Deborah Michel for training on mass spectrometer.

I would like to acknowledge College of Pharmacy and Nutrition and NSERC for the financial support.

I will never forget the time spent with my lab mates, Dr. Ravi Singh, Dr. Jatinder Kaur, Yunyun Di, Joshua Buse, Jessie Lin and Heather Hodgson, thanks for their support and friendship.

DEDICATION

This thesis is dedicated to my loving parents, Krishna Maini and Vipan Maini. Thanks for their constant love and support.

TABLE OF CONTENTS

LIST OF FIGURES

LIST OF TABLES

LIST OF ABBREVIATIONS

AIF	Apoptosis inducing factor
AP-1	Activator protein-1
APCI	Atmospheric pressure chemical ionization
API	Atmospheric pressure ionization
BCC	Basal-cell carcinoma
CID	Collision induced dissociation
COX-2	Cyclo-oxygenase-2
CPD	Cyclobutane pyrimidine dimer
CREB	cyclic-AMP-response-element-binding protein
CUR	Curtain gas
DMEM	Dulbecco's Modified Eagle Medium
DMS/MS	Differential mobility spectrometry/mass spectrometry
DNA	Deoxyribonucleic Acid
DPBS	Dulbecco's phosphate buffered saline
ELISA	Enzyme-linked immunosorbant assay
EPI	Enhanced product ion
ESI	Electrospray ionization
ESI-MS/MS	Electrospray ionization/tandem mass spectrometry
GS1	Ion source gas 1
HPLC	High pressure liquid chromatography
HPLC-MS	High performance liquid chromatography-Mass spectrometry
HPLC-UV	High-pressure liquid chromatography/ UV detection
HQC	High quality control
LLOQ	Lower limit of quantification
LOD	Limit of detection
LQC	Low quality control
MMP	Matrix metalloproteinase
MQC	Middle quality control
MRM	Multiple reaction monitoring

MS/MS	Tandem mass spectrometry
NER	Nucleotide excision repair
QC	Quality control
RIA	Radioimmuno assay
ROS	Reactive oxygen species
SCC	Squamous-cell carcinoma
SGLT1	sodium dependent glucose transporter 1
SPF	Sun Protection Factor
TNF-α	Tumor necrosis factor - alpha
T<>T	Cyclobutane thymine dimer
UVR	Ultraviolet radiation
8-oxoGua	8-Oxo-7,8-dihydroguanosine

1. Abstract

Flavonols constitute a class of polyphenolic compounds, which are known to protect a number of plant species from UV-radiation induced damage. Flavonols have received much interest because of the beneficial role of polyphenols in chemoprevention. The overall goal of this study was to investigate the sun screening properties of flavonols. We had 5 objectives to accomplish our goal: developing an analytical method to measure UV radiation-induced damage to DNA; determining the ability of flavonols to protect against UV radiation-induced damage to an artificial skin mimic; determining the UVA and aqueous stability properties of a range of flavonols; determine the decomposition products of the stability studies; general trend of flavonol photochemistry using a prototype compound 3-hydroxyflavone.

Objective 1: To develop an analytical method to quantify direct UV radiation-induced DNA damage. The quantitative analysis of DNA lesion was achieved by validating a simple and robust analytical method based on HPLC-APCI-MS/MS technology to quantify cyclobutane pyrimidine dimers involving two thymines, the major DNA lesions produced in human skin when exposed to UV radiation.

Objective 2: To use the analytical method for thymine dimer damage to determine the ability of three flavonols (quercetin, kaempferol and galangin) to protect EpiDerm™, an artificial skin mimic, against UV radiation-induced thymine dimer formation. We found that all three flavonols (4nmol/cm^2) protected EpiDerm™ against UVB radiation-induced DNA damage. The levels of thymine dimer formation from UVA radiation were below the limit of quantification of our method.

Objective 3: To determine the stability of a series of flavonols (galangin, kaempferol, quercetin and myricetin) to UVA radiation and aqueous media. The stability of flavonols was achieved by monitoring the levels of a range of flavonols remaining over time to UVA radiation and aqueous media by using HPLC-UV detection. We determined that stability of the flavonols was inversely related to the number of hydroxyl groups on the B-ring.

Objective 4: To determine the decomposition products of the stability studies. This was accomplished by using HPLC-MS/MS and we determined that the flavonols (galangin,

kaempferol, quercetin and myricetin) mainly decomposed to depside and its hydrolysis products in both systems and produced additional aldehyde products in the UVA experiment.

Objective 5: To study the general trend of flavonol photochemistry using a prototype compound 3-hydroxyflavone. In order to identify whether there exists a general trend of photodecomposition of flavonols, we chose to investigate decomposition of 3-OH-F.

2. Review of literature

2.1. Introduction

UV-radiation is one of the major environmental factors responsible for the induction of skin cancer [1]. The relationship between elevated levels of UV-radiation and skin cancer is widely reported [2]. The harmful effects of UV-radiation are mostly associated with both direct and indirect DNA damage [2].

The absorption of UV-radiation results in a photochemical reaction leading to the formation of dimeric pyrimidine photoproducts which are highly lethal to cells [3]. The photoproducts formed by UV-radiation can lead to errors in DNA replication thus inducing mutations [2]. Cyclobutane pyrimidine dimers (CPD) involving two thymine residues (T<>T) are predominant DNA lesions produced in skin when exposed to UV-radiation [4].

In order to reduce the harmful biological effects of UV-radiation, it is necessary to reduce the amount of UV-radiation received by the population. The application of sunscreen results in significant reduction of cyclobutane pyrimidine dimer and (6-4) photoproduct formation [5]. But the majority of sunscreens currently available in the market have the potential to screen only the UVB portion of the sunlight [6]. Since the UVA portion of sunlight also contributes to skin cancer, there is a need to develop broad spectrum sunscreens that would protect against both UVA and UVB radiation [6].

In an effort to identify new broad spectrum sunscreens, compounds derived from plant extracts are being investigated for their potential sunscreen properties [7]. A large number of plants produce secondary metabolites, many of which have important roles in plant defense mechanisms [8]. Flavonols such as quercetin and kaempferol are generally produced by a variety of plant species in response to UV-induced damage [9, 10]. The photoprotective properties of the flavonol quercetin may be due to its ability to absorb UV-radiation at 255 and 365nm. The potential of flavonols to absorb UV-radiation can be exploited for human use as sunscreen agents. The initial work from our lab has established that quercetin is a sunscreen against UVA and UVB induced TNF-α and MMP-1 production [11]. In order to further investigate the mechanism of action of flavonols as topical sunblock agents, we focused our research on

inhibition of DNA adduct formation (cyclobutane thymine dimer), with respect to treatment with flavonols.

The purpose of our study is to develop a simple and selective HPLC-APCI-MS/MS method for the quantification of cyclobutane thymine dimer not containing the phosphate backbone. I have developed and validated an easy and robust *in vitro* analytical method for measuring T<>T formation by exposure of DNA to UV-radiation. Our study aims to determine the topical sunscreen properties of series of flavonols in UVA/B exposed human skin model (EpiDerm^{TM}). The potential of flavonols to act as sunscreen agents is in turn directly dependent upon their stability to UV-radiation. However, quercetin has been reported to be unstable in cell culture media [12, 13]. So as the part of investigation on sun protectant properties of flavonols, we have also studied the stability of flavonols to UV-radiation and aqueous medium. We have used HPLC-MS/MS technology to determine the decomposition products of flavonols in UV-radiation and DMEM. The mechanism of UV radiation-induced decomposition of flavonol will provide us an insight into its photoprotective properties.

2.2. UV-radiation

The stratospheric ozone layer protects the surface of the earth by absorbing the most harmful component of sunlight with a wavelength range lower than 320 nm [14]. The decreasing concentration of the ozone layer has significantly affected the ground level distribution of UV-radiation [14]. An Antarctic ozone hole with a size three times larger than the entire land mass of the United States was indicated in ozone mapping data [15]. The current scientific suggestions indicate that the depletion of ozone layer over the past 2 decades has been the primary cause of the observed increases in skin cancer [14].

The amount of UV-radiation reaching the Earth's surface is influenced by a number of factors including ozone concentration, aerosols, clouds and climate. The depletion of the ozone layer has increased the intensity of UV-radiation reaching the surface of Earth. The presence of clouds has been reported to lower the ground level on UV-radiation. The attenuation of UV-radiation in presence of clouds depends upon the amount, thickness and number of cloud layers [16]. In contrast to clouds, snow reflects most of the UV-radiation into the atmosphere and which is then scattered back into Earth's surface by aerosols, thus increasing the overall levels of UV-radiation [16].

UV-radiation is subdivided into UVC (100-280 nm), UVB (280-315 nm) and UVA (315-400 nm) [17]. Of the total amount of UV-radiation that reaches the atmosphere of earth, 90 to 99% UVB and 100% of the UVC is absorbed by ozone. As a result, only part of the total UV-radiation which can reach the surface of earth can cause biological damage [18].

The biological effects of UV-radiation greatly depend upon the wavelength of incident light. The lower the wavelength of UV light, the more is the biological damage. UV wavelengths longer than 320nm (UVA) have limited ability to induce mutations in DNA. UVB spectrum between 280-320nm is the major cause of DNA damage leading to mutations [18]. However the intensity of UVA radiation reaching the surface of earth is 20 times more abundant as compared to UVB [18].

The increased amount of UV-radiation reaching Earth's surface, tends to increase the risk of human skin cancer. UV-radiation accounts for the major environmental factor responsible for

pathogenesis of skin cancer [18]. Hence, greater attention should be paid to the potential hazards of exposure to UV-radiation.

2.2.1. Role of UV-radiation in skin carcinogenesis

The rate of increase of human skin cancer in North America, Europe, and Australia has surpassed all other types of cancers [19]. The depletion of the stratospheric ozone layer has increased the amount of UV-radiation reaching the Earth's surface [18]. Skin exposure to UV-radiation is the major risk factor in the development of skin cancer. Chronic exposure to UV-radiation induces the formation of non-melanomic skin carcinoma (NMSC), making UV-radiation a complete carcinogen [14].

In 2012, more than 75,000 new cases of melanoma are expected in the United States [20]. The American Cancer Society estimates more than 2 million new cases of NMSC each year in the United States [20]. The Canadian Cancer Society has estimated 81,300 new cases and 320 deaths from NMSC are expected to occur in Canada in 2012 [21]. In Australia, the incidence of NMSC comprises the most common group of skin cancer [22]. The Australian Cancer Network Management has recommended surgical management of BCC and SCC [22]. It was reported that 1% depletion in ozone concentration may increase the incidence of NMSC by 2.0% [14]. However, the increase in the incidence of skin cancer cases over the past two decades is much higher than predicted [14].

Events involving induction of skin carcinogenesis by UV-radiation can be divided into three parts including tumor initiation, promotion and progression [23]. Initiation of skin carcinogenesis by UV-radiation involves formation of DNA photoproducts, which if unrepaired can lead to errors in DNA replication and mutations. UV-radiation-induced tumor promotion involves induction of various transcriptional factors like activator protein-1 (AP-1) and activation cyclooxygenase-2 (COX-2). Finally progression of skin cancer involves metastasis of the benign tumor [23].

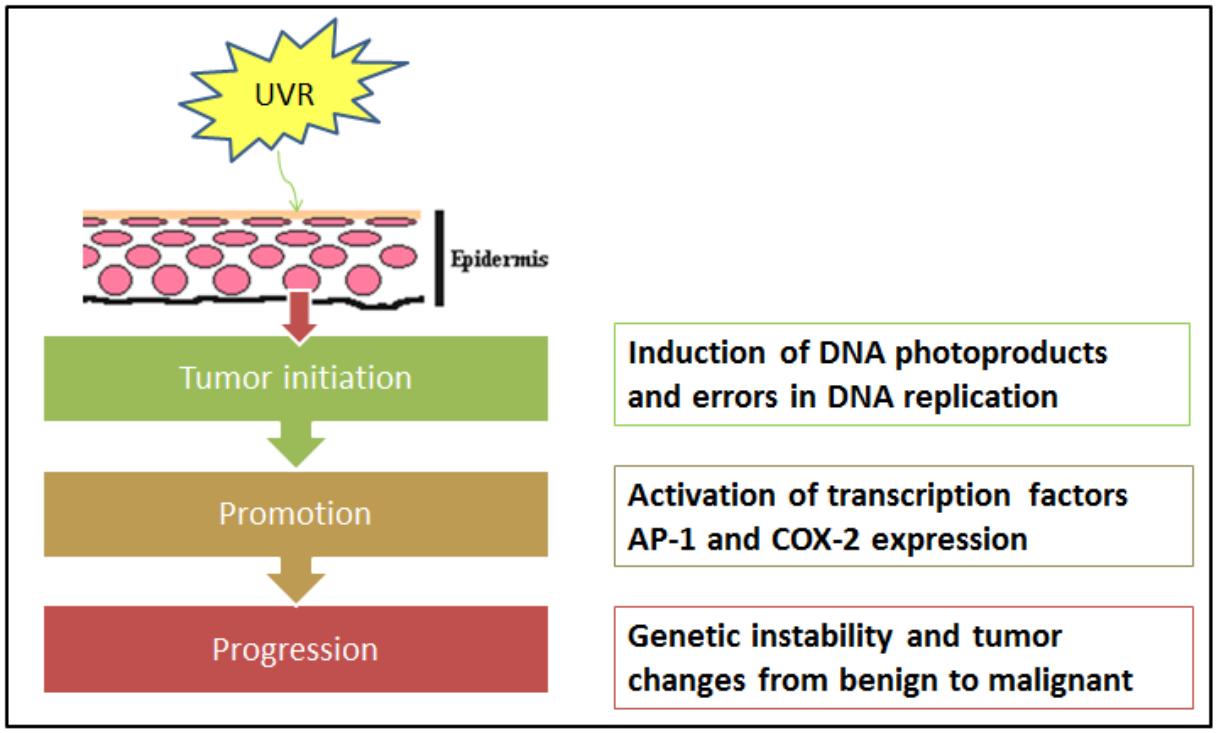

Figure 2.1: Stages of UVB-radiation induced skin carcinogenesis involving tumor initiation, promotion and progression (adapted from reference [23])

Skin cancer can be divided into two broad categories including malignant melanomas and non-melanomic skin cancers [24]. Melanomas are the result of either a single or a few intense exposures to UV-radiation, resulting in severe sunburn. On the other hand NMSC occurs primarily on the sun exposed areas of the body [25]. NMSC have been strongly associated with excess exposure of the body to chronic sun radiations. The UV exposed sites of body are more predisposed for development of NMSC [14].

In clinical practice, non-melanomic skin cancers can be subdivided into squamous cell carcinomas (SCC) and basal cell carcinomas (BCC) [24]. BCC are benign and slow growing in contrast to SCC which are fast growing and more likely to metastasize [26]. Unlike BCC, SCC is more common and metastasizes within 5 years in about 5% of cases, increasing mortality rates [27]. Of the total diagnosed cases of skin cancer, 80% are basal-cell carcinoma (BCC), 16% are squamous-cell carcinoma (SCC) and 4% are melanomas [19].

The correlation between the amount of UV exposure and the development of skin cancer has been well documented. An epidemiological study has reported that the development of NMSC is a UV dose dependent response [28]. Geographical parameters and climate also markedly influence the development of skin cancer [14]. Depending upon geographical factors, people living in tropical areas have more risk of sunburn, as compared to those living far from the equator [14].

The risk of occurrence of NMSC tends to be higher in elderly and immune suppressed members of the population [29]. Studies have shown that after UV exposure the individuals with impaired immune systems are more prone to develop skin cancer [29, 30], in addition, a survey done in the United States found that the risk of SCC is more common in men than in women [31].

2.2.2. Cellular damage by UVA and UVB

DNA is one of the key targets for UV-induced damage in a variety of organisms. The formation of DNA lesions greatly depends upon the wavelength of the incident photons [32]. In contrast to UVB, UVA radiation is more abundant but its effect on human skin remains poorly understood [33]. UVA radiation is not directly absorbed by DNA but is suspected to play a major role in the induction of oxidative stress through the formation of reactive oxygen species (ROS) [34].

On the other hand, UVB radiation being the most energetic component of solar radiation which hits the earth's surface is directly absorbed by DNA. UVB radiation-induced direct damage to DNA involves the formation of dimeric photoproduct among adjacent pyrimidine bases, thymine and cytosine [35]. The two major classes of photoproducts are cyclobutane-pyrimidine dimers (CPD) and pyrimidine – pyrimidone (PP) photoproducts [36]. This DNA damage can lead to the formation of DNA adducts and cross-linking of DNA strands.

In 2006, Mouret *et al* determined the distribution of UV radiation-induced photoproducts in human skin cells [36]. HPLC coupled with tandem mass spectroscopy was used for quantitative analysis based of UV-induced photoproducts. The authors suggested that CPDs are the predominant DNA lesions produced in whole human skin when exposed to UVB or UVA radiation [36]. The mechanism that triggers the formation of photoproducts is different for UVA and UVB radiation [37]. UVB radiation is directly absorbed by DNA and leads to the formation

of CPDs and (6-4) PPs (Figure 2.2). UVA induced CPDs are formed by either direct photochemical mechanism or through photosensitized triple energy transfer [37].

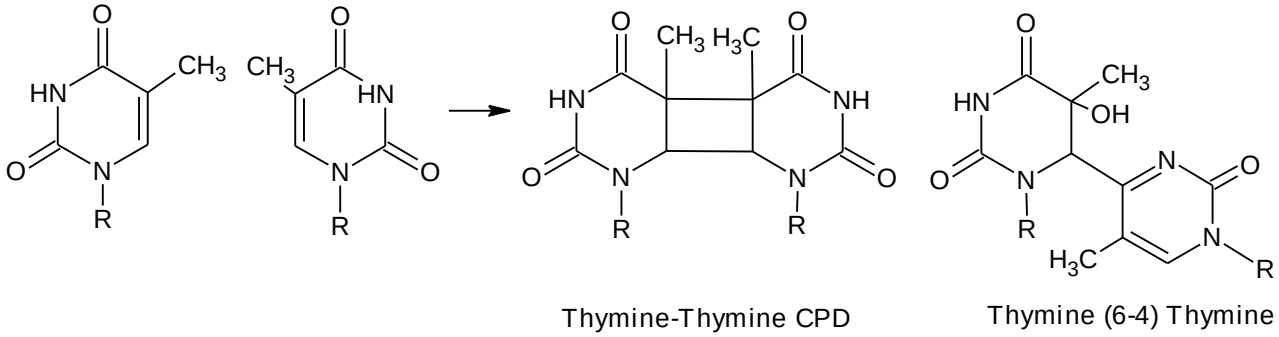

Figure 2.2: Formation of thymine cyclobutane dimer and thymine (6-4) photoproduct from thymine

In 2010, Mouret and coworkers investigated the relative distribution of bipyrimidine photoproducts from UV-radiation induced damage [37]. CPDs were reported to be formed in larger amounts than oxidative lesions in both cultured cells and whole skin. The CPDs involving two thymines accounted for 90% of the total photoproducts [37].

UV irradiation of a frozen solution of thymine in water produces covalently bound photoproducts. Freezing the solution tends to hold the nucleic acids in place and facilitate dimerization-suggesting a steric requirement in restricting movement of the nucleic acid chain [38]. The covalent bond formation between two thymine residues upon exposure of frozen thymine solution to UV-radiation was found to be a reversible process [39]. There exits an equilibrium between thymine and thymine dimer (T<>T), which is mainly dependent upon the wavelength of incident UV-radiation. The equilibrium between thymine and thymine dimer tends to shift with the change in wavelength of UV-radiation, with the longer wavelength ($\lambda > 280$nm) the equilibrium has been reported to shift towards dimer, whereas with shorter wavelength ($\lambda <$ 240nm) the more formation of thymine was observed [39].

Cyclobutane pyrimidine dimer and 6-4 photoproducts involving two thymines are the major DNA lesions induced by UV-radiation. The UV-induced pyrimidine dimers, if not repaired, can lead to a variety of mutations like deletion, substitution and frame shift mutations. The UV portion of sunlight is involved in formation of pre-mutagenic lesions by C to T transition mutation [40]. The anti-mutagenic response to UVB-induced damage is greater as compared to UVA, so the authors speculate that UVA radiation is more carcinogenic [40].

2.2.2.1. UVB-induced damage:

The adverse effects of solar radiation on living systems are mostly due to direct absorption of UVB radiation.

i. UVB-radiation induced formation of CPDs

UVB radiation is highly lethal and mutagenic to cells. The direct absorption of UVB light by DNA leads to the formation of dimeric pyrimidine photoproducts [41, 42]. In 2001, Douki *et al* found that CPDs are produced preferentially at TT site as compared to CC bipyrimidine products [42]. The three main UVB-induced dimeric photoproducts are cyclobutane T<>T, 6-4PP at T<>T and T-C [42]. Significant amount of TC to TT or CC to TT transitions mutations were detected at bipyrimidine sites in the p53 gene [40]. However, it was proposed that the probability of CC to TT transition mutation was the highest of all mutations [40].

ii. UVB-induced formation of 8-oxoGua and cytosine photohydrate

UVB radiation is involved in the formation of 8-oxo-7,8-dihydroguanosine (8-oxoGua) and cytosine hydrate. Pelle *et al* have recently suggested the mechanism of formation of 8-oxoGua induced by UVB involves the oxidation of the guanine base by •OH radical [43]. Another DNA photoproduct formed by UVB radiation is 6-hydroxy-5,6-dihydrocytosine known as cytosine photohydrate [44]. With respect to CPDs, 8-oxoGua and cytosine hydrate contribute less than 10% of the overall cellular DNA damage resulting from UV radiation [44]. This suggests that a minor role is played by 8-oxoGuo and cytosine hydrate in induction of mutation.

2.2.2.2. UVA-induced damage:

The International Agency of Research on Cancer emphasized the deleterious effects of UVA radiation on human skin [45]. Although UVA has a lower energy as compared to UVB, it accounts for more than 90% of UV radiation reaching the surface of earth [18]. Until 1980, it was thought that only UVB is responsible for adverse health effects of UV radiation. However these deleterious effects are also produced by UVA radiation [45]. In contrast to UVB, UVA radiation preferentially induces CPDs without any detectable formation of pyrimidine (6-4) pyrimidone [36].

i. UVA-radiation induced formation of CPDs

UVA-induced formation of CPD was first observed in bacteria [46]. This research was followed by a study in Chinese hamster ovary cells for the distribution of photoproducts. It was found that the level of UVA-induced CPDs were much higher as compared to 8-oxoGua, an oxidatively induced lesion in cellular DNA [44]. Enlightened by the previous research, in 2006 Mouret *et al* found that CPDs are the predominant DNA lesions induced by UVA radiation in cellular DNA [36].

ii. UVA-radiation induced cellular effects

UVA radiation can have harmful effects on cells due to the formation of reactive oxygen species (ROS) [44]. ROS formed in the epidermal cells can play a role in the promotion phase of UV-radiation induced skin carcinogenesis. In human cells, UVA radiation generates GC to AT transition mutations. UVA radiation also forms a minimal amount of 8-oxoGua [44], which suggests that 8-oxoGua contributes very little to the overall biological effects of UVA damage.

2.2.3. Biological events leading to skin carcinogenesis

In addition to genetic damage, UVB-radiation is also known to induce skin cancer by alterations in transcription factors [47]. UVB-radiation can initiate skin carcinomas and cell proliferation through various signaling pathways. An association between increased Activator protein-1 (AP-1) activity and promotion of skin cancer has been widely studied [47]. The mechanism underlying the promotion of UVB-induced skin cancer includes activation of regulators of

transcription factors like p38, extracellular-activated protein kinase, and mitogen activated protein kinase (MAPK). The stimulation of transcriptional factor regulators causes the phosphorylation of cyclic-AMP-response-element-binding protein (CREB) and stimulation of serum-response-element, leading to an increased expression of cFos gene. Homo- or hetero-dimer complexes of cFos and JunD proteins bind to DNA at a specific site and play a role in tumor promotion [23]. Phosphorylation of CREB at serine 133 also stimulates COX-2 expression leading to cell proliferation, skin cancer and angiogenesis.

UVB-radiation induced activation of AP-1 via PI3K-AKT signaling pathway was claimed to be through elevated levels of cFos protein and COX-2 expression by UVB-radiation. An elevated level of transcription factor AP-1 has been reported in tumor-promotion sensitive cells and not in normal cells [23]. Activation of p38 and PI3K signaling pathways plays a role in cell proliferation, tumor promotion and angiogenesis.

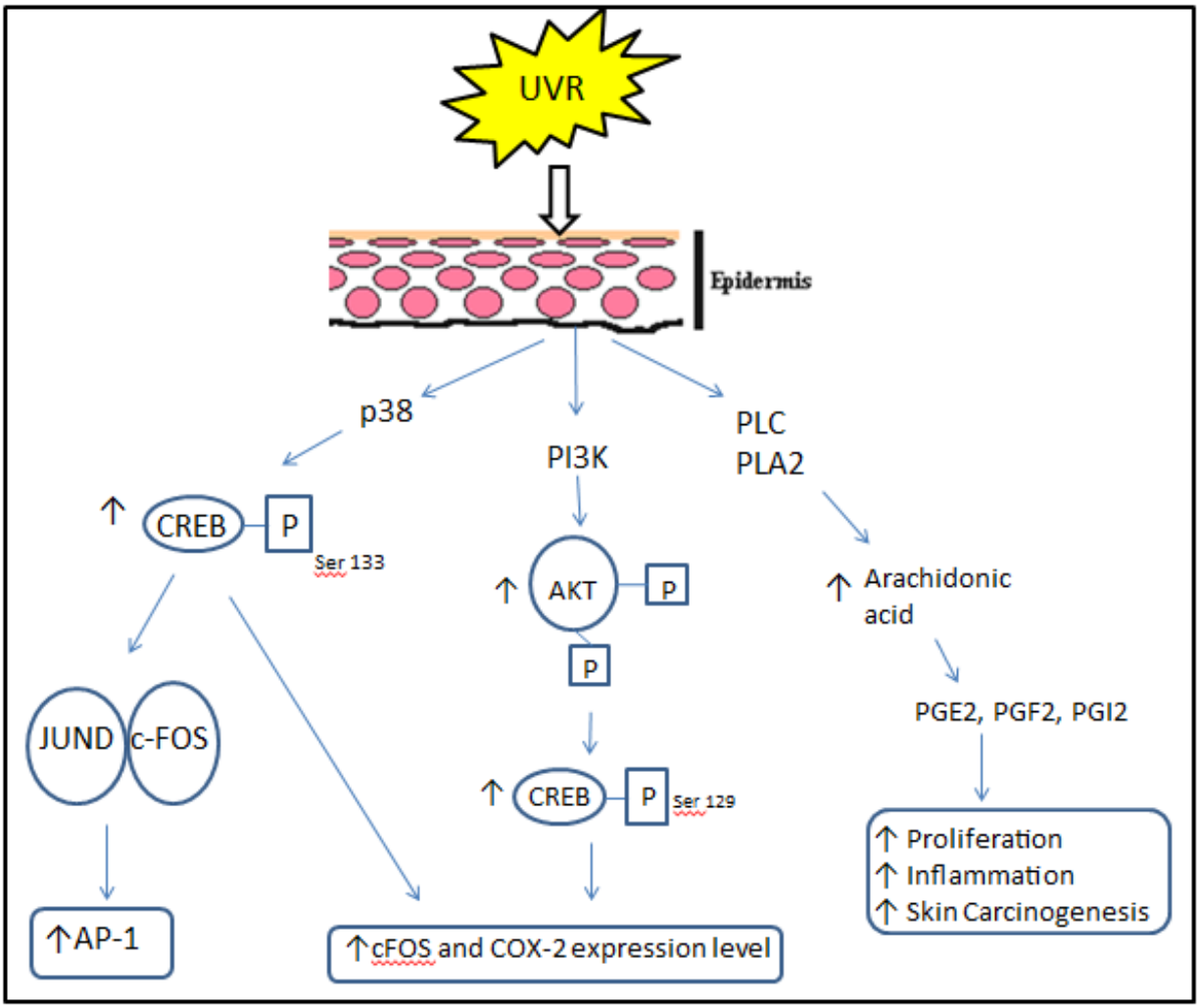

Figure 2.3: UVB radiation-induced signaling pathways involving p38, PI3K, AKT and prostaglandins leading to altered phosphorylation of CREB with increased levels of cFos and COX-2 promotors (adapted from ref [23])

2.2.4. Other biological effects of UV radiation

A number of studies have cited the relation between the amount of UV-exposure and photoaging in skin cells [48, 49]. Photoaging is characterized by increased production of ROS and matrix metalloproteinases (MMPs) upon UV-exposure, leading to winkle formation and recoil capacity [48]. MMP is an endopeptidase which is known to play a role in photoaging via breakdown of collagen protein [49]. The induction of MMP-1 in the skin by UV-radiation causes the unwinding of the helical proteins and hydrolysis of peptide bonds, resulting in denaturated

collagen. MMP-9 causes further degradation of the breakdown of collagen protein, leading to photoaging. However, the balance between the loss and synthesis of the collagen protein is the determining factor for the extent of skin damage in a healthy young individual [49].

2.2.5. Repair of cyclobutane DNA damage

UV-radiation induced DNA damage results in a stress response, which causes activation of nucleotide excision repair mechanism. Nucleotide excision repair (NER) involves 20-30 proteins by which bulky DNA damage are repaired [50]. NER removes a wide variety of UV-induced DNA lesions especially 6-4PPs and CPDs. NER has better ability to excise 6-4PPs as compared to CPDs, though the amount of CPD is higher than 6-4PPs. There are a number of steps which are involved in NER including: recognition of damaged DNA, opening of the DNA double helix, excision followed by synthesis of a DNA fragment and ligation of the repair batch [50].

Specific DNA damage involving cyclobutane pyrimidines can also be repaired by CPD photolyase, using UV light to repair the lesions [51]. CPD photolyase is a globular protein, carrying two cofactors, flavin adenine dinucleotide in its reduced form ($FADH^-$) and folate. The part of DNA involving lesions or CPDs is excised out of the double helix, and binds to the substrate binding site near to the cofactor $FADH^-$. Following the binding of CPD to the substrate, UV radiation is required to excite electrons from $FADH^-$ to CPD, either directly or by energy transfer [51]. Consequently, the bonds between pyrimidines break and the electron is returned to restore $FADH^-$ [51]. The enzymatic photo repair of CPD involves excitation of two electrons from the cofactor, resulting in restoration of two thymines. Thus UV radiation induced DNA damage can be repaired by either cascade of enzymes involving NER or photo-repair. However, unrepaired pyrimidine dimers can lead to errors in DNA replication and mutations, which clearly indicates the link between UV-radiation and skin cancer.

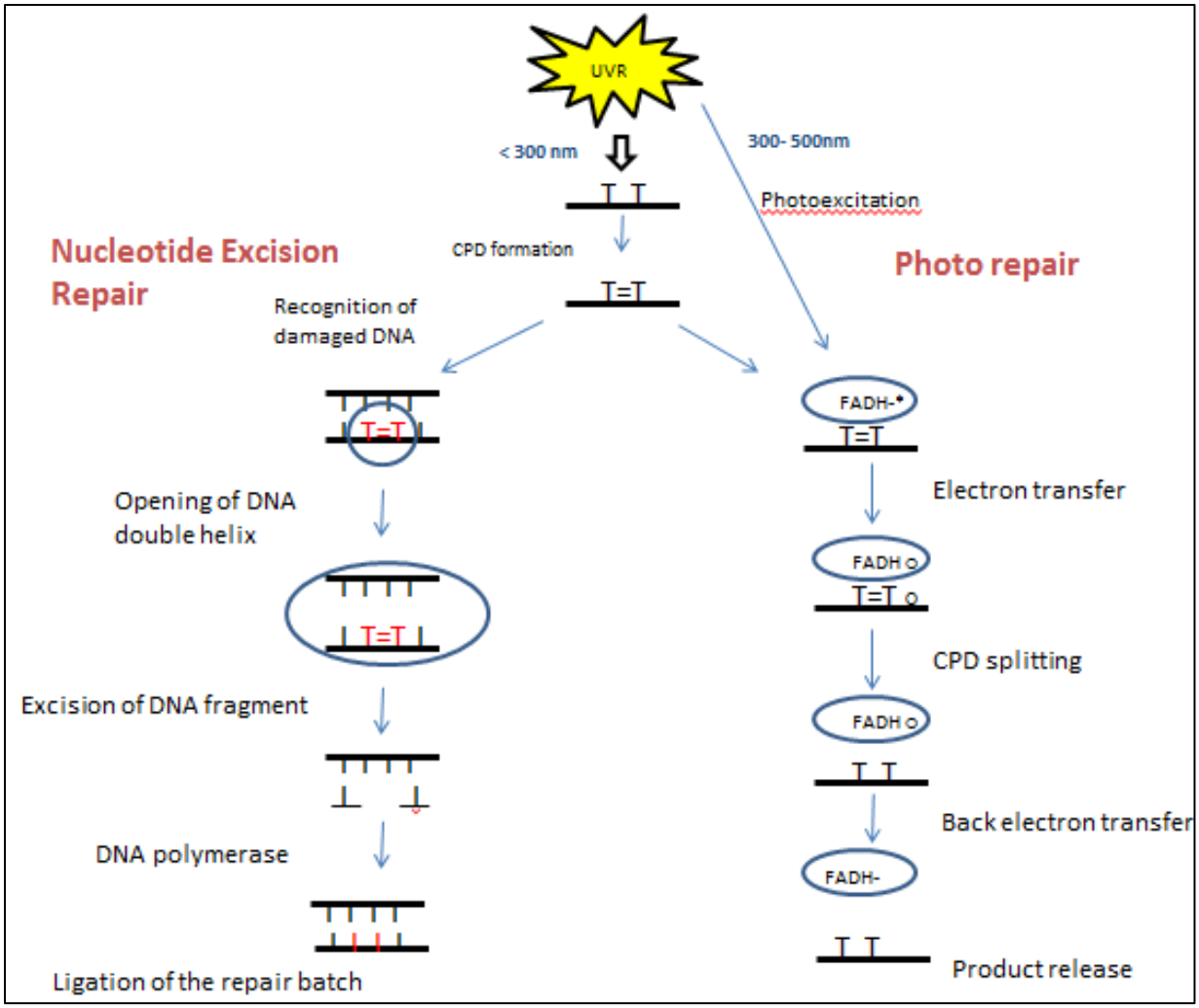

Figure 2.4: NER and photorepair removes UV-induced DNA lesions. NER includes stepwise process involving recognition of damaged DNA, opening of DNA double helix, excision followed by synthesis of DNA fragment and ligation of the repair batch. Photorepair involves a reaction cycle of CPD repair by photolyase (adapted from [50], [51])

2.3. Sunscreens

In many populations, the incidence of skin cancer continues to rise possibly due to reduced awareness of deleterious effects of UV radiation on skin [52]. The number of skin cancer cases continues to rise in North America, and similar trends can also be observed for the rest of the world including Australia and Europe [53]. The dramatic rise in skin cancer cases can be attributed to change in life style and increased exposure to sun light. In order to minimize the number of skin cancer cases, changes in life style can be the only modifiable factor. An effort to educate the public, to decrease sunlight exposure, can actually result in changes in the number of skin cancer cases round the world [54].

The simple and most widely recommended strategy, to protect the skin from negative effects associated with exposure to solar UVR, includes the use of sunscreen. The American Academy of Dermatology has recommended limited exposure to sun, to wear protective clothing, wearing a hat and the use of sunscreens when exposed to sunlight [54]. The prevention of excess exposure to solar radiation has been a first primary preventive measure, to decrease the incidence of skin aging, NMSC and malignant melanomas cases. Due to changing lifestyles, limiting exposure to sunlight for prevention of skin cancer has proven insufficient [55].

Out of all the primary preventive measures, the application of sunscreen seems to be the most popular method of protection from UV light. However, the use of primary measures to prevent skin damage largely depends upon the behavior of the people to skin protection [56]. Young children's behavior for sun protection was found to be influenced by parent's knowledge of skin cancer and skin protection [56]. The parents who had more information on sun protection and use of sunscreen were more likely to protect themselves and their children from sunlight damage [56]. The survey found that among adolescents, females were more likely to use sunscreen protection than males, and among adults, people with sensitive skin were most likely to be using sunscreen. However, very young children and older people were the most likely to use hats and clothes for sun protection [56]. Overall, the study suggested that the use of sunscreen is the most frequent method of protection from UV radiation, in all age groups including children, adolescents and adults [56].

2.3.1. Measures to determine UV protection ability of sunscreens

During the past two decades, there has been debates regarding the efficacy of sunscreens, however recent clinical studies have reported that the use of sunscreen for prolonged period of time can prevent NMSC [53]. Sunscreens are unique products because on proper application they prevent the sunburn [5]. The selection of a sunscreen or the combination of sunscreens is evaluated for their efficacy to prevent sunburn. Sun protection provided by the sunscreen is based on the Sun Protection Factor (SPF). The SPF is defined as "the ratio of sun exposure that skin can tolerate before burning with and without sunscreen protection" [5]. SPF therefore reflects the protection ability of sunscreens from UVB-radiation induced skin damage/erythema. Photoprotection of topical sunscreens is determined by their SPF, higher the SPF means higher efficacy.

Since the portion of sun light responsible for UV radiation-induced sunburn is similar to that of DNA damage, it was suggested that protection against sunburn is the same as protection against DNA damage [52].

2.3.2. Types of sunscreens

Traditionally topical sunscreens are divided into two broad categories including:

a. Organic sunscreens

A number of formulations containing organic sunscreens have been present in the market for decades. Some of the examples of organic sunscreens include para-aminobenzoic acid (PABA), PABA esters, cinnamates, benzophenones, salicylates, butylmethoxydibenzoylmethane, drometrizole trisulphonic (Mexoryl XL), terephthalydene dicamphor sulphonic acid (Mexoryl SX), methylene bisbenzotriazol tetramethylbutylphenol (Tinasorb M), anisotriazine (Tinasorb S) [52].

However, organic sunscreens have a major drawback of relatively narrow absorption spectrum. In order to overcome this drawback, organic sunscreens are majorly used in combinations, to provide an effective sun protection [52].

b. Inorganic sunscreens

The two most commonly used inorganic sunscreens are titanium dioxide and zinc oxide [52]. These sunscreens are photostable and effectively provide protection against UVA radiation [52]. Inorganic sunscreens provide sun protection by reflecting or scattering UV radiation.

The reflection/scattering of UV-radiation by inorganic sunscreens has a major problem of whitening of the skin. Inorganic sunscreens are cosmetically unacceptable, due to white appearance. In order to overcome such disadvantage, the average particle size of metal oxides were (titanium dioxide and zinc oxide) reduced to micro or nanoparticle size, to appear invisible on the skin [52, 57]. The transparency of inorganic sunscreens is more likely to provide increased consumer satisfaction. However, a few studies have shown safety concerns due to percutaneous absorption of micro/nanoparticle metals from the sunscreens [58-60].

Topical sunscreen agents can act either by either reflecting/ scattering UV-radiation or by absorbing the incident photon on the skin. The broad spectrum topical sunscreens protect the skin from UVA and UVB induced DNA damage and ROS formation. Examples of topical sunscreen agents:

2.3.3 Sunscreens available in the market

Sunscreens available in the U.S. market are rated according to their UVB protection, whereas those available in Europe are graded similarly but for both UVA and UVB protection. Recently, the FDA issued new regulations for labeling of OTC sunscreen products. In 2011, FDA finalized these guidelines, which recommended the use of broad spectrum sunscreen products that protect the skin from both UVA and UVB induced damage. Under the new guidelines the sunscreens which protect the skin from all types of sun-induced damage (both UVA and UVB) will be labeled “broad spectrum” and “SPF 15” (or greater) [54]. The broad spectrum sunscreen products with higher SPF, indicates higher levels of overall sun protection [54].

Today, sunscreen products with a combination of organic and inorganic ingredients are becoming popular in the market. Efforts are being made to design the broad spectrum sunscreens, to provide photoprotection from UVB and UVA portion of the solar light.

FDA monograph sunscreen ingredients	Protection type	Type of protection	Commercial use (Brand names)
Zinc oxide	Physical	UVA & UVB	Aveeno, Neutrogena
Titanium dioxide	Physical	UVB & considerable level of UVA	Aveeno, Neutrogena
Avobenzone (Butyl Methoxydibenzoylmethane)	Chemical	UVA & limited amount of UVB	No-Ad sunblock
Octyl methoxycinnamate	Chemical	UVA & limited amount of UVB	Johnson's Baby Sunblock Extra Protection
Aminobenzoic Acid	Chemical	UVB	Neutrogena
Octyl salicylate	Chemical	UVB	-
Mexoryl XL	Chemical	UVB & considerable level of UVA	L'Oréal
Phenylbenzimidazole	Chemical	UVB	-

Table 2.1: List of commercial sunscreen ingredients (adapted from [54]).

Considering the harmful effects of UVA radiation, USFDA guidelines have approved the use of avobenzone, ZnO and TiO_2 for sun protection [61]. Among these ingredients avobenzone is an organic molecule and ZnO and TiO_2 are inorganic molecules. The combination of avobenzone and ZnO sunscreen ingredients tends to provide broad spectrum of sun protection by both absorption and scattering of UVradiation [61].

Currently, US FDA are considering the approval of Tinosorb® M (also called Bisoctrizole), which is a broad spectrum sunscreen agent [54].

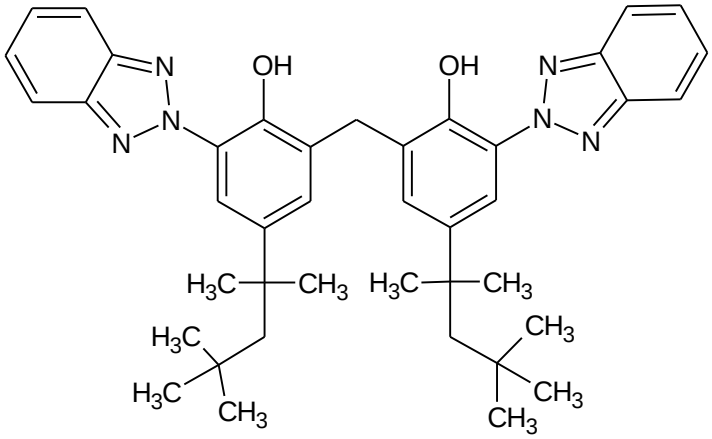

Tinsorb M

Figure 2.5: Structure of Tinsorb M, a broad spectrum organic sunscreen agent

Tinosorb® M is an organic sunscreen agent, which is stable to photodegradation. Unlike physical sunscreens, Tinosorb® M appears invisible on the skin and provides protection similar to physical sun block agents. It acts as a sunscreen agent in multiple ways, being photostable organic molecules absorb the UV-radiation and its micronized structure scatters/ reflects the light.

2.4. Flavonols

Flavonols constitute a class of polyphenolic compounds, which are mostly found in the form of plant glycosides [62]. Flavonols are secondary metabolites, generally produced by variety of different plant species. Flavonols belong to one of the most prevalent class of compounds found in vegetables, fruits, nuts and beverages such as tea, coffee and red wine [62].

A large number of plants produce secondary metabolites, derived from shikimic acid or aromatic amino acids, many of which have important roles in plant defense mechanisms [8]. Flavonols are secondary metabolites, generally produced by a variety of plant species in response to defense against UV radiation-induced damage [9]. Due to the presence of a number of phenolic hydroxyl groups on flavonols, they are also known for their significant antioxidant properties [9].

Flavonols have a wide range of biochemical and biological properties. Flavonols are naturally occurring phytochemicals, which are structurally characterized by the presence of a diphenylpropane (C6C3C6) skeleton [63]. Flavonols are present in diet in the form of *O*-glycosides, and the most common glycosidic unit being glucose [63]. The glycone unit in flavonols can also be glucorhamnose, galactose, arabinose, and rhamnose.

Flavonols like quercetin, kaempferol, myricetin and galangin constitute important members of the class of dietary flavonols [63]. Quercetin (3,5,7,3',4'-pentahydroxyflavone), kaempferol (3,5,7,3'-terahydroxyflavone), myricetin (3,5,7,3',4',5'-hexahydroxyflavone) and galangin (3,5,7-trihydroxyflavone) differ by hydroxyl group substitution on the benzopyrone skeleton.

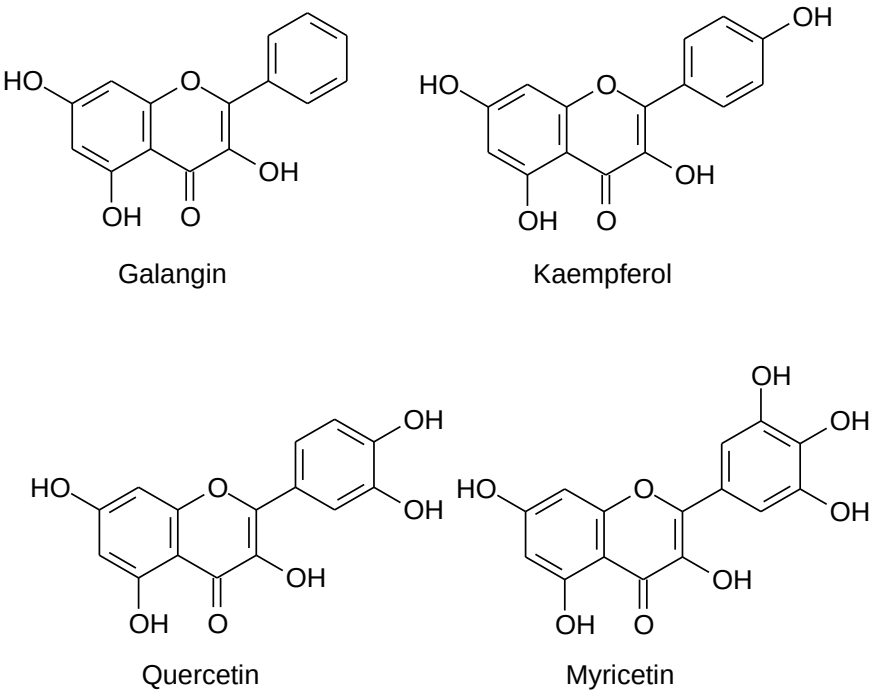

Figure 2.6: Structure of galangin, kaempferol, quercetin and myricetin

2.4.1. Role of flavonols in plants

Flavonols constitute the major class of naturally occurring polyphenolic compounds, which are mostly found in the form of plant glycosides. Plants like *Vicia faba*, *Brassica napus* and *Pinus sylvestris* show significant increase in the biosynthesis of flavonol content, particularly quercetin and kaempferol, after exposure to UV radiation [9]. In general flavonols have the ability to absorb in the region of 280-315 nm of sunlight thus act as a UV filters [9]. The photoprotective property of flavonol quercetin may be due to its maximal UV absorbance bands at 256nm and 368nm of sunlight [64]. Increases in flavonol content of plant species appear to be related to increased protection from UVB radiation.

Plant species vary in the levels of flavonol expression on exposure to UV radiation and thus, differ in their ability to resist UV damage [9]. UV radiation does not show a general increase in the content of all flavonols in plants, rather there is a preferential synthesis of flavonols, depending upon the level of hydroxylation. *Brassica napus* show higher levels quercetin as compared to kaempferol in response to UV radiation [65]. The selective synthesis of quercetin

over kaempferol was proposed to be related to the higher capacity of quercetin to scavenge UV-generated oxidative stress [65].

2.4.2. Role of flavonols in photoprotection: biological strategies

2.4.2.1. Endogenous photoprotection (oral levels):

Quercetin and kaempferol are predominantly present in the human diet [66]. Among all flavonols, the dietary intake of the flavonol quercetin accounted for the highest followed by kaempferol. Myricetin occurs less frequently in nature, compared to quercetin and kaempferol [66]. Flavonols are generally described as health-promoting and disease preventing supplements [67]. The various beneficial effects flavonols, has led to an increase in the dietary intake, as well as, the consumption of quercetin supplements by consumers [68]. The use of supplements has elevated the levels of quercetin by 25-60 folds [68].

In view of the studies conducted to date, it can be suggested that flavonol glycosides are hydrolyzed and the aglycone is absorbed. Oral dosing with a quercetin glycone such as rutin results in the absorption of quercetin aglycone from the intestine [69]. Yet, some studies confirm that low levels of flavonol glycosides can also be detected in the circulation. In addition to that, the plasma concentration of flavonols is also influenced by the apical efflux transporter multidrug resistance associated protein-2, which tends to excrete the flavonols increasing urinary flavonol elimination [70]. Data on flavonol metabolism indicates that the aglycone undergoes a high degree of plasma protein binding and rapid metabolism [71]. The biological effects of the flavonol aglycones are influenced by phase I and phase II metabolizing enzymes [62]. CYP450 mediated oxidation of flavonols are not generally observed, this is due to the fact that the abundance of hydroxyl groups on flavonol makes it resistant to phase I metabolism [72]. Flavonols undergo extensive phase II metabolism by enzymes, such as UDP-glucuronosyltransferase, glutathione S-transferase (GST) and sulfonyl transferase [68].

The most commonly studied flavonol, quercetin, has been evaluated as a potential anti-cancer agent [12, 13, 73-75]. However, the effect in prevention of skin cancer by increased dietary levels of flavonols is still unclear. In one study, the dietary level of quercetin has been reported to have no effect in prevention of UV-radiation induced SCC [75]. On the other hand, topical

application of flavonols has been widely reported to protect the skin from UV-radiation induced skin damage [12, 13][74].

2.4.2.2. Topical Application:

The flavonols have gained attention as protective agents against UV-radiation induced damage. The chemopreventive effect of flavonols is believed to be because of its inhibitory activities on variety of signaling pathways associated with UV-radiation induced damage [12, 13][74].

Kato *et al,* reported the chemopreventive effect of topically applied quercetin on mouse skin [74]. The authors performed analysis using mouse epidermis, and found that the topical application of quercetin inhibits epidermal tumor promotion through inhibition of lipoxygenase [74]. However the study done by Bowden *et al* in 2010 indicated, that the topical application of quercetin has no significant reduction on tumor growth, at the dose, five times less concentrated as compared to their previous study [12].

The anti-inflammatory activity of flavonols could be related to its ability to inhibit the cyclooxygenase or the 5-lipoxygenase pathways of arachidonic acid metabolism [76]. In previous studies, the glycosides of flavonols such as quercetin, kaempferol have shown an anti-inflammatory activity against carrageenan-induced inflammation in rats [76].

a) Anti-cancer:

Interestingly, myricetin was claimed to induce apoptosis in UVB-irradiated keratinocytes by inhibiting AKT (protein kinase) activity [77]. The underlying mechanism was reported to involve binding of myricetin to the ATP binding site of AKT and a decrease in phosphorylation of Bad (pro-apoptotic protein) [77]. Treatment with myricetin in UVB-irradiated cells, promoted translocation of Bad into mitochondria resulting in change of mitochondrial membrane potential and mitochondrial dysfunction [77]. Subsequently, mitochondrial apoptosis inducing factor (AIF) was released into the cytosol leading to cell death [77].

b) Photoprotection:

Quercetin is a known inhibitor of phosphoinositol-3-kinase (PI3K), a signal regulator for tumor promotion. However later in 2010 Bowden *et al* claimed that quercetin caused increased

expression of cFOS protein levels in UVB exposed HaCat cells [12]. The increased cFOS protein levels can be directly related to elevated levels of p38 and CREB phosphorylation. Interestingly, the authors found that the stability of quercetin in DMEM was the underlying cause for increased cFOS protein levels in HaCat cells. Quercetin was reported to degrade rapidly when incubated under normal cell conditions in DMEM [12]. Quercetin degradation in DMEM caused increased AP-1 activity and thus opposed its chemopreventive action. To achieve stability of quercetin in DMEM, the media was complemented with ascorbic acid. The study established that the treatment of UVB-irradiated HaCat cells with stabilized quercetin leads to inhibition of cFOS promoter activity and induces apoptosis [12]. This indicates that the stability of flavonols is a contributing factor to their chemopreventive action.

In 2008, a study done by Jung *et al* on mouse skin epidermal cells claimed that myricetin can suppress UVB radiation-induced skin cancer by directly targeting Fyn kinase [78]. Fyn, a member of Src family kinase, plays an important role in development of skin cancer. The authors suggested that the docking of myricetin to the ATP binding site of Fyn resulted in lowering of COX-2 expression via regulation of AP-1 and NF-κB activity [78]. Hence suppression of COX-2 expression by blocking of active site of Fyn kinase can be another strategy for the chemopreventive activity [78].

Later in 2010, Jung *et al* reported that, topical application of myricetin can also inhibit UVB-irradiated angiogenesis by regulating PI3-kinase activity [79]. Since angiogenesis is a critical part of cancer progression, the inhibition of hypoxia inducing factor through the PI3K-AKT signaling pathway leads to interference in the release of major growth factors like vascular endothelial growth factor and matrix metalloproteinase (MMP). The study indicated that the inhibition of PI3-kinase activity by myricetin, suppressed angiogenesis in UVB-irradiated mouse skin [79].

In addition to known cellular mechanisms of photoprotection by a range of topically applied flavonols, they may also acts as physical sunscreen agents as they absorb in the UVA and UVB ranges. Topical application of flavonol can act as a barrier between the sun and the skin, thus limiting the amount of damage caused by UV-radiation. They may act either by reflecting/ scattering UV-radiation or more likely by absorbing the incident photons.

2.4.2.3. Dietary versus topical:

The beneficial health effects of nutritional flavonol are gaining attention in today's world. However, the dietary levels are inadequate in providing protection from UV-radiation induced damage to the skin. The difference in UV-protection ability of dietary and topical levels of flavonol might be due to number of reasons. The most possible reason can be due to inadequate distribution of dietary flavonols to skin [12]. Secondly, the chemopreventive effect of dietary flavonols is dependent on the time frame to accumulation of required levels, which can take from eight to ten weeks [74]. So the action of topical application of flavonol can be practically instantaneous as compared to the dietary levels.

2.4.3. Other biological effects of flavonols

The total average intake of flavonols in the United States was estimated to be 1g/day [80]. Due to the large consumption of dietary polyphenols, it is essential to understand the biological effects of flavonols and their metabolites.

Flavonols are reported to have various beneficial health effects, including anti-oxidant, anti-tumaoral, anti-allergic, and anti-inflammatory activities [81]. A number of epidemiologic studies have also suggested the protective role of flavonols including against cardiovascular diseases and neurodegenerative disorders [82]. For example, polyphenols like quercetin and resveratrol, which are constituents of red wine, have been suggested to lower the incidence of coronary atherosclerosis. The French people were suggested to have less number of cardiac patients as compared to other western countries, despite the fact that French diet is rich in saturated fats. The protective effect of red wine is due to presence of high levels of polyphenols (resveratrol and quercetin) and this in turn became the explanation for the 'French paradox' [83]. Flavonols also have inhibitory effects on various enzymes like lipoxygenase, cyclooxygenase, monoxygenase and β-glucuronidase [81].

UV radiation-induced generation of reactive oxygen species (ROS) in skin cells results in photoaging [84]. ROS result in oxidative damage to lipids, proteins and DNA of skin cells. The anti-oxidant activity of the flavonol depends upon the ability to donate a hydrogen atom to the free radicals [84]. UV radiation-induced ROS results in the generation of collagenases and

matrix metalloproteinase (MMP-1) in skin cells. Recent studies have correlated the efficacy of flavonols as anti-oxidants to their ability to reduce the expression of MMP-1 [84].

The comparison of anti-oxidant capacity of flavonols include various structural features like 3-OH group on ring C and a 2, 3- double bond in conjugation with the 4-oxo group and hydroxyl group substitution on ring-B. The structural features of flavonols including the spatial arrangement of hydroxyl groups on ring-B play a significant role in its antioxidant activity [84]. The anti-oxidant activity of flavonols such as quercetin, kaempferol and myricetin depends on the number of hydroxyl groups present to scavenge the free radicals. Previous research suggested that the comparison of anti-oxidant activity of flavonols is in the order of myricetin (six OH) > quercetin (five OH) > kaempferol (four OH) [84].

2.5. Current analytical methods for detection and quantification of thymine dimer

2.5.1. Immunoassays

During the last four decades, extensive work has been reported for the qualitative and quantitative analysis of thymine dimers by using immunoassays and HPLC technologies [85, 86]. In order to determine the dimeric pyrimidine photoproducts, a number of antibodies against CPDs were used for analysis using enzyme linked immunosorbant assay (ELISA) and radioimmunoassay (RIA) techniques.

In 1982, Klocker *et al* developed a sensitive RIA method for the detection of photoproducts [87]. However, it was found that thymine dimers have high affinity to bind with antiserum, but with low specificity. Hence, there was a need to establish specific antibodies to recognize specific DNA lesions among the different photoproducts.

2.5.2. HPLC-Fluorescence

In 1999, Robinson *et al* developed an analytical method based on HPLC and fluorescence technology for detection of thymine photoproducts [85]. Since DNA photoproducts, including cyclobutane thymine dimers are not naturally fluorescent; the authors used 4-Bromomethyl 7-methoxycoumarin for detection of thymine and its photodimers. However, HPLC-florescence detection technique had a drawback of low selectivity for the type of thymine dimer formed.

Overall, HPLC-florescence detection technique did not allow the detection of different UV-radiation induced DNA adducts.

2.5.3. High performance liquid chromatography- tandem Mass spectrometry (HPLC-MS/MS):

HPLC-MS/MS technology is preferred for the identification and quantification of thymine dimer over existing methods like immunoassays and HPLC-florescence. UV-induced DNA adducts, especially pyrimidine photoproducts, have been extensively studied by coupling mass spectrometry technique to HPLC. Chromatographic method of separation is the significant separation of pyrimidine bases from their photoproducts. Reason being pyrimidine bases are more retained on octadecylsilyl silica gel columns due to hydrophobic interactions as compared to their photoproducts. The structural characterization of cyclobutane dimer and 6,4-

photoproducts either in the form of bases, nucleosides or dinucleotide monophosphates has been reported in the literature [88].

The choice of ionization technique depends upon the type of analyte of interest for analysis. Today, the most commonly used ionization sources for identification of thymidine dimer includes the use of electrospray ionization (ESI). ESI works well for thymidine dimers, not so well for thymine dimers since they lack the ionizable phosphate groups. However, other ionization techniques including Atmospheric pressure chemical ionization (APCI) and Atmospheric pressure photoionization (APPI) might also prove to be promising for analysis of thymine dimer without phosphate.

There are both strength and weaknesses of ESI, APCI and APPI ionization sources. More polar, relatively high molecular weight compounds are preferably analyzed by ESI, whereas, low molecular weight, thermally stable, non-polar to relatively polar compounds are preferably analyzed by APCI [89]. Some of the most commonly used ionization sources which can be coupled with LC-MS/MS for analysis of DNA adducts include:

i. Electrospray ionization (ESI):

In the ESI process, several processes occur: 1) a voltage is applied on the end of a capillary to form charged droplets; 2) an electric field gradient attracts the charged droplets; 3) a drying gas reduces the size of the droplets; 4) the repulsive forces between the charged ions in a droplet lead to conversion of ions from liquid phase to gas phase; 5) the ions are then forced into the mass analyzer. ESI is a softer ionization method as compared to other known ionization methods [89]. However, the analyte can undergo collision induced dissociation (CID) in the region between the capillary exit and skimmer.

ii. Atmospheric Pressure Chemical Ionization (APCI):

Atmospheric pressure chemical ionization (APCI) is a soft ionization technique, although less soft than ESI. ESI and APCI ionization sources differ in their structure by the presence of a heater and a corona discharge needle in APCI. The process of formation of ions in APCI involves chemical ionization. The heater around the capillary produces a temperature between 350-550°C, which converts the liquid-phase sample into the gas-phase. The corona discharge

needle provides charge to the carrier gas nitrogen, which in turn reacts with the gas-phase analyte. The gas phase ions generated at atmospheric pressure around the capillary are then forced into mass analyzer.

iii. Atmospheric pressure photoionization (APPI):

The compounds which remain poorly ionized or cannot be ionized by ESI or APCI might get ionized by atmospheric pressure photoionization ionization (APPI). In those cases APPI, might be the ionization of choice. The APPI process is based on the formation of ions in the ionization chamber by radiation from a far ultraviolet (UV) lamp [90]. An APPI ionization source can provide sufficiently high energy to ionize many organic compounds [91]. Ionization of DNA adducts by UV lamp in APPI source might be an interesting approach for future study.

2.5.3.1. HPLC-ESI-MS/MS:

The use of HPLC-MS/MS technology provides an ease for DNA photoproduct analysis over other existing methods, involving immunoassays including ELISA and RIA. In 2000, Douki *et al* developed an analytical method based on electrospray ionization/tandem mass spectrometry (ESI-MS/MS) for characterization of UV-induced DNA adducts [88]. The authors characterized fragmentation of thymine photoproducts at the base, dinucleoside monophosphate as well as at dinucleotide (pTpT) levels. They used a triple quadrupole mass spectrometer operated in negative ion ESI mode, coupled with HPLC for selective identification of thymidine monophosphate (TpT) adducts (Figure 2.7).

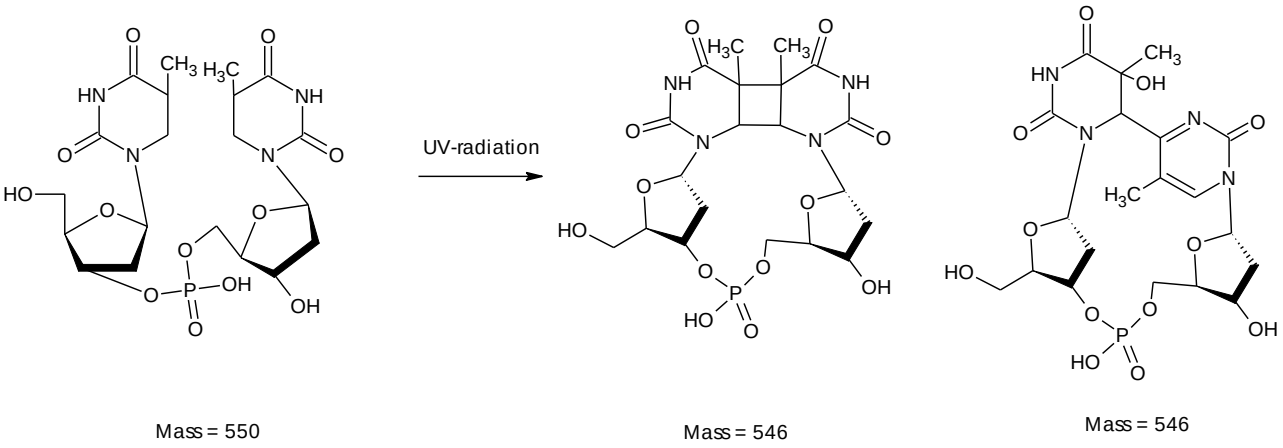

Figure 2.7: Formation of dinucleoside phosphate cyclobutane thymidine dimer and 6,4-PP adducts of TpT [88])

The authors used ESI-MS/MS to also develop the fragmentation behavior of the thymine adducts [88]. The ESI was operated in the negative ion mode. Selective parent to product ion transitions were monitored in multiple reaction monitoring (MRM) mode to increase the specificity of the method. The analysis of cyclobutane thymidine dimers (Figure 2.8A) and the (6–4) adducts was performed by monitoring two MRM transitions: 545→447 and 545→432 respectively. The ion trap was used in positive ion mode to determine the multistage mass spectrometry (MS^n) of thymidine dimer (Figure 2.8B).

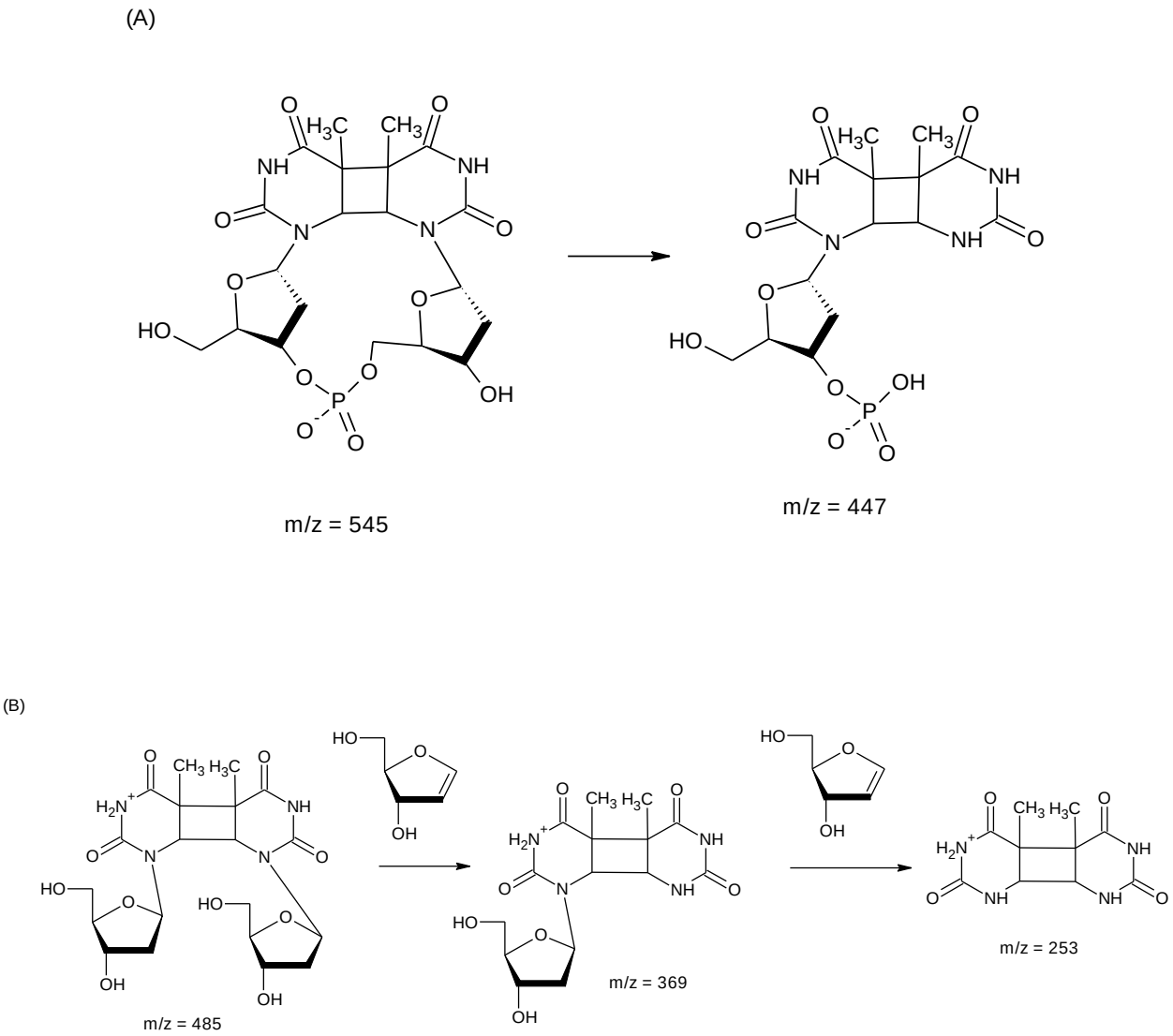

Figure 2.8: (A) Structural representation of fragmentation of cyclobutane dimer TpT with m/z transition 545→447 using ESI-MS/MS in negative ion mode on a triple-quadruple; (B) MS4 fragmentation of cyclobutane thymine dimer with parent ion: 485.1→369.1→253.1 using ion-trap.

The use of electrospray a soft ionization technique clearly showed the advantage of controlled fragmentation pattern of photoproducts. This study provides an interesting fragmentation behavior of thymine dimer in different levels DNA including base, nucleoside and dinucleotide monophosphate. In addition to characterization of fragmentation, the authors also developed

HPLC-ESI-MS/MS method in negative MRM mode for quantification of thymine dinucleotide phosphate [88].

2.5.3.2. ESI-DMS-MS/MS:

In 2010 St- Jacques and coworkers developed a sensitive and selective method for detection and structure elucidation of thymine dimers using differential mobility spectrometry/mass spectrometry (DMS/MS) [38]. They investigated the formation of isomeric structures of thymine adduct after exposure to UV-radiation, specifically cyclobutane adduct and 6,4-adduct of thymine nucleobase and thymine dideoxynucleotide.

Differential mobility spectrometry (DMS) cell was interfaced between the ionization source (ESI) and the mass analyzer (linear ion trap MS) [38]. The concept of differential mobility spectrometry was based upon the separation of isomeric ions of thymine dimer based on the drift velocity. The ions formed in the ionization region are drifted in an accelerating electric field by the application of drift velocity. The ions, which enter the drift tube, travel against the drift gas to reach the detector. The separation of structural isomers of DNA adducts was based upon the concept of differences in velocity of ions when they drift through change in electric field. Based on their results, the authors confirmed the presence of proton-bound isomer in addition to cyclobutane and 6-4PPs adducts (figure 2.9).

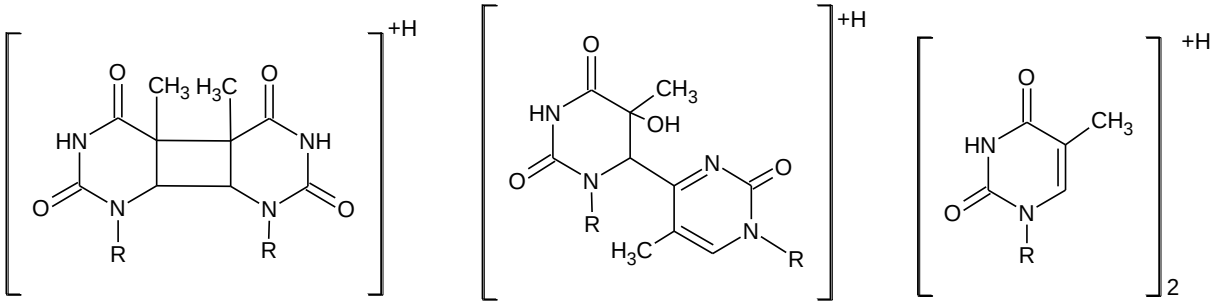

Figure 2.9: Structure represent the protonated forms of the [1] Cyclobutane Photoproduct, [2] 6,4-Photoproduct and [3] the Proton-Bound Dimer

The fragmentation of isomeric adducts of thymine were characterize by tandem mass spectrometry (MS/MS) of the separated photoproducts. The MS/MS analysis was performed in

positive ion mode with MRM transition of *m/z* 253/210 for cyclobutane thymine dimer, transition of *m/z* 253/235 corresponds to protonated 6,4-adduct, and transition *m/z* 253/127 was distinctive for the proton-bound thymine dimer. The largest shift in the position of peak was observed with cyclobutane isomer with MRM transition *m/z* 253/210. The least shift in peak was observed for 6-4 PP with the MRM transition *m/z* 253/235 with the loss of water whereas the protonated thymine dimer showed an intermediate shift with MRM transition *m/z* 253/127 [38]. However, the authors do not specify the structure of proposed product ions [38].

Differential mobility spectrometry interfaced between ESI and linear ion trap allowed the separation of isomeric thymine adducts, which were specifically monitored by specific MRM transitions. ESI-DMS-MS/MS provided the structural information and fragmentation pattern of UV-radiation induced isomeric adducts of thymine. Lastly, the study confirmed the presence of various isomeric products of thymine after exposure to UV radiation [38].

2.5.3.3. HPLC-APCI-MS/MS:

The use of atmospheric pressure chemical ionization (APCI) may be a promising ionization technique for the analysis of thymine dimer without phosphate backbone for the following reasons:

The advantages of using APCI for analysis of DNA adducts includes, less signal suppression due to matrix effect as compared to ESI. Secondly, APCI can be effectively used for ionization of small molecules and with wide range of polarity [89]. Moreover, DNA adducts identified by using ESI-MS/MS method require phosphate linked to thymidine dimers, which can readily form ions in negative mode.

In addition, the purpose of using HPLC-APCI-MS/MS method will be to quantify thymine dimers that did not contain phosphate. Since various enzymes are required to prepare samples retaining the phosphate and sugar moieties on thymine. The advantage for analysis of cyclobutane thymine dimer being that it avoids the use of exonucleases, nuclease P1, and an alkaline phosphatase in sample preparation [42].

The fact that sensitivity of ESI-MS/MS method has not been reported, so it is hard to justify which of the two techniques either ESI or APCI, is better for quantitative analysis. It is usually

the nature of analyte which governs the method of choice for ionization, yet there is not set criteria. However, it is a common procedure to try both APCI and ESI and determine which works better.

2.6. EpiDerm™:

EpiDerm™ is a highly differentiated model of human epidermis [92]. EpiDerm™ is derived from normal human epidermal keratinocytes. It is cultured to form a multilayered, human epidermis with a well-developed basement membrane human

Advantages of using EpiDerm™ [92]:

1. Three dimensional highly differentiated tissues
2. Both metabolically and mitotically active
3. Cost effective alternative to animal and human clinical testing
4. Easy to handle
5. Quantifiable biomarkers of UVR induced damage
6. Ideal for photo-damage and keratinocyte signaling studies

Histology of EpiDerm: EpiDerm™ tissues are mitotically and metabolically active and both structurally and biochemically mimics the normal human epidermis. Like human epidermis, EpiDerm™ [92] consists of organized basal, spinous and granular layers and spinous corneum layers. The layers are arranged in the pattern as those found in human skin (figure 2.10). The tissues are cultured on cell culture inserts, using serum free medium. The EpiDerm exhibits in vivo-like morphological and growth characteristics which are uniform and highly reproducible.

Uses: EpiDerm™ tissue models have become vital replacements for traditional animal based testing in the cosmetics, chemical and pharmaceutical industries to assess the dermal irritancy and toxicology [92].

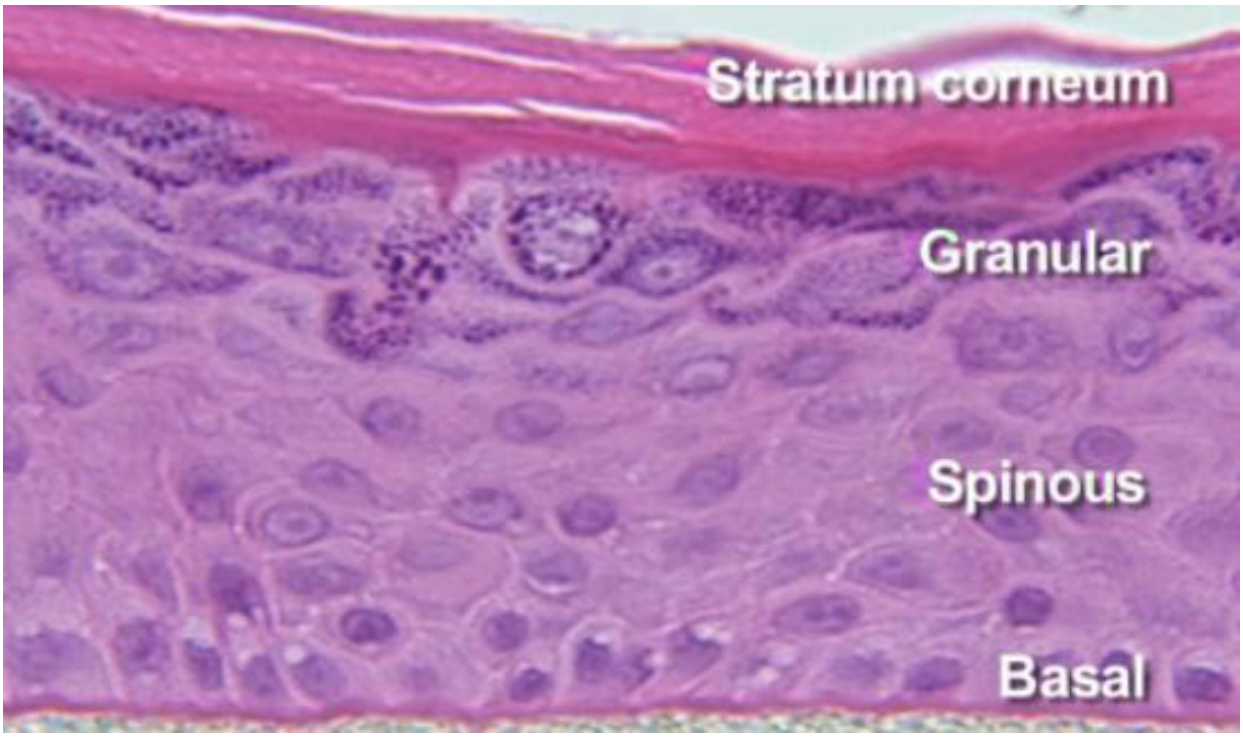

Figure 2.10: Section of EpiDerm™ reveals the presence of basal, spinous, granular keratinocytes and stratum corneum [93].

References

[1] D. Kulms, T. Schwarz, 20 years after - Milestones in molecular photobiology, J. Invest. Dermatol. Symposium Proceedings. 7 (2002) 46-50, doi: 10.1046/j.1523-1747.2002.19638.x.

[2] A.A. Lamola, Specific formation of thymine dimers in DNA., Photochem. Photobiol. 9 (1969) 291-294.

[3] F.R. de Gruijl, Photocarcinogenesis: UVA vs. UVB radiation, Skin Pharmacol. Appl. Skin Physiol. 15 (2002) 316-320, doi: 10.1159/000064535.

[4] J.-. Ravanat, T. Douki, J. Cadet, Direct and indirect effects of UV radiation on DNA and its components, J. Photochem. Photobiol. B: Biol. 63 (2001) 88-102.

[5] M. Al Mahroos, M. Yaar, T.J. Phillips, J. Bhawan, B.A. Gilchrest, Effect of sunscreen application on UV-induced thymine dimers, Arch. Dermatol. 138 (2002) 1480-1485.

[6] T. Maier, H.C. Korting, Sunscreens - Which and what for?, Skin Pharmacology and Physiology. 18 (2005) 253-262.

[7] L. Padmavathy, L. Rao, N. Ethirajan, B. Swamy, Malignant melanoma - Cutaneous metastases, Indian J. Dermatol. 53 (2008) 212-214.

[8] D. Treutter, Significance of flavonoids in plant resistance and enhancement of their biosynthesis, Plant Biology. 7 (2005) 581-591.

[9] J.B. Harborne, C.A. Williams, Advances in flavonoid research since 1992, Phytochem. 55 (2000) 481-504.

[10] A. Solovchenko, M. Schmitz-Eiberger, Significance of skin flavonoids for UV-B-protection in apple fruits, J. Exp. Bot. 54 (2003) 1977-1984, doi: 10.1093/jxb/erg199.

[11] Brian Michael Fahlman, *In vitro* studies to assess the potential of Quercetin as a topical sunscreen; photooxidative properties, photostability and inhibition of UV radiation-mediated skin damage (2010).

[12] E.R. Olson, T. Melton, S.E. Dickinson, Z. Dong, D.S. Alberts, G.T. Bowden, Quercetin potentiates UVB-induced c-Fos expression: Implications for its use as a chemopreventive agent, Cancer Prev. Res. (Philadelphia, Pa.). 3 (2010) 876-884.

[13] E.R. Olson, T. Melton, Z. Dong, G.T. Bowden, Stabilization of quercetin paradoxically reduces its proapoptotic effect on UVB-irradiated human keratinocytes., Cancer Prev. Res. (Philadelphia, Pa.). 1 (2008) 362-368.

[14] F. Urbach, Ultraviolet radiation and skin cancer of humans, J. Photochem. Photobiol. B: Biol. 40 (1997) 3-7.

[15] NASA HQ Press Release #00-137 NASA Science News "Record-setting Ozone Hole", NASA Science News "Record-setting Ozone Hole : Antarctica's ozone hole has expanded to cover an area three times larger than the United States" Link : http://science.nasa.gov/science-news/science-at-nasa/2000/ast08sep_1/, Acessed on Jan10, 2012 (Sep 8, 2000).

[16] J. Calbó, D. Pagès, J.-. González, Empirical studies of cloud effects on UV radiation: A review, Rev. Geophys. 43 (2005) 1-28.

[17] Y. Jiang, M. Rabbi, M. Kim, C. Ke, W. Lee, R.L. Clark, P.A. Mieczkowski, P.E. Marszalek, UVA generates pyrimidine dimers in DNA directly, Biophys. J. 96 (2009) 1151-1158.

[18] D.E. Godar, UV doses worldwide, Photochem. Photobiol. 81 (2005) 736-749.

[19] W.P. Coleman III, Skin Cancer: Recognition and Management, 2nd Edition by Robert A. Schwartz, Dermatologic Surgery. 34 (2008) 1702-1702, doi: 10.1111/j.1524-4725.2008.34351.x.

[20] American Cancer Society, American Cancer Society, http://www.cancer.org/Cancer/CancerCauses/SunandUVExposure/skin-cancer-facts. 2012 (2012).

[21] Canadian Cancer Society, Date accessed 10 March, http://www.cancer.ca/Canada-wide/About%20cancer/Cancer%20statistics.aspx?sc_lang=en. 2012 (2012).

[22] G.G. Giles, R. Marks, P. Foley, Incidence of non-melanocytic skin cancer treated in Australia, Br. Med. J. 296 (1988) 13-17.

[23] G.T. Bowden, Prevention of non-melanoma skin cancer by targeting ultraviolet-B-light signalling, Nat. Rev. Cancer. 4 (2004) 23-35.

[24] J. Longstreth, F.R. de Gruijl, M.L. Kripke, S. Abseck, F. Arnold, H.I. Slaper, G. Velders, Y. Takizawa, van der Leun, J. C., Health risks. 46(1-3) (1998) 20-39.

[25] R.E. Kwa, K. Campana, R.L. Moy, Biology of cutaneous squamous cell carcinoma, J. Am. Acad. Dermatol. 26 (1992) 1-26.

[26] J.G. Einspahr, S.P. Stratton, G.T. Bowden, D.S. Alberts, Chemoprevention of human skin cancer, Crit. Rev. Oncol. 41 (2002) 269-285.

[27] M. Alam, D. Ratner, Cutaneous squamous-cell carcinoma, N. Engl. J. Med. 344 (2001) 975-983.

[28] U. Leiter, C. Garbe, Epidemiology of melanoma and nonmelanoma skin cancer - The role of sunlight, Sunlight, Vitamin D and Skin Cancer. 624 (2008) 89-103.

[29] M.A. Weinstock, Death from skin cancer among the elderly: Epidemiological patterns, Arch. Dermatol. 133 (1997) 1207-1209.

[30] J.W. Streilein, J.R. Taylor, T. Yoshikawa, I. Kurimoto, Immunology of human skin and its relationship to skin cancers, Cancer Bull. 45 (1993) 225-231.

[31] D.L. Miller, M.A. Weinstock, Nonmelanoma skin cancer in the United States: Incidence, J. Am. Acad. Dermatol. 30 (1994) 774-778.

[32] R.B. Setlow, E. Grist, K. Thompson, A.D. Woodhead, Wavelengths effective in induction of malignant melanoma, Proc. Natl. Acad. Sci. U. S. A. 90 (1993) 6666-6670.

[33] E.A. Drobetsky, J. Turcotte, A. Châteauneuf, A role for ultraviolet A in solar mutagenesis, Proc. Natl. Acad. Sci. U. S. A. 92 (1995) 2350-2354.

[34] S.Q. Wang, R. Setlow, M. Berwick, D. Polsky, A.A. Marghoob, A.W. Kopf, R.S. Bart, Ultraviolet A and melanoma: A review, J. Am. Acad. Dermatol. 44 (2001) 837-846.

[35] B.E. Johnson, Formation of thymine containing dimers in skin exposed to ultraviolet radiation, Bull. Cancer. 65 (1978) 283-297.

[36] S. Mouret, C. Baudouin, M. Charveron, A. Favier, J. Cadet, T. Douki, Cyclobutane pyrimidine dimers are predominant DNA lesions in whole human skin exposed to UVA radiation, Proc. Natl. Acad. Sci. U. S. A. 103 (2006) 13765-13770.

[37] S. Mouret, C. Philippe, J. Gracia-Chantegrel, A. Banyasz, S. Karpati, D. Markovitsi, T. Douki, UVA-induced cyclobutane pyrimidine dimers in DNA: A direct photochemical mechanism?, Org. Biomol. Chem. 8 (2010) 1706-1711.

[38] A. St-Jacques, J. Anichina, B.B. Schneider, T.R. Covey, D.K. Bohme, UV-induced bond modifications in thymine and thymine dideoxynucleotide: Structural elucidation of isomers by differential mobility mass spectrometry, Anal. Chem. 82 (2010) 6163-6167.

[39] R.B. Setlow, J.K. Setlow, Evidence that ultraviolet-induced thymine dimers in DNA cause biological damage., Proc. Natl. Acad. Sci. U. S. A. 48 (1962) 1250-1257.

[40] T.M. Rünger, C→T transition mutations are not solely UVB-signature mutations, because they are also generated by UVA, J. Invest. Dermatol. 128 (2008) 2138-2140.

[41] J. Cadet, P. Vigny, The photochemistry of nucleic acids: In Bioorganic Photochemistry, Photochemistry and the Nucleic Acids (Edited by H.Morrison). 1 (1990) 1-272.

[42] T. Douki, J. Cadet, Individual determination of the yield of the main UV-induced dimeric pyrimidine photoproducts in DNA suggests a high mutagenicity of CC photolesions, Biochemistry (N. Y.). 40 (2001) 2495-2501.

[43] E. Pelle, X. Huang, T. Mammone, K. Marenus, D. Maes, K. Frenkel, Ultraviolet-B-induced oxidative DNA base damage in primary normal human epidermal keratinocytes and inhibition by a hydroxyl radical scavenger, J. Invest. Dermatol. 121 (2003) 177-183.

[44] J. Cadet, E. Sage, T. Douki, Ultraviolet radiation-mediated damage to cellular DNA, Mutation Research - Fundamental and Molecular Mechanisms of Mutagenesis. 571 (2005) 3-17.

[45] F. El Ghissassi, R. Baan, K. Straif, Y. Grosse, B. Secretan, V. Bouvard, L. Benbrahim-Tallaa, N. Guha, C. Freeman, L. Galichet, V. Cogliano, A review of human carcinogens—Part D: radiation, The Lancet Oncology. 10 (2009) 751-752, doi: DOI: 10.1016/S1470-2045(09)70213-X.

[46] R.M. Tyrrell, Induction of pyrimidine dimers in bacterial DNA by 365 nm radiation., Photochem. Photobiol. 17 (1973) 69-73.

[47] W.R. Stanton, M. Janda, P.D. Baade, P. Anderson, Primary prevention of skin cancer: a review of sun protection in Australia and internationally, Health Promot. Internation. 19 (2004) 369-378, doi: 10.1093/heapro/dah310.

[48] M. Berneburg, H. Plettenberg, J. Krutmann, Photoaging of human skin, Photodermatol. Photoimmunol. Photomed. 16 (2000) 239-244, doi: 10.1034/j.1600-0781.2000.160601.x.

[49] K. Scharffetter-Kochanek, M. Wlaschek, P. Brenneisen, M. Schauen, R. Blaudschun, J. Wenk, UV-induced reactive oxygen species in photocarcinogenesis and photoaging, Biol. Chem. 378 (1997) 1247-1257.

[50] J. De Boer, J.H.J. Hoeijmakers, Nucleotide excision repair and human syndromes, Carcinogenesis. 21 (2000) 453-460.

[51] V. Thiagarajan, M. Byrdin, A.P.M. Eker, P. Müller, K. Brettel, Kinetics of cyclobutane thymine dimer splitting by DNA photolyase directly monitored in the UV, Proc. Natl. Acad. Sci. U. S. A. 108 (2011) 9402-9407.

[52] F.P. Gasparro, M. Mitchnick, J.F. Nash, A Review of Sunscreen Safety and Efficacy, Photochem. Photobiol. 68 (1998) 243-256.

[53] U. Osterwalder, B. Herzog, S.Q. Wang, Advance in sunscreens to prevent skin cancer, Expert Review of Dermatology. 6 (2011) 479-491.

[54] U.S. Food and Drug Administration Protecting and promoting your health, http://www.fda.gov/forconsumers/consumerupdates/ucm258416.htm. 2012 (June/14/2011).

[55] T.I. Ellison, M.K. Smith, A.C. Gilliam, P.N. MacDonald, Inactivation of the vitamin D receptor enhances susceptibility of murine skin to UV-induced tumorigenesis, J. Invest. Dermatol. 128 (2008) 2508-2517.

[56] W.R. Stanton, M. Janda, P.D. Baade, P. Anderson, Primary prevention of skin cancer: a review of sun protection in Australia and internationally, Health Promot. Internation. 19 (2004) 369-378, doi: 10.1093/heapro/dah310.

[57] M. Lergenmüller, New titanium dioxide for improved UV-A protection, COSSMA. 5 (2004) 39.

[58] D.T. Tran, R. Salmon, Potential photocarcinogenic effects of nanoparticle sunscreens, Australas. J. Dermatol. 52 (2011) 1-6, doi: 10.1111/j.1440-0960.2010.00677.x.

[59] M.H. Tan, C.A. Commens, L. Burnett, P.J. Snitch, A pilot study on the percutaneous absorption of microfine titanium dioxide from sunscreens., Australas. J. Dermatol. 37 (1996) 185-7, doi: 10.1111/j.1440-0960.1996.tb01050.x.

[60] M.S. Agren, Percutaneous-Absorption of Zinc from Zinc-Oxide Applied Topically to Intact Skin in Man, Dermatologica. 180 (1990) 36-39.

[61] D.G. Beasley, T.A. Meyer, Characterization of the UVA Protection Provided by Avobenzone, Zinc Oxide, and Titanium Dioxide in Broad-Spectrum Sunscreen Products, Am. J. Clin. Dermatol. 11 (2010) 413-421.

[62] Y.J. Moon, X. Wang, M.E. Morris, Dietary flavonoids: Effects on xenobiotic and carcinogen metabolism, Toxicol. in Vitro. 20 (2006) 187-210.

[63] J.B. Harborne, C.A. Williams, Advances in flavonoid research since 1992, Phytochem. 55 (2000) 481-504.

[64] B. Durbeej, L.A. Eriksson, On the Formation of Cyclobutane Pyrimidine Dimers in UV-irradiated DNA: Why are Thymines More Reactive?, Photochem. Photobiol. 78 (2003) 159-167.

[65] G.J. Smith, K.R. Markham, Tautomerism of flavonol glucosides: Relevance to plant UV protection and flower colour, J. Photochem. Photobiol. A. 118 (1998) 99-105.

[66] M.G.L. Hertog, P.C.H. Hollman, B. Van de Putte, Content of potentially anticareinogenic flavonoids of tea infusions, wines, and fruit juices, J. Agric. Food Chem. 41 (1993) 1242-1246.

[67] J.V. Formica, Review of the biology of quercetin and related bioflavonoids, Food Chem. Toxicol. 33 (1995) 1061-1080.

[68] H. Van Der Woude, M.G. Boersma, J. Vervoort, I.M.C.M. Rietjens, Identification of 14 quercetin phase II mono- and mixed conjugates and their formation by rat and human phase II in vitro model systems, Chem. Res. Toxicol. 17 (2004) 1520-1530.

[69] T. Walle, Absorption and metabolism of flavonoids, Free Radic. Biol. Med. 36 (2004) 829-837.

[70] R.A. Walgren, J. Karnaky K.J., G.E. Lindenmayer, T. Walle, Efflux of dietary flavonoid quercetin 4'-β-glucoside across human intestinal Caco-2 cell monolayers by apical multidrug resistance-associated protein-21, J. Pharmacol. Exp. Ther. 294 (2000) 830-836.

[71] D.W. Boulton, U.K. Walle, T. Walle, Extensive binding of the bioflavonoid quercetin to human plasma proteins, J. Pharm. Pharmacol. 50 (1998) 243-249.

[72] V.M. Breinholt, E.A. Offord, C. Brouwer, S.E. Nielsen, K. Brøsen, T. Friedberg, In vitro investigation of cytochrome P450-mediated metabolism of dietary flavonoids, Food Chem. Toxicol. 40 (2002) 609-616.

[73] B. Ying, T. Yang, X. Song, X. Hu, H. Fan, X. Lu, L. Chen, D. Cheng, T. Wang, D. Liu, D. Xu, Y. Wei, F. Wen, Quercetin inhibits IL-1 beta-induced ICAM-1 expression in pulmonary epithelial cell line A549 through the MAPK pathways, Mol. Biol. Rep. 36 (2009) 1825-1832.

[74] R. Kato, T. Nakadate, S. Yamamoto, T. Sugimura, Inhibition of 12-O-tetradecanoylphorbol-13-acetate-induced tumor promotion and ornithine decarboxylase activity by quercetin: Possible involvement of lipoxygenase inhibition, Carcinogenesis. 4 (1983) 1301-1305.

[75] P.A. Steerenberg, J. Garssen, P. Dortant, H. Van De Vliet, L. Geerse, A.P.J. Verlaan, W. Goettsch, Y. Sontag, M. Norval, N.K. Gibbs, H.B. Bueno-de-Mesquita, H. Van Loveren, Quercetin prevents UV-induced local immunosuppression, but does not affect UV-induced tumor growth in SKH-1 hairless mice, Photochem. Photobiol. 65 (1997) 736-744.

[76] R.K. Goel, V.B. Pandey, S.P.D. Dwivedi, Y.V. Rao, Antiinflammatory and antiulcer effects of Kaempferol, a flavone, isolated from Rhamnus procumbens, Indian. J. Exp. Biol. 26 (1988) 121-124.

[77] W. Kim, H.J. Yang, H. Youn, Y.J. Yun, K.M. Seong, B. Youn, Myricetin Inhibits Akt Survival Signaling and Induces Bad-mediated Apoptosis in a Low Dose Ultraviolet (UV)-B-irradiated HaCaT Human Immortalized Keratinocytes, J. Radiat. Res. 51 (2010) 285-296, doi: 10.1269/jrr.09141.

[78] S.K. Jung, K.W. Lee, S. Byun, N.J. Kang, S.H. Lim, Y. Heo, A.M. Bode, G.T. Bowden, H.J. Lee, Z. Dong, Myricetin suppresses UVB-induced skin cancer by targeting Fyn, Cancer Res. 68 (2008) 6021-6029, doi: 10.1158/0008-5472.CAN-08-0899.

[79] S.K. Jung, K.W. Lee, S. Byun, E.J. Lee, J. Kim, A.M. Bode, Z. Dong, H.J. Lee, Myricetin inhibits UVB-induced angiogenesis by regulating PI-3 kinase in vivo, Carcinogenesis. 31 (2010) 911-917, doi: 10.1093/carcin/bgp221.

[80] J. Kühnau, The flavonoids and their role in human nutrition, Qualitas Plantarum Plant Foods for Human Nutrition. 23 (1973) 119-127.

[81] M.G.L. Hertog, P.C.H. Hollman, M.B. Katan, D. Kromhout, Intake of potentially anticarcinogenic flavonoids and their determinants in adults in The Netherlands, Nutr. Cancer. 20 (1993) 21-29.

[82] H. Schroeter, C. Boyd, J.P.E. Spencer, R.J. Williams, E. Cadenas, C. Rice-Evans, MAPK signaling in neurodegeneration: Influences of flavonoids and of nitric oxide, Neurobiol. Aging. 23 (2002) 861-880.

[83] S. Renaud, M. De Lorgeril, Wine, alcohol, platelets, and the French paradox for coronary heart disease, Lancet. 339 (1992) 1523-1526.

[84] G.-. Sim, B.-. Lee, S.C. Ho, W.L. Jae, J.-. Kim, D.-. Lee, J.-. Kim, H.-. Pyo, C.M. Dong, K.-. Oh, P.Y. Yeo, T.H. Jin, Structure activity relationship of antioxidative property of flavonoids and inhibitory effect on matrix metalloproteinase activity in UVA-irradiated human dermal fibroblast, Arch. Pharm. Res. 30 (2007) 290-298.

[85] J.K. Robinson, W.G. Scott, K.L. Rowlen, J.W. Birks, Derivatization of thymine and thymine photodimers with 4-bromomethyl-7-methoxycoumarin for fluorescence detection in high-performance liquid chromatography, J.Chromatogr. B: Biomed. Sci. Appl. 731 (1999) 179-186.

[86] L. Roza, K.J. van der Wulp, S.J. MacFarlane, P.H. Lohman, R.A. Baan, Detection of cyclobutane thymine dimers in DNA of human cells with monoclonal antibodies raised against a thymine dimer-containing tetranucleotide., Photochem. Photobiol. 48 (1988) 627-633.

[87] H. Klocker, B. Auer, H. Burtscher, A sensitive radioimmunoassay for thymine dimers, Mol. Gen. Genet. 186 (1982) 475-477.

[88] T. Douki, M. Court, J. Cadet, Electrospray-mass spectrometry characterization and measurement of far-UV-induced thymine photoproducts, J. Photochem. Photobiol. B: Biol. 54 (2000) 145-154.

[89] L L Geerse, Understanding operational differences between APCI and ESI., J. Chromatogr. Sci. 46 (2008) 88.

[90] F.P. Lossing, I. Tanaka, Photoionization as a Source of Ions for Mass Spectrometry, J. Chem. Phys. 25 (1956) 1031-1034, doi: 10.1063/1.1743092.

[91] H.W. Jochims, M. Schwell, H. Baumgartel, S. Leach, Photoion mass spectrometry of adenine, thymine and uracil in the 6-22 eV photon energy range, Chem. Phys. 314 (2005) 263-282, doi: 10.1016/j.chemphys.2005.03.008.

[92] MatTek Corporation (http://www.mattek.com/pages/in-vitro-toxicology). 2012.

[93] MatTek Corporation, An *In Vitro* Skin Irritation Test using the EpiDerm Reconstructed Human Epidermal Model (2012).

3. Hypothesis and objectives

Hypothesis 1: HPLC-APCI-MS/MS can be used to quantify cyclobutane thymine dimer, a biomarker of UV-radiation induced damage.

Hypothesis 2: flavonols would inhibit UVA and UVB induced photodamage to artificial skin mimics.

Hypothesis 3: aqueous and photostability of flavonols may depend on hydroxyl group substitution on the B-ring.

In order to test these hypotheses, five major objectives for this research project were established.

Objective 1- To develop and validate bio-analytical method for detection and quantification of cyclobutane thymine dimer: A simple analytical method based on HPLC-APCI-MS/MS technology to be used to quantify cyclobutane pyrimidine dimers, major DNA lesions produced in human skin when exposed to UV radiation.

Objective 2- To apply the analytical method to determine the topical sunscreen properties of flavonols in UVA/B exposed artificial skin mimics (EpiDerm™): To use the analytical method for thymine dimer damage to determine the ability of three flavonols (quercetin, kaempferol and galangin) to protect EpiDerm™, an artificial skin mimic, against UV radiation-induced thymine dimer formation.

Objective 3- To determine the effect of B-ring substitution on the UVA and the aqueous stability of flavonols (galangin, kaempferol, quercetin and myricetin): The stability of flavonols would be achieved by monitoring the levels of a range of flavonols remaining over time to UVA radiation and aqueous media by using HPLC-UV detection.

Objective 4- To determine the UVA and aqueous decomposition products of flavonols (galangin, kaempferol, quercetin and myricetin): The determination of decomposition products of the stability studies will be accomplished by using HPLC-MS/MS technology.

Objective 5- To determine the UV-induced decomposition of the flavonol 3-hydroxyflavone in polar and non-polar solvents. The general trend of flavonol photochemistry will be studied by using a prototype compound 3-hydroxyflavone.

4. Objective 1

To develop and validate bio-analytical method for detection and quantification of cyclobutane thymine dimer

Quantitative analysis of cyclobutane thymine dimers by High Performance Liquid Chromatography Atmospheric Pressure Chemical Ionization Tandem Mass Spectrometry: method development and validation.

Authors: Sabia Maini, Brian M. Fahlman[1] and Ed S. Krol*

Submitted to the Journal of Pharmaceutical and Biomedical Analysis

NOTE:

In this paper the role of Sabia Maini includes- Optimization of HPLC and MS/MS conditions, method validation, HaCaT cell experiments.

In this paper the role of Brian Fahlman includes- Pilot studies on ionization techniques ESI and APCI.

Paper was written by Sabia Maini and Ed Krol

4.1. Abstract

We report a rapid and sensitive High-performance liquid chromatography-Atmospheric-pressure chemical ionization-tandem mass spectrometry (HPLC-APCI-MS/MS) method to quantify cyclobutane thymine dimer, a biomarker of ultraviolet radiation-induced skin damage. An Allsphere ODS-2 reversed phase column (2.1mm by 150mm, 3µ) was used for separation of internal standard, thymine and cyclobutane thymine dimers under isocratic conditions with a mobile phase consisting of water-methanol (99:1, v/v) with 0.1% formic acid at a flow rate of 200µL/min. The HPLC-APCI-MS/MS method was validated for the levels of cyclobutane thymine dimers by multiple reaction monitoring in the presence of known quantities of cyclobutane thymine dimers (standard) and 5-fluorouracil (internal standard). This assay involves rapid and simple sample preparation; the extracted DNA from skin cells was hydrolyzed by treatment with 88% formic acid at 125ºC for 20 min. The samples were evaporated to dryness and reconstituted in 200 µL of water. The method was linear over the range of 0.0195 µM - 0.6 µM, with a limit of detection of 0.009 µM. The bioanalytical method validation was performed to achieve accuracy, precision, selectivity, sensitivity, reproducibility, and stability as per to USFDA guidelines. The *in vitro* application of selective and sensitive HPLC-APCI-MS/MS method was used to determine the sunscreen properties of the flavonol galangin, by monitoring the decrease in the levels of cyclobutane thymine dimers in flavonol treated UVB-exposed HaCaT cells.

KEYWORDS: cyclobutane thymine dimer, tandem mass spectrometry, APCI, fragmentation pattern, method validation.

Abbreviations

CPDs: cyclobutane pyrimidine dimers; DMS/MS: differential mobility spectrometry/mass spectrometry; DMEM: Dulbecco's modified Eagle medium; ELISA: enzyme linked immunosorbant assay; FBS: fetal bovine serum; HPLC-APCI-MS/MS: High Performance Liquid Chromatography-Atmospheric Pressure Chemical Ionization-tandem mass spectrometry; HQC: high quality control; LQC: low quality control; LLOD: lower limit of detection; LLOQ: lower limit of quantification; MRM: multiple reaction monitoring; PBS: phosphate buffered saline; MQC: middle quality control; RIA: radioimmunoassay;T<>C: thymine-cytosine dimer; T<>T: thymine-thymine dimer; UV: ultraviolet.

4.2. Introduction

The amount of ultraviolet (UV) radiation reaching the Earth's surface has increased, in part due to the depletion of the stratospheric ozone layer [1]. Increased exposure to UV-radiation is one of the major environmental factors responsible for induction of skin cancer [2] in many parts of the world namely North America, Europe, and Australia [3]. The American Cancer Society estimates that there are more than 2 million new cases of non-melanomic skin cancer annually in the United States [4].

The relationship between elevated levels of UV radiation and skin cancer is widely reported [5]. Chronic exposure to sunlight has a major role in the development of skin carcinoma [6], with DNA being one of the key targets for UV-induced damage in a variety of organisms. The formation of DNA photoproducts depends upon the nature of the incident photons [7, 8]. Radiation in the UVB range (280-315 nm) is widely known to cause direct photochemical damage to DNA [9-12]. The damage caused by radiation in the less energetic UVA range (315-40 nm) is mainly the result of oxidative stress [13-15] although formation of dimeric pyrimidine photoproducts has also been observed [16].

Two major classes of UV- radiation induced photoproducts are known, cyclobutane pyrimidine dimers (CPDs) and 6-4 dimers (Figure 4.1). The CPDs arise from cycloaddition at the C5-C6 double bond between two pyrimidine residues such as Thymine-Thymine (T<>T) and Thymine-Cytosine (T<>C) [8, 16, 17]. CPDs are produced preferentially at sites containing adjacent thymines versus those possessing adjacent cytosines and account for 90% of the total photoproducts [8, 12]. T-C to T-T or C-C to T-T transition mutations have been detected at bipyrimidine sites, however the probability of C-C to T-T transition mutation was the highest of all the mutations [18]. Based on the work done [8, 16] on the relative distribution of UV radiation induced photoproducts, CPDs are the predominant DNA lesions produced by both UVA and UVB radiations and T<>T is a useful biomarker of UV radiation-induced biological damage. The dimeric pyrimidine photoproducts formed by UV radiation, if unrepaired can cause errors in DNA replication, leading to mutagenesis and carcinogenesis [17].

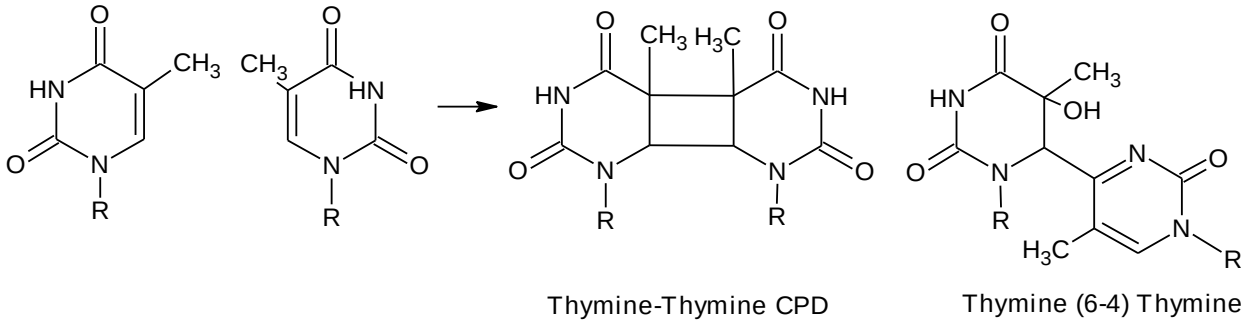

Figure 4.1: Formation of thymine cyclobutane dimer and thymine (6-4) photoproducts from thymine.

A number of methods have been used to identify and quantify dimeric pyrimidine photoproducts. Earlier methods used enzyme linked immunosorbant assay (ELISA) or radioimmunoassay (RIA) approaches [19, 20], however a drawback to this technique was the observation that thymine dimers bind with high affinity but low specificity to antiserum [20]. An analytical method based on HPLC with fluorescence detection was developed for detection of thymine and its photodimers using 4-bromomethyl 7-methoxycoumarin derivatization [21]. The fluorescence detection technique, however, showed low selectivity for the CPDs. A sensitive gas chromatography-electron capture detection method which was used to measure thymine dimer formation could differentiate between different T<>T dimers, although this method required HPLC separation followed by pentafluorobenzyl derivatization [22]. Douki *et al* developed a tandem mass spectrometric technique using electrospray ionization for detection of specific dimeric pyrimidine photoproducts, based on the ionization in negative mode of the phosphate groups of the thymidine dimers [23]. More recently St- Jacques and coworkers developed a method for detection and structure elucidation of thymine dimers using differential mobility spectrometry/mass spectrometry (DMS/MS) [24].

We are currently studying the ability of naturally-occurring flavonols to provide protection against UV radiation-induced damage to skin [25-27]. A large number of plant species are known to produce flavonols, such as quercetin and kaempferol, in response to UV radiation exposure [28, 29]. These flavonols are believed to protect plants from UV radiation-

induced damage, likely as a result of their ability to absorb UV radiation at 255 and 365nm. In an effort to determine the photoprotective properties of flavonols we sought an analytical method for quantification of direct UV radiation damage to DNA in vitro.

The purpose of our study is to develop a simple and selective HPLC-APCI-MS/MS method for the quantification of CPD thymine dimers (i.e. not containing the phosphate backbone). We have developed and validated an easy and robust method for measuring T<>T caused by exposure of DNA to UV-radiation *in vitro*. The use of LC-MS/MS in our method provides an improvement for ease of DNA photoproduct analysis over other methods involving immunoassays including ELISA and RIA. In addition, our technique avoids the use of exonucleases, nuclease P1, and an alkaline phosphatase in sample preparation [12]. In order to demonstrate the utility of this method, we have applied this technique to assess the ability of the naturally-occurring flavonol galangin, a compound which we are investigating for its photoprotective properties, to prevent T<>T formation in UVB exposed HaCaT cells.

4.3. Materials and Methods

4.3.1. General

Thymine ($C_5H_6N_2O_2$, minimum 99%), 5-fluorouracil ($C_4H_3FN_2O_2, \geq 99\%$) and formic acid were purchased from Sigma-Aldrich Canada Ltd (Oakville, ON). LC/MS grade water and methanol were purchased from Fisher Scientific Canada (Ottawa, ON). HaCaT cells were obtained from Cell Lines Service (Eppelheim, Germany). Dulbecco's modified Eagle medium (DMEM), fetal bovine serum (FBS), phosphate buffered saline (PBS), versene and trypsin were from Invitrogen (Burlington, ON). DNeasy Blood & Tissue Kits were purchased from Qiagen (Toronto, ON)

UVB irradiations were carried out using two FS20T12/UVB lamps (National Biological Corp., Beachwood, OH). The output of the lamps was filtered to remove UVC radiation at an emission of 310nm. UVC irradiations were carried out using a Rayonet Preparative Photochemical Reactor (The So. New England Ultraviolet Co., Middletown, CT) fitted with UVC bulbs.

4.3.2. Preparation of Cyclobutane thymine photodimer standard

Cyclobutane thymine photodimer was prepared in water using the method of Ramsey and Ho (42). An aqueous solution of thymine at a concentration of 2 mM was frozen and then exposed to UVC light in a reactor for 30 min. Following the irradiation, the frozen sample was thawed in a water bath at 40 ^{0}C. The 'freeze-irradiation-thaw' process was repeated five times daily for 10 days to prepare the standard.

4.3.3. *Chromatographic conditions*

HPLC-PDA analysis was performed on a Waters Alliance system (Waters Corp., Milford, MA) which consisted of a pump, autosampler, and photodiode array detector (Waters 2996). Elution of T<>T was carried out on an Allsphere ODS-2, 3µ column (2.1 mm × 150 mm) with isocratic flow using a solvent system of water-methanol (99:1, v/v) with 0.1% formic acid at a flow rate of 200 µL/min. Data was processed using Waters Empower software.

The separation and isolation of cyclobutane thymine dimer was performed by using semi preparative LC with an Allsphere ODS-2 5µ column (10 mm × 300 mm). The solvent system consisted of gradient flow of water-methanol with 0.1% formic acid at a flow rate of 3 ml/min. The gradient for T<>T collection was as follows: 0 to 15 min, linear gradient from 100% A to 90% A; 15 to 18 min, isocratic 90% A; 18 to 19 min, linear gradient from 90% A to 100% A; 19 to 20 min, isocratic 100% A. Aliquots of 100 µL were injected onto the column and T<>T (R_t = 14.4 min) was collected using a fraction collector. The column was maintained at room temperature (22ºC) and washed with (50:50) water: methanol after every use. The fractions of the T<>T sample were combined and the solvent was removed by freeze drying (Labconco Freezone 6 Plus, Labconco Corp., Kansas City, MO). Stock solutions (100 µM) were prepared by dissolving known amounts of T<>T in 100% water.

4.3.4. *HPLC-MS/MS analysis*

HPLC-MS/MS analysis was carried out at room temperature on an Agilent 1100 system coupled to quadrupole linear ion trap mass spectrometer. The HPLC system consisted of a pump (Agilent 1100 G1311A) and an autosampler (Agilent 1100 G1329A) (Agilent Technologies, Mississauga, ON). Mass spectrometry was performed using an AB SCIEX 4000 QTRAP (AB SCIEX instruments). HPLC flow was diverted to waste for the first 2 minutes of each run through an electronic vaco valve, and then from 13 to 20 min when no data acquisition was taking place. Aliquots of 10 µL of processed samples were injected onto an ODS-2 3µ column (2.1 mm × 100 mm). The column and autosampler were maintained at room temperature. The analytes were eluted under isocratic flow of water- methanol (99:1. v/v) with 0.1% formic acid at a flow rate of 200 µL/min with a run time of 20 min.

The mass spectrometer was used in multiple reaction monitoring (MRM) mode, equipped with a heated nebulizer (Atmospheric pressure chemical ionization (APCI)) interface used in positive mode. The precursor and product ion spectra were determined by direct infusion of standards and internal standards into the ion source with a syringe pump. Quantitative analysis of the processed samples was performed using sum of two MRM transitions for the standard (cyclobutane thymine dimer) from *m/z* 253 → 210 and *m/z* 253 → 139. For the internal standard (5-fluorouracil) the Q1/Q3 transition was monitored from *m/z* 131 → 114.

All of the mass spectrometry conditions for ionization of the standard and internal standard were optimized by direct infusion using a syringe pump at a flow rate of 10 µL/min. Nitrogen was used as the nebulizer, collision and curtain gas. The optimized mass spectrometer parameters were as follows: curtain gas 45psi, collision-activated dissociation (CAD) 5psi, nebulizer gas (GS1) 40psi, entrance potential (EP) 10eV and temperature 450ºC. The optimized APCI-MS/MS parameters are given in table 1.

SAMPLE ID	Q1 (*m/z*)	Q3 (*m/z*)	Time (msec)	DP (volts)	CE (volts)	CXP (volts)	Ionization mode
Standard (T<>T)	253	210	500	56	17	12	+
Standard (T<>T)	253	139	500	56	31	12	+
I.S. (5-FU)	131	114	500	41	25	20	+

Table 4.1: Optimized APCI-MS/MS parameters for T<>T and internal standard

4.3.5. Processing of data

Analyst 1.5.1 software from AB SCIEX was used for controlling the equipment and acquiring and processing of data.

4.3.6. Preparation of stock and working standard solutions

All of the primary and working stock solutions of standard T<>T and that of internal standard (5-fluorouracil) were prepared in LC-MS grade water. 100 µM primary stock solutions of standard and internal standard were prepared in water and stored at −20ºC. The 10 times concentrated working stock solutions of standard and quality control samples were made by

serial dilution of primary stock solution in water. The QC samples including low quality control (LQC), middle quality control (MQC) and high quality control (HQC) were prepared as per United States Food and Drug Administration (USFDA) guidelines with concentrations of 0.05 µM, 0.25 µM, and 0.5 µM respectively. The LQC is 3-times the lower limit of quantification (LLOQ) and HQC is 80% of the upper limit of quantification. The stocks stored at −20ºC were used to prepare fresh standard curve and quality control samples on each day of analysis.

4.3.7. Preparation of calibration curve samples and quality control (QC) samples

The standard and quality control samples were prepared fresh on each day of analysis. DNA was extracted from blank unexposed HaCaT cells using a DNeasy kit. After isolation of DNA, the samples were spiked with 20µL of working stock solution of standard/ quality control and internal standard. Each sample was subjected to hydrolysis in 200 µL of 88% formic acid at 125ºC for 20min (39). The hydrolysate of all the standard, quality control and blank samples were evaporated and redissolved in 200 µL of water. The samples were vortex-mixed for 30 sec and injected into the HPLC-MS/MS system with an injection volume of 10 µL.

4.3.8. Validation procedures

A complete validation for the assay of cyclobutane thymine dimer in human skin was performed according to USFDA guidelines [30], by spiking the DNA from human skin cells with the standard (calibration) and quality control samples. The method was validated in terms of accuracy, precision, selectivity, sensitivity, reproducibility, and stability. Each analytical run consisted of a blank sample (without internal standard), double blank (with internal standard), six standard samples for calibration (n = 3), and replicate sets (n = 6) of quality control samples.

4.3.8.1. Calibration curve

Each calibration curve consisted of an extracted blank (without internal standard), double blank (with internal standard) and six standard samples. The limit of detection (LOD) was the lowest detectable concentration with a signal-to-noise ratio of 3. The lowest limit of quantification (LLOQ) was the lowest sample point on the calibration curve with a signal-to-noise ratio of 10.

*C*alibration curves were constructed by plotting the ratio of peak areas of analyte and internal standard (y) against the nominal concentrations of analyte (x) using Analyst software. The best fit for the calibration curve was determined by using the least-square quadratic regression model $y = ax^2 + bx + c$, weighted by $1/x^2$.

4.3.8.2. *Selectivity and carry-over*

To determine selectivity, six blank HaCaT cell samples were compared with the QC samples, to determine the presence of interference for each MRM transitions standard and internal standard. Injection of blanks (100% water) after the highest calibration curve concentration were done to determine the absence of autosampler carry-over.

4.3.8.3. Accuracy and precision

Accuracy and precision were determined by analyzing replicates (n = 6) of each of LLOQ, LQC, MQC and HQC samples on three separate days. The precision was expressed as % relative standard deviation (RSD) of the concentrations measured at each QC level. Accuracy was measured as the mean of [(calculated amount/ nominal value) × 100].

The LLOQ and QC samples meet the following acceptance criteria with:

(a) The a*ccuracy* should be within ±15% of the nominal value except for LLOQ which can be within ±20%.
(a) The precision around the mean value should not exceed 15% of RSD except for LLOQ which should not be more than 20% of RSD.

4.3.8.4. Recovery and matrix effect

The extent of recovery was analyzed by comparing the peak areas of the QC samples with the peak areas of post-extraction spiked samples of the corresponding concentrations. The matrix effect was evaluated by comparing the peak areas of the analyte in post-extraction spiked samples with the peak areas of the standard solutions.

[% Recovery = (Mean peak area of extracted samples/ Mean peak area of post-extraction spiked samples) × 100]

[% Matrix effect = *(*Mean peak area of post-extraction samples/ Mean peak area of non-extracted pure samples) × 100]

4.3.8.5. Stability study

Freeze/thaw stability, autosampler stability, bench top stability, and long-term stability studies were accomplished by analyzing replicates (n = 3) of freshly prepared LLOQ, LQC, MQC, and HQC. For freeze/thaw stability, samples frozen at -80ºC were allowed to thaw unassisted at room temperature and then refrozen for 24 h prior to the next cycle. The samples were measured for freeze/thaw stability after three 24 h freeze/thaw cycles at 24 h, 48 h and 72h.

The bench top stability was measured using three aliquots each of LQC, MQC and HQC. The samples were allowed to thaw at room temperature and kept at room temperature for 6 h and analyzed. The autosampler stability was measured by keeping the replicates (n = 3) of LQC, MQC, and HQC in the autosampler for 24 h prior to injection. The long term stability was measured by storing the replicates (n = 3) of LQC and HQC at -80ºC for 30 days prior to analysis. The QC samples assessed for stability studies were compared with the freshly prepared samples and were used to determine the deviation from the nominal concentration.

4.3.9. Cell Culture

HaCaT cells were obtained from Cell Lines Service (Eppelheim, Germany) and cultured as a monolayer in DMEM containing 10% FBS. The cells were plated onto T-75 culture flasks and incubated at 37ºC with 5% CO_2. When cells reached 90% confluency they were treated with 0.05% EDTA / 0.1% trypsin in phosphate buffered saline (PBS) and incubated for 15 min at 37ºC to aspirate and dispense the cells onto 6 well plates at a density of $5x10^3$ cells/cm^2. The plates were incubated in media at 37ºC with 5% CO_2 until 90% confluency was reached. The blank unexposed HaCaT cells were removed from the incubator, collected and placed in a -80°C freezer for preparation of the standard curve and method validation.

4.3.10. Galangin Treatment

For dosing with galangin, each well containing HaCaT cells at 90% confluency was washed with PBS, and 2 mL DMEM with 10% FBS was added. To the media, 4.0 µL of 50mM

of galangin in DMSO was added to obtain concentrations of 100 μM. The dark and UVB control had neither DMSO nor galangin added to the media. The vehicle control contained 4.0μL DMSO added to the media. Following the treatment with galangin, the cells were returned to the incubator at 37°C with 5% CO2 for 24 hrs.

4.3.11. UVB exposure

For UVB exposure, the cells were removed from the incubator and the media was replaced with PBS. The 6-well plates were then placed under UVB lamps without covers. The galangin treated cells were exposed to UVB radiation at a dose of 0.05J/cm^2. UVB-control samples were also irradiated in a similar manner. For the dark control, plates were wrapped in aluminum foil and placed under UVB lamps. Following UV irradiation, PBS was removed and the cells were placed in a -80°C freezer for analysis.

4.3.12. Statistics

Significant differences in the amount of T<>T in UVB exposed control and galangin treated samples were assessed with one-way analysis of variance with Tukey's test for pairwise multiple comparisons using SPSS software (IBM SPSS statistics version 19, Markham, ON, Canada). The level of significance was set at $P < 0.05$.

4.4. Results and Discussion

We have developed a HPLC-APCI-MS/MS method for detection and quantification of T<>T, the major DNA lesion produced in skin on exposure to UV radiation. Our analytical method is simple and selective for quantitative analysis of T<>T, as opposed to analysis of the phosphate linked thymidine dimers which requires the use of exonuclease, nuclease P1, and alkaline phosphatase sample preparation steps [12]. Although the reported GC-ECD method also detects T<>T, our method does not require the additional HPLC purification and derivatization steps [22].

4.4.1. *LC-MS/MS analysis*

We initially tested two ionization sources, ESI and APCI, and determined that APCI was a superior ionization method to ESI as the sensitivity of APCI for T<>T was an order of magnitude greater (data not shown). The detection and quantification of T<>T was achieved by optimizing mass spectrometric conditions operated in positive mode. T<>T was monitored for two fragment ions with *m/z* 253→210 and *m/z* 253→139 (figure 4.2), which are specific for the cyclobutane thymine dimer.

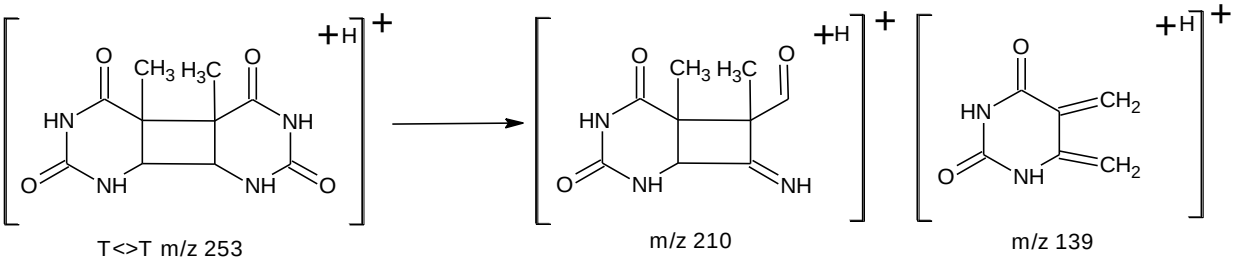

Figure 4.2: Structural representation of product ions of cyclobutane thymine dimer with *m/z* transition (a) 253→210 (b) 253→139

We used an internal standard in our experiments to account for the undesired effects of sample preparation, matrix effects and instrument error. Isotopically labeled internal standards would be a superior option; however, these are not commercially available for thymine dimer. 5-FU was selected as an internal standard because of its structural similarity with thymine, its elution within the same chromatographic time frame, and most importantly, 5-FU does not occur naturally. 5-FU was monitored with Q1/ Q3 transition of *m/z* 131→114.

4.4.2. Retention times

The standard (T<>T) and internal standard (5-FU) were efficiently separated from thymine using reversed phase HPLC. Under our chromatographic conditions, T<>T and 5-FU eluted at retention times of 6.83 min and 4.07 min respectively. The extracted ion chromatogram of spiked samples corresponding to internal standard (*m/z* 131→114) and standard (*m/z* 253→210 and *m/z* 253→139) are shown in Figure 4.3.

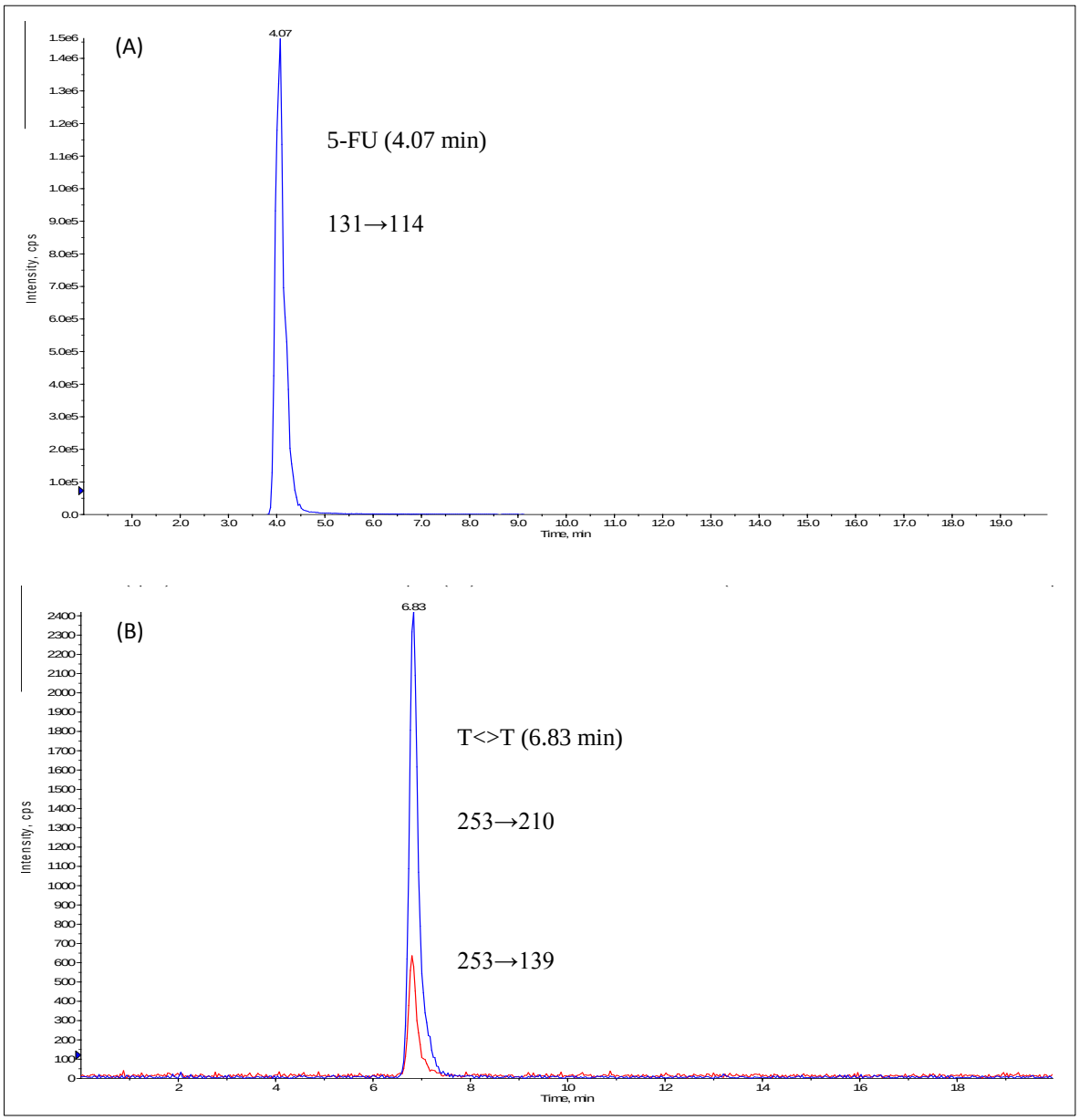

Figure 4.3: Extracted total ion chromatograms for spiked sample corresponding to (A) internal standard (5-FU) with *m/z* 131→114 and (B) standard (T<>T) with *m/z* 253→210 and 253→139.

4.4.3. *Linearity*

The calibration curve was quadratic over a range of 0.0195 µM – 0.60 µM at six concentrations (0.0195 µM, 0.0391 µM, 0.0781 µM, 0.156 µM, 0.313 µM, 0.6*0* µM). We

determined a limit of detection (LOD) of 0.0097 µM and a lower limit of quantification (LLOQ) of 0.0195 µM. The sum of two MRM transitions in replicates of three gave the equation $y = -0.109\ x^2 + 0.385\ x + -0.000273$ with a correlation coefficient of ≥ 0.998 (Figure 4.4). During development of the standard curve, LLOQ and the remaining standard curve samples were within ±15% deviation from the nominal concentrations (table 2).

Nominal and calibration curve concentrations of T<>T after extraction from spiked HaCat cells (n = 3)			
Nominal concentration (µM)	Calculated concentration (µM)	Precision	Accuracy
0.0195	0.020	1.2	100.6
0.039	0.039	3.4	99.2
0.078	0.076	1.3	97.1
0.156	0.158	5.1	101.1
0.313	0.326	0.6	104.3
0.600	0.586	5.3	97.6

Table 4.2: Accuracy and precision of calibration curve concentrations of T<>T after extraction from spiked HaCat cells (n = 3).

[Precision is expressed as % RSD = (SD/mean) ×100%].

[Accuracy = (Mean determined concentration/Nominal concentration) ×100%]

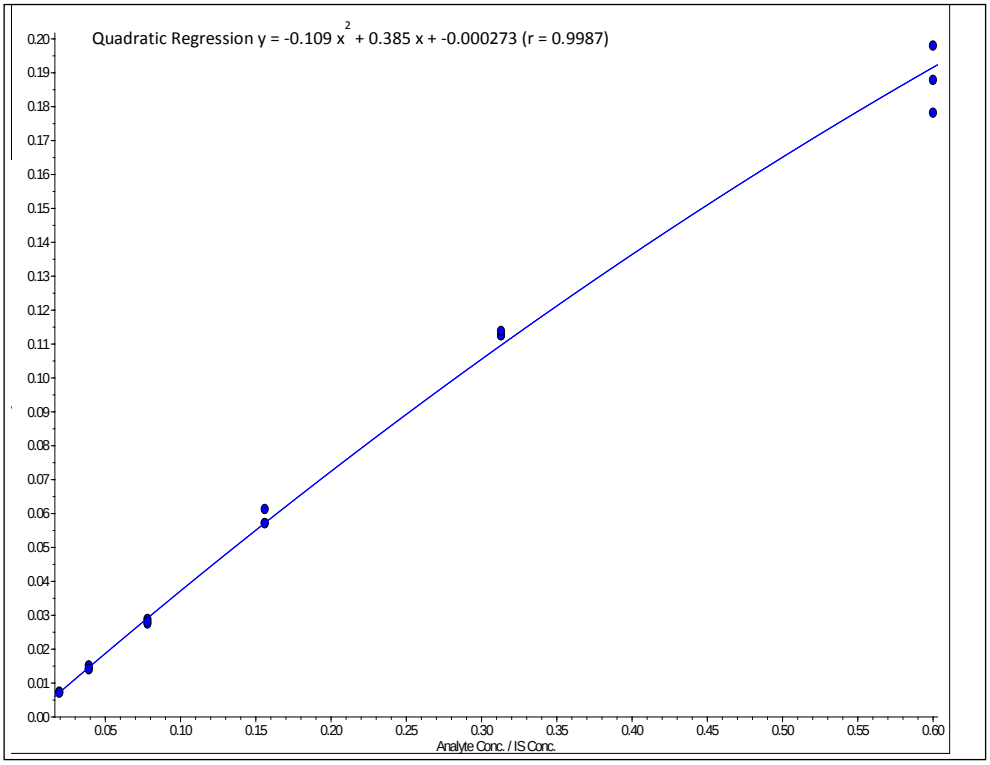

Figure 4.4: Calibration curves for spiked standard samples corresponding to sum of ions of both MRM transitions (*m/z* 253→210 and *m/z* 253→139) with n = 3.

4.4.4. *Selectivity and carryover*

We analyzed extracted blank HaCaT cell samples and found no interfering peaks in the blank and QCs. We observed no carry-over in the blank sample inserted after the highest calibration curve concentration.

4.4.5. Accuracy and precision

Table 3 and 4 represents intra-day and inter-day accuracy and precision for spiked QC samples at LLOQ, LQC, MQC and HQC in replicates (n = 6) on three separate days. Intra-day precision for each of LLOQ, LQC, MQC and HQC was lower than 11.4% of relative standard deviation. Intra-day accuracy for LQC, MQC and HQC were within ±15% of the nominal value (LLOQ within ±20%). Inter-day precision for each of LLOQ, LQC, MQC and HQC samples

were less than 7.7% of relative standard deviation and accuracy was from 91.8 to 113.5% of the nominal value.

Intra-day Assay Precision and Accuracy for extracted T<>T samples from spiked HaCat cells			
QC samples	N	Precision	Accuracy
LLOQ (0.0195µM)			
(Day 1)	6	7.2	116.4
(Day 2)	6	4.4	114.3
(Day 3)	6	6.0	112.3
LQC (0.050µM)			
(Day 1)	6	4.8	112.7
(Day 2)	6	3.8	94.7
(Day 3)	6	4.0	113.7
MQC (0.25µM)			
(Day 1)	6	7.1	89.5
(Day 2)	6	8.5	92.3
(Day 3)	6	11.4	96.3
HQC (0.50µM)			
(Day 1)	6	9.3	103.7
(Day 2)	6	2.4	97.0
(Day 3)	6	5.1	102.0

Table 4.3: Intra-day precision and accuracy for extracted QC samples from spiked HaCat cells.

[Precision is expressed as % RSD = (SD/mean) ×100%].

[Accuracy = (Mean determined concentration/Nominal concentration) ×100%]

Inter-day Assay Precision and Accuracy for extracted T<>T samples from spiked HaCat cells				
QC levels	Nominal Concentration	n	Precision	Accuracy
LLOQ	0.0195µM	18	1.7	113.5
LQC	0.05 µM	18	7.7	106.4
MQC	0.25 µM	18	3.4	91.8
HQC	0.5 µM	18	2.6	101.1

Table 4.4: Inter-day precision and accuracy for extracted QC samples from spiked HaCat cells. [Precision is expressed as % RSD = (SD/mean) ×100%].

[Accuracy = (Mean determined concentration/Nominal concentration) ×100%]

4.4.6. Recovery and matrix effect

Table 5 represent the % recoveries of T<>T and IS. The % recovery of T<>T from QC samples at LQC, MQC, HQC was 64.7%, 67.0% and 69.6% respectively. The % recovery of IS at LQC, MQC, HQC was 40.2%, 39.2% and 40.3% respectively, which was lower than expected. However, the recovery of T<>T after normalization to the IS was consistently within 1.6-1.7. Matrix effects for T<>T and IS were found to be within ±15% of the nominal value.

Recovery of extracted QC samples (n = 5)							
Sample type	$PA_{T<>T}$ in extracted sample ±SD	$PA_{T<>T}$ in non-extracted spiked sample ±SD	% Recovery of T<>T ± SD	PA_{IS} in extracted sample ±SD	PA_{IS} in non-extracted spiked sample ±SD	% Recovery of IS ±SD	IS normalized recovery of T<>T ±SD
LQC	3.7E+004 ±3.2E+003	5.7E+004 ±2.3E+003	64.7 ±8.0	5.6E+006 ±3.6E+005	1.4E+007 ±1.9E+006	40.2 ±5.5	1.6 ±0.1
MQC	2.2E+005 ±4.4E+003	3.3E+005 ±1.3E+004	67.0 ±2.0	5.5E+006 ±3.3E+005	1.4E+007 ±1.8E+006	39.2 ±5.0	1.7 ±0.2
HQC	4.8E+005 ±4.0E+004	6.9E+005 ±2.3E+004	69.6 ±5.9	5.5E+006 ±2.1E+005	1.4E+007 ±1.9E+006	40.3 ±5.6	1.7 ±0.1

Table 4.5: % Recovery for extracted QC samples from spiked HaCat cells compared to unextracted samples.

PA = mean peak area

% Recovery of T<>T = [(PA of T<>T in extracted sample/ PA of T<>T in non-extracted spiked sample) ×100]

% Recovery of IS = [(PA of IS in extracted sample/ PA of IS in non-extracted spiked sample) ×100]

IS normalized recovery = [recovery of T<>T/ recovery of IS]

4.4.7. Stability studies

The bench top stability of QC samples at LQC, MQC and HQC were found to be acceptable with the accuracy of 90.7%, 88.3% and 93.4% of the nominal value respectively. The mean accuracy of the autosampler stability of QC samples at LQC, MQC and HQC was 73.6 % of the nominal value. The mean accuracy of the freeze thaw and long term (stored at - 80ºC) stability for T<>T was 60.7% and 79 % respectively of the nominal value (Table 6).

Bench top stability (6h) study of extracted QC samples (n = 6)				
Sample type	Nominal Concentration	Precision	Accuracy	Average Accuracy ± SD
LQC	0.05 µM	4.2	90.7	90.8 ± 2.5
MQC	0.25 µM	4.6	88.3	
HQC	0.5 µM	6.3	93.4	
Autosampler stability (24h) study of extracted QC samples (n = 3)				
Sample type	Nominal Concentration	Precision	Accuracy	Average Accuracy ± SD
LQC	0.05 µM	5.5	72.3	73.6 ± 4.3
MQC	0.25 µM	2.3	70.0	
HQC	0.5 µM	2.9	78.3	
Freeze thaw stability of QC samples after three (24h) freeze thaw cycles (n= 3)				
Sample type	Nominal Concentration	Precision	Accuracy	Average Accuracy ± SD
LQC (low)	0.05 µM	9.8	56.6	60.7 ± 5.8
HQC (high)	0.5 µM	2.9	64.9	

Long term storage (at -80ºC) of extracted QC samples (n = 3)				
Sample type	Nominal Concentration	Precision	Accuracy	Average Accuracy ± SD
LQC (low)	0.05 µM	0.1	83.7	79 ± 6.7
HQC (high)	0.5 µM	2.0	74.3	

Table 4.6: Bench top, autosampler, freeze thaw and long term stability study results for extracted QC samples.

[Precision is expressed as % RSD = (SD/mean) ×100%].

[Accuracy = (Mean determined concentration/Nominal concentration) ×100%]

4.4.8. Ability of galangin to attenuate UVB radiation-induced T<>T formation in HaCaT cells

We recently published a report outlining a study on the stability of several flavonols in cell culture media. We concluded that flavonols bearing fewer hydroxyl groups on the B-ring (galangin, kaempferol) were more stable in DMEM than flavonols with extensive B-ring substitution (quercetin, myricetin) [26]. Several studies have reported photoprotective properties for myricetin [31, 32], quercetin [25, 33, 34] and kaempferol [35], however there are no reports on the photprotective properties of galangin. To test the application of this method and to determine whether galangin should be pursued further as a topical skin photoprotectant, we treated UVB-exposed HaCaT cells with a single concentration of galangin. Our results, shown in figure 4.5, demonstrate that HaCaT cells treated with galangin (100 µM) there is a 34.4% decrease in UVB radiation-induced T<>T formation compared to the untreated HaCaT cells. Thus, our method was able to detect and quantify T<>T in a cell culture system and show that galangin can protect HaCaT cells against UVB radiation-induced T<>T formation. This has provided us with a robust analytical method to study T<>T formation in biological systems and also has provided us with pilot data to further pursue the study of galangin as a photoprotectant.

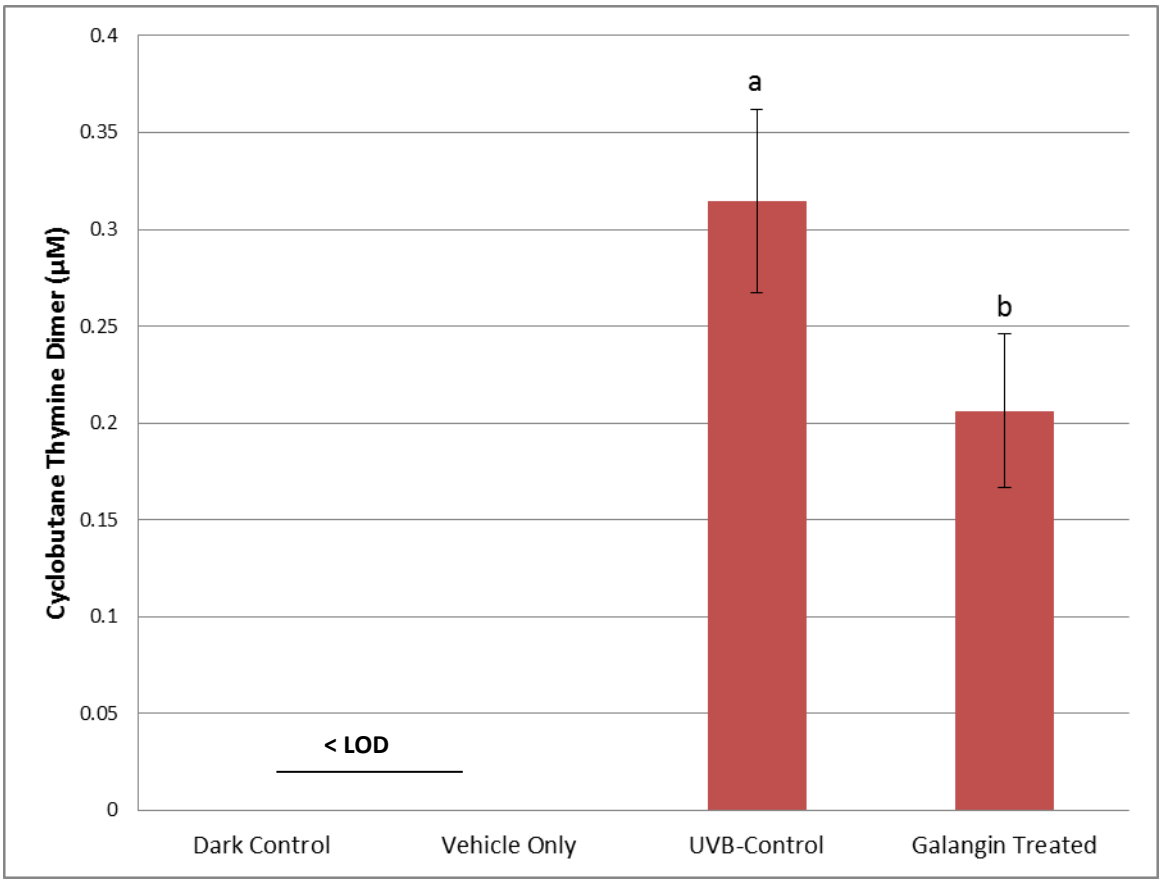

Figure 4.5: The graph represents the decrease in the mean levels of UVB radiation (0.05J/cm^2) induced T<>T formation (±SD) in galangin treated HaCaT cells (100 µM) compared to the UVB control. These results are the mean of three independently performed experiments, and statistically significant differences ($p < 0.05$) between groups are indicated by labels containing different letters.

4.5. Conclusion

We have developed an HPLC-APCI-MS/MS method which is an efficient analytical technique for quantification of UV-radiation induced DNA lesions involving two thymine residues. This method is an easy and robust *in vitro* analytical method which we developed and validated as per FDA guidelines. The major advantages of our method over previous techniques are improved selectivity and relatively simple and swift sample preparation. The application of this assay allows accurately to measure the amount of T<>T produced *in vitro* after exposure to UV radiation.

Acknowledgements

E.S.K. is supported by the Natural Sciences and Engineering Research Council (NSERC) and the College of Pharmacy & Nutrition, B.M.F. is a recipient of an Rx&D award and S.M. is a recipient of a University of Saskatchewan GTA. We wish to give our special thanks to Dr. Jane Alcorn and Ravi Singh for guidance on method validation, Deb Michel and Joshua Buse for technical assistance and Dr. John Headley and Kerry Peru at Environment Canada for help with the initial APCI studies.

4.6. References

[1] D.E. Godar, UV doses worldwide, Photochem. Photobiol. 81 (2005) 736-749.

[2] D. Kulms, T. Schwarz, 20 years after - Milestones in molecular photobiology, J.Invest. Dermatol. Symposium Proceedings. 7 (2002) 46-50.

[3] W.P. Coleman III, Skin Cancer: Recognition and Management, 2nd Edition by Robert A. Schwartz, Dermatologic Surgery. 34 (2008) 1702-1702.

[4] American Cancer Society, American Cancer Society, http://www.cancer.org/Cancer/CancerCauses/SunandUVExposure/skin-cancer-facts. 2012 (2012).

[5] A.A. Lamola, Specific formation of thymine dimers in DNA., Photochem. Photobiol. 9 (1969) 291-294.

[6] J. Cadet, E. Sage, T. Douki, Ultraviolet radiation-mediated damage to cellular DNA, Mutat. Res. - Fundamental and Molecular Mechanisms of Mutagenesis. 571 (2005) 3-17.

[7] R.B. Setlow, E. Grist, K. Thompson, A.D. Woodhead, Wavelengths effective in induction of malignant melanoma, Proc. Natl. Acad. Sci. U. S. A. 90 (1993) 6666-6670.

[8] S. Mouret, C. Philippe, J. Gracia-Chantegrel, A. Banyasz, S. Karpati, D. Markovitsi, T. Douki, UVA-induced cyclobutane pyrimidine dimers in DNA: A direct photochemical mechanism?, Org. Biomol. Chem. 8 (2010) 1706-1711.

[9] F.R. de Gruijl, Photocarcinogenesis: UVA vs. UVB radiation, Skin Pharmacol. Appl. Skin Physiol. 15 (2002) 316-320.

[10] B.E. Johnson, Formation of thymine containing dimers in skin exposed to ultraviolet radiation, Bull. Cancer. 65 (1978) 283-297.

[11] J. Cadet, P. Vigny, The photochemistry of nucleic acids: In Bioorganic Photochemistry, Photochemistry and the Nucleic Acids (Edited by H.Morrison). 1 (1990) 1-272.

[12] T. Douki, J. Cadet, Individual determination of the yield of the main UV-induced dimeric pyrimidine photoproducts in DNA suggests a high mutagenicity of CC photolesions, Biochemistry (N. Y.). 40 (2001) 2495-2501.

[13] F.R. de Gruijl, Photocarcinogenesis: UVA vs UVB, Singlet Oxygen, Uv-A, and Ozone. 319 (2000) 359-366.

[14] E.A. Drobetsky, J. Turcotte, A. Châteauneuf, A role for ultraviolet A in solar mutagenesis, Proc. Natl. Acad. Sci. U. S. A. 92 (1995) 2350-2354.

[15] S.Q. Wang, R. Setlow, M. Berwick, D. Polsky, A.A. Marghoob, A.W. Kopf, R.S. Bart, Ultraviolet A and melanoma: A review, J. Am. Acad. Dermatol. 44 (2001) 837-846.

[16] S. Mouret, C. Baudouin, M. Charveron, A. Favier, J. Cadet, T. Douki, Cyclobutane pyrimidine dimers are predominant DNA lesions in whole human skin exposed to UVA radiation, Proc. Natl. Acad. Sci. U. S. A. 103 (2006) 13765-13770.

[17] J.-. Ravanat, T. Douki, J. Cadet, Direct and indirect effects of UV radiation on DNA and its components, J. Photochem. Photobiol. B: Biol. 63 (2001) 88-102.

[18] T.M. Rünger, C→T transition mutations are not solely UVB-signature mutations, because they are also generated by UVA, J. Invest. Dermatol. 128 (2008) 2138-2140.

[19] L. Roza, K.J. van der Wulp, S.J. MacFarlane, P.H. Lohman, R.A. Baan, Detection of cyclobutane thymine dimers in DNA of human cells with monoclonal antibodies raised against a thymine dimer-containing tetranucleotide., Photochem. Photobiol. 48 (1988) 627-633.

[20] H. Klocker, B. Auer, H. Burtscher, A sensitive radioimmunoassay for thymine dimers, Mol. Gen. Genet. 186 (1982) 475-477.

[21] J.K. Robinson, W.G. Scott, K.L. Rowlen, J.W. Birks, Derivatization of thymine and thymine photodimers with 4-bromomethyl-7-methoxycoumarin for fluorescence detection in high-performance liquid chromatography, J. Chromatogr. B: Biomed. Sci. Appl. 731 (1999) 179-186.

[22] M. McVean, D.C. Liebler, Inhibition of UVB induced DNA photodamage in mouse epidermis by topically applied α-tocopherol, Carcinogenesis. 18 (1997) 1617-1622.

[23] T. Douki, M. Court, J. Cadet, Electrospray-mass spectrometry characterization and measurement of far-UV-induced thymine photoproducts, J. Photochem. Photobiol. B: Biol. 54 (2000) 145-154.

[24] A. St-Jacques, J. Anichina, B.B. Schneider, T.R. Covey, D.K. Bohme, UV-induced bond modifications in thymine and thymine dideoxynucleotide: Structural elucidation of isomers by differential mobility mass spectrometry, Anal. Chem. 82 (2010) 6163-6167.

[25] B.M. Fahlman, E.S. Krol, Inhibition of UVA and UVB radiation-induced lipid oxidation by quercetin, J. Agric. Food Chem. 57 (2009) 5301-5305.

[26] S. Maini, H.L. Hodgson, E.S. Krol, The UVA and Aqueous Stability of Flavonoids Is Dependent on B-Ring Substitution, J Agric Food Chem; dx.doi.org/10.1021/jf3016128 (2012).

[27] B.M. Fahlman, E.S. Krol, UVA and UVB radiation-induced oxidation products of quercetin, J. Photochem. Photobiol. B: Biol. 97 (2009) 123-131.

[28] J.B. Harborne, C.A. Williams, Advances in flavonoid research since 1992, Phytochem. 55 (2000) 481-504.

[29] A. Solovchenko, M. Schmitz-Eiberger, Significance of skin flavonoids for UV-B-protection in apple fruits, J. Exp. Bot. 54 (2003) 1977-1984.

[30] U.S. Department of Health and Human Services Food and Drug Administration Center for Drug Evaluation and Research (CDER) Center for Veterinary Medicine (CVM), Guidance for Industry Bioanalytical Method Validation (May 2001).

[31] S.K. Jung, K.W. Lee, S. Byun, E.J. Lee, J.-. Kim, A.M. Bode, Z. Dong, H.J. Lee, Myricetin inhibits UVB-induced angiogenesis by regulating PI-3 kinase in vivo, Carcinogenesis. 31 (2009) 911-917.

[32] S.K. Jung, K.W. Lee, S. Byun, N.J. Kang, S.H. Lim, Y. Heo, A.M. Bode, G.T. Bowden, H.J. Lee, Z. Dong, Myricetin suppresses UVB-induced skin cancer by targeting Fyn, Cancer Res. 68 (2008) 6021-6029.

[33] F.T.M.C. Vicentini, T. He, Y. Shao, M.J.V. Fonseca, W.A. Verri, G.J. Fisher, Y. Xu, Quercetin inhibits UV irradiation-induced inflammatory cytokine production in primary human keratinocytes by suppressing NF-κB pathway, J. Dermatol. Sci. 61 (2011) 162-168.

[34] Y.-. Yang, Y.-. Son, S.-. Lee, Y.-. Jeon, J.-. Lee, Quercetin inhibits α-MSH-stimulated melanogenesis in B16F10 melanoma cells, Phytother. Res. 25 (2011) 1166-1173.

[35] K.M. Lee, K.W. Lee, S.K. Jung, E.J. Lee, Y.-. Heo, A.M. Bode, R.A. Lubet, H.J. Lee, Z. Dong, Kaempferol inhibits UVB-induced COX-2 expression by suppressing Src kinase activity, Biochem. Pharmacol. 80 (2010) 2042-2049.

5. Objective 2

To apply the analytical method to determine the topical sunscreen properties of flavonols in UVA/B exposed artificial skin mimics (EpiDerm™)

Topical Application of Quercetin Decreases UV Radiation-Induced Formation of MMP-1, TNF-α and Dimeric Thymine Photoproduct in Reconstructed Human Skin Model.

Authors: Sabia Maini, Brian M. Fahlman†, and Ed S. Krol*

Prepared for submission to Journal of Photochemistry and Photobiology B: Biology

Lab based experiments were performed by Brian Fahlman and Sabia Maini with supervisory consultation with Ed Krol.

NOTE:

In this paper the role of Sabia Maini includes- Topically application of flavonols on the surface of EpiDerm™ samples, to determine the decrease in the formation of dimeric pyrimidine photoproduct T<>T.

In this paper the role of Brian Fahlman includes- Topically application of quercetin on the surface of EpiDerm™ samples, to determine the decrease in UV-radiation induced formation of MMP-1 and TNF-α.

This paper was written equally by all the authors.

5.1. Abstract

Exposure of skin to ultraviolet light has been shown to have a number of deleterious effects including photoaging, photoimmunosuppression and photoinduced DNA damage which can lead to the development of skin cancer. In this paper we present a study on the ability of flavonols to prevent UV radiation-induced damage. Pilot studies with the flavonol quercetin were shown to decrease two secondary biomarkers of UV radiation-induced damage, in EpiDerm™, a commercially available artificial skin mimic. InEpiDerm™ samples treated topically with quercetin immediately prior to UVA or UVB exposure, a concentration of 2nmol/cm^2 quercetin significantly decreased UVA induced matrix metalloprotease (MMP-1) secretion, but 4nmol/cm^2 of quercetin was required to significantly reduce UVB induced MMP-1 secretion. Tumor necrosis factor-α (TNF-α) secretion in EpiDerm™ samples was significantly reduced at 2nmol/cm^2 quercetin for both UVA and UVB radiation. We followed this study by determining the ability of three flavonols (quercetin, kaempferol and galangin) to prevent a direct biomarker of UV damage, cyclobutane thymine dimer (T<>T) formation. Topical application of the three flavonols at a concentration of 4nmol/cm^2 on the surface of EpiDerm™ samples significantly decreased the formation of T<>T, suggesting that flavonols may protect against direct UVB-induced DNA damage in skin.

Keywords

Quercetin; sunscreen; EpiDerm; MMP-1; TNF-α; T<>T

5.2. Introduction

Ultraviolet radiation (UVR), defined as electromagnetic radiation in the range of 100nm to 400nm, accounts for 10% of the solar radiation that reaches the earth [1]. Of this radiation, the ultraviolet C (UVC) portion (<280nm) and 90% to 99% of the ultraviolet B (UVB) (280nm-315nm) is filtered by atmospheric ozone, leaving ultraviolet A (UVA) (315nm-400nm) as the major component of ultraviolet radiation to reach the earth's surface [1].

The ultraviolet radiation that reaches the earth's surface has a number of effects on mammalian systems. Positive effects of UVR include regulation of circadian rhythm and of the conversion of 7-dehydrocholesterol to pre-vitamin D_3, a precursor of vitamin D, which has a wide range of beneficial effects as reviewed by Goltzman [2] and Dixon et. al. [3]. Exposure to ultraviolet radiation also has a number of negative biological effects including lipid peroxidation leading to cell dysfunction or necrosis [4,5] destruction of skin collagen leading to photoaging [6], immunosuppression [7], and DNA damage leading to skin cancer, through either oxidative [8] or direct photochemical processes [9,10].

UVR induced photoaging is primarily associated with the UVA (315nm-400nm) wavelengths and is characterized by increased wrinkle formation relative to unexposed skin, a loss of skin recoil capacity and an increase in skin fragility [11-13]. Most prominently UVA, and to a lesser extent UVB (280nm-315nm) radiation, cause photoaging through induction of matrix metalloprotease-1 (MMP-1) which is responsible for the breakdown of collagen [11,15-19]. It is well known that both UVA and UVB radiation can induce the formation of reactive oxygen species (ROS) in the skin [4,20] and there is good evidence that it is these ROS that initiate the photoaging process. The level of H_2O_2, an inducer of MMP-1 [21], has been found to be elevated in photoaged skin relative to naturally aged skin, perhaps accounting for the differences in MMP activities [15].

Exposure to ultraviolet radiation, particularly UVB, has also been associated with immunosuppression, both local and systemic [6,7]. This immunosuppression is believed to reduce the risk of harmful, excessive inflammation in the skin following UVR exposure [6] and

has been found to result from both acute [7] and chronic [25] exposure to UVR. UVB induced immunosuppression occurs via down regulation of T-cell mediated immunity through the induction of immunomodulating cytokines [6,26]. UVB radiation has been shown to induce TNF-α [28], IL-10 [27,28], IL-4[28] and IL-6 [29].

The initial skin chromophore involved in immunosuppression has been shown to be DNA, and UVR absorption by DNA resulting in the formation of thymine dimers is also the initiating step in photocarcinogenesis [9,30]. UVB radiation is directly absorbed by pyrimidines, especially thymine, resulting in the formation of pyrimidine dimers [31,32]. These dimers can be formed between two adjacent thymines (T-T), two adjacent cytosines (C-C) or between adjacent thymine-cytosine pairs (T-C). The pyrimidine dimers can take a number of forms but are most commonly found as cyclobutane pyrimidine dimers (CPD's) which are formed by [2+2] cycloaddition between the C5-C6 double bonds of adjacent pyrimidines [31,33]. Other dimers observed include 6-4 dimers (6-4) and their Dewer isomers. The relative frequency of occurrence of these dimers in sun exposed skin is: T-T(CPD) > T-C(6-4) > T-C(CPD) > T-T(6-4) [31].

Due to the negative effects associated with overexposure to solar UVR, a large number of topically applied sunscreens are available on the market and the development of new sunscreens is an active area of research. One family of phytochemicals which are believed to have photoprotective properties in plants are the flavonols (Figure 1). The flavonols have absorption bands in both the UVA and UVB range [42] and several flavonols and their glycosides, such as quercetin and kaempferol, have been shown to be upregulated in response to UVR exposure in a number of plant species [43], [44] [45]. The majority of studies have focussed on quercetin, due in part to its relative abundance and low cost. Use of quercetin as a photoprotectant has proven effective in both human fibroblasts, which showed a decrease in photoinduced MMP-1 production following quercetin treatment [46], and in mice where dietary intake of quercetin by mice has been shown to decrease UVR induced immunosuppression [47,48]. Previously we have reported on the favorable antioxidant [49] properties of quercetin as a potential protective mechanism against UVR damage, but quercetin may also provide protection from UVR induced damage as a result of direct UV absorbance. One concern that has however arisen is the stability

of quercetin [36, 53]. Several studies have determined that quercetin is unstable in cell media and decomposes under typical cell culture conditions [53,55,56]. Addition of ascorbic acid can stabilize quercetin but causes a loss in apoptotic activity [53]. Our own studies on the stability of quercetin to UVR and DMEM indicate that increased B-ring hydroxylation of the flavonols leads to a decrease in stability, suggesting that other flavonols such as kaempferol and galangin may be preferable [50,56]. However there are very few studies on the photoprotective properties of kaempferol and galangin.

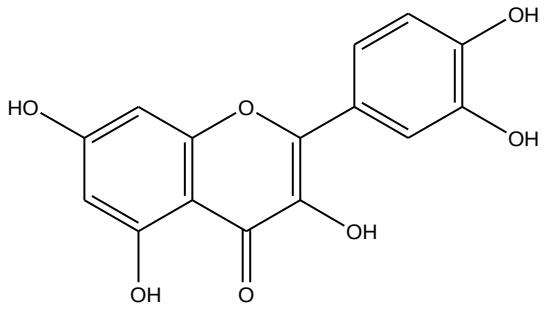

Figure 5.1: Structure of quercetin (3, 3', 4', 5, 7-pentahydroxyflavone)

We hypothesize that flavonols can reduce UVR induced oxidative damage, including photoaging, and direct DNA damage in skin *in vitro*. To study this hypothesis we determined the ability of three flavonols, quercetin, kaempferol and galangin, to prevent UVR induced damage in a reconstructed human skin model (EpiDerm™). As a pre-assessment of flavonol photoprotective ability, we first measured the ability of quercetin to protect EpiDerm™ against two secondary biomarkers, MMP-1 (photoaging), and TNF-α (immunosuppression and a secondary marker for UVR induced DNA damage, specifically CPD formation). The results from this pre-assessment led us to examine the ability of quercetin, kampferol and galangin to protect EpiDerm™ from UVR induced T<>T formation.

Recently we developed and validated an analytical method to quantify cyclobutane thymine dimer (T<>T), a biomarker of UVR induced DNA damage. The calibration curve was quadratic over a range of 0.0195 µM – 0.60 µM, with a limit of detection (LOD) of 0.0097 µM and a lower limit of quantification (LLOQ) of 0.0195 µM. In this present work, we report the application of this analytical method to determine the topical sunblock properties of a range of flavonols (quercetin, galangin and kaempferol) in preventing UVR induced DNA damage in the reconstructed human skin model.

5.3. Materials and methods

5.3.1. General

Quercetin dihydrate ($C_{15}H_{10}O_7.2H_2O$, M_W= 338.26), kaempferol ($C_{15}H_{10}O_6$, M_W= 286.23), galangin ($C_{15}H_{10}O5$, M_W= 270.24) were purchased from Sigma (St. Louis, MO). LC/MS grade water and methanol was purchased from Fisher Scientific Canada (Ottawa, ON). Thymine ($C_5H_6N_2O_2$, minimum 99%), 5-fluorouracil ($C_4H_3FN_2O_2$, ≥99%) and formic acid were purchased from Sigma-Aldrich Canada Ltd (Oakville, ON).

2 FS20T12/UVB lamps (National Biological Corp., Beachwood, OH) filtered to remove UVC with an intensity of 1300 $\mu W \bullet cm^{-2}$ at 310 nm as measured with a UVP UVX-31 sensor. 2 F20T12/BL/HO UVA lamps (National Biological Corp., Beachwood, OH) filtered to remove UVC with an intensity of 740 $\mu W \bullet cm^{-2}$ at 365 nm as measured with a UVP UVX-36 sensor were used for irradiation. The output of the lamps was filtered to remove UVC radiation.

Standard T<>T was prepared in water using the method of Ramsey and Ho (42). UVC irradiations were carried out using a Rayonet Preparative Photochemical Reactor (The So. New England Ultraviolet Co., Middletown, CT) fitted with UVC bulbs.

Quantikine® Human pro-MMP-1 ELISA kits and Quantikine® Human TNF-α/TNFSF1A ELISA kits were purchased from Cedarlane Laboratories Ltd., Burlington, ON and read using a Synergy™ HT Multi-Detection Microplate Reader (BioTek Instruments Inc., Winooski, VT). DNeasy Blood & Tissue Kits were purchased from Qiagen (Toronto, ON).

5.3.2. EpiDerm™ Skin Mimics

EpiDerm™ skin mimics (EPI-200 and EPI-606) and media were purchased from MatTek Corporation (Ashland, MA). EPI-200 and EPI-606 tissues differ in their surface area, EPI-200 tissues had a diameter of 9mm and EPI-606 tissues were of 22mm. Upon receipt of the EpiDerm shipment, the tissues were handled as per the protocol provided by MatTek Corporation. Briefly, individual tissues from EPI-200 were placed in each well of a 6-well culture plate along with 1mL of maintenance media. Similarly, EPI-606 tissues on the day of shipment were placed in

100mm petri dishes containing 6.3ml of maintenance media. The tissues were incubated at 37°C with 5% CO_2 overnight to recover from the stress of the shipment.

5.3.3. Flavonol Treatment

5.3.3.1. EPI-200

EPI-200 tissues were treated topically with quercetin in acetone immediately prior to UVR exposure. The amount of quercetin used was 50µL and 100µL of 26µM quercetin in acetone to achieve the amount equivalent to 2nmol/cm^2 and 4nmol/cm^2. Both doses were done in duplicate for three different days. Following application of the quercetin in acetone, EpiDerm samples were left for 10min to allow acetone to evaporate leaving a thin layer of quercetin on the skin prior to UVR exposure.

5.3.3.2. EPI-606

EPI-606 tissues were treated topically with range of flavonols including galangin, kaempferol and quercetin in acetone immediately prior to UVR exposure. The amount of flavonol delivered on to the skin was 4nmol/cm^2. To achieve the set dose, the tissues were treated with 600µL of 26µM flavonol in acetone. Experiment with three different flavonols was performed in duplicate for three different days. Following application of the flavonol in acetone, EpiDerm™ samples were left for 10min to allow acetone to evaporate leaving a thin layer of flavonol on the skin prior to UVR exposure.

5.3.4. UVR Exposure

5.3.4.1. EPI-200 (MMP-1 and TNF-α assay)

EPI-200 samples were placed under lamps without covers. UVB irradiations at the dose of 0.9 J/cm^2 were performed using two FS20T12/UVB lamps and UVA irradiations at the dose of 10 J/cm^2 were performed using two F20T12/BL/HO UVA lamps. For the dark samples, plates were wrapped in aluminum foil and placed under UV lamps for the similar exposure. Following UVR exposure, EPI-200 samples were also placed in the incubator at 37°C with 5%

CO_2. Tissues were removed from the incubator 24 hours after exposure and media collected and placed in a -80°C freezer for later analysis.

5.3.4.2. EPI-606 (T<>T assay)

After the flavonol treatment, once the acetone vehicle had evaporated from the surface, EPI-606 tissues were placed under UV-lamps without covers. UVB irradiations at the dose of 0.05 J/cm^2 were performed using two FS20T12/UVB lamps and UVA irradiations at the dose of 8.5 J/cm^2 were performed using two F20T12/BL/HO UVA lamps. UV-control samples were also irradiated in the similar way. For the dark samples, plates were wrapped in aluminum foil and placed under UV lamps for the similar exposure. Following the irradiation, the tissues were washed with PBS, and were carefully removed from the tissue culture inserts and placed in a -80°C freezer for later analysis.

5.3.5. ELISA Analysis

5.3.5.1. pro-MMP-1

Extracellular pro-MMP-1 produced in response to UVR in the presence or absence of quercetin was measured using a Quantikine® Human pro-MMP-1 ELISA kit (R&D Systems, Minneapolis, MN) following the manufacturer's directions. Briefly, 100µL of culture media and 100µL of diluent solution were added to each well of a 96-well plate and shaken at room temperature for 2 hours. The samples were aspirated, the plate was washed four times with PBS and 200µL of conjugate was added to each well and the plate shaken at room temperature for 2 hours. Conjugate solution was aspirated, the plate was washed four times and 200µL substrate solution was added to each well followed by a 20 min incubation protected from light. 50µL of stop solution was then added to each well and the absorbance at 450nm and 570nm was recorded using a BioTek Instruments (Winooski, VT) plate reader. An eight point calibration curve was prepared using standards provided by the supplier and the pro-MMP-1 concentration of each well was determined by interpolation. Results are reported as mean ± standard deviation.

5.3.5.2. TNF-α

Extracellular TNF-α produced in response to UVR in the presence or absence of quercetin was measured using a Quantikine® Human TNF-α/TNFSF1A ELISA kit (R&D Systems, Minneapolis, MN) following the manufacturer's directions. Briefly, 50µL of culture media and 200µL of diluent solution were added to each well of a 96-well plate and incubated at room temperature for 2 hours. The samples were aspirated, the plate was washed four times and 200µL of conjugate was added to each well and the plate incubated at room temperature for 1 hour. Conjugate solution was aspirated, the plate was washed four times and 200µL substrate solution was added to each well followed by a 20 min incubation protected from light. 50µL of stop solution was then added to each well and the absorbance at 450nm and 570nm was recorded using a BioTek Instruments (Winooski, VT) plate reader. An eight point calibration curve was prepared using standard provided by the supplier and the TNF-α concentration of each well was determined by interpolation. Results are reported as mean ± standard deviation.

5.3.6. HPLC-APCI-MS/MS Analysis

A sensitive and selective HPLC-APCI-MS/MS method was used to quantify T<>T, a biomarker of UVR induced damage in skin. Bioanalytical method validation for the assay of cyclobutane thymine dimer in human skin was performed according to USFDA guidelines for accuracy, precision, selectivity, sensitivity, reproducibility, and stability.

Instrumentation:

Analysis was carried out at room temperature on an Agilent 1100 system coupled to quadrupole linear ion trap AB SCIEX 4000 QTRAP (AB SCIEX instruments) mass spectrometer. The HPLC system consisted of a pump (Agilent 1100 G1311A) and an autosampler (Agilent 1100 G1329A) (Agilent Technologies, Mississauga, ON). The mass spectrometer was used in multiple reaction monitoring (MRM) mode, equipped with a heated nebulizer (Atmospheric pressure chemical ionization (APCI)) interface used in positive ion mode.

5.3.6.1. LC-MS/MS parameters

T<>T and internal standard (IS) were eluted under isocratic flow of 99% Water/ 1% methanol with 0.1% formic acid at a flow rate of 200µL/min with a run time of 20 min. Aliquots of 80 µL of processed samples were injected onto an ODS-2 3µ column (2.1 mm × 100 mm). Quantitative analysis of the processed samples was performed using sum of two MRM transitions for the standard (cyclobutane thymine dimer) from *m/z* 253 → 210 and *m/z* 253 → 139. For the IS (5-fluorouracil) the Q1/Q3 transition was monitored from *m/z* 131 → 114. The optimized mass spectrometer parameters were used for analysis. Analyst 1.5.1 software from AB SCIEX was used for controlling the equipment and acquiring and processing of data.

5.3.6.2. Preparation of calibration curve samples

The standard curve and quality control samples were prepared on the day of analysis. DNeasy blood and tissue kit was used to extract DNA from unexposed EpiDerm™. Or DNA extraction, the tissues were incubated at 56^0C in the presence of buffer ATL and proteinase K for 4 hours. Following tissue lysis, the remaining steps were performed as per the protocol of DNeasy kit. In the final step DNA was eluted from the spin columns by twice washing with 200µl of water. For each tissue sample, three DNA extraction columns were used.

After DNA isolation, the elution from three columns was combined and spiked with 20µL of working stock solution of standard/quality control and internal standard. Each sample was subjected to hydrolysis with 88% formic acid at 125ºC for 20min (39). The hydrolysate of all the standard, quality control and blank samples were evaporated and re-suspended in 100 µL of water. The samples were vortex-mixed for 30 sec and injected into the HPLC-MS/MS system with the injection volume of 80 µL.

5.3.6.3. Preparation of treated, control and dark samples

Similarly, DNA was extracted from each of the treated, UVB control, and dark control tissue samples by using DNeasy kit. The extracted DNA was spiked with internal standard (5-FU), followed by hydrolysis with 88% formic acid at 125ºC for 20 min. The hydrolysate of all the treated, control and dark samples were evaporated and resuspended in 100 µL of water. The

samples were vortex-mixed for 30 sec and injected into the HPLC-MS/MS system with the injection volume of 80 μL.

5.3.7. Statistics

Statistical analyses were performed using GraphPad Prism 5.0 (GrpahPad Software Inc., La Jolla, CA). MMP and TNF-a data was analyzed by one-way ANOVA with a Bonferroni's Multiple Comparison Test. Significant difference in amount of T<>T formation in UVB exposed control and flavonol treated samples were assessed with one-way analysis of variance with Tukey's test for pairwise multiple comparisons using SPSS software (IBM SPSS statistics version 19, Markham, ON, Canada). The level of significance was set at $P < 0.05$.

5.4. Results

5.4.1. Effect of Quercetin on UVR-mediated MMP-1 excretion

The effectiveness of quercetin as a photoprotectant was assessed using the reconstructed human skin model. The methodology involved topical application of quercetin to the stratum corneum of the EpiDerm™ immediately prior to UVR exposure. The topical application relies primarily on photoabsorptive processes and intercellular and cellular membrane antioxidant activity to provide photoprotection.

The effect of topical quercetin treatment of EpiDerm^{TM} on MMP-1 excretion is presented in Figure 5.2. Both UVA and UVB exposed samples treated with either 2nmol/cm^2 or 4nmol/cm^2 of quercetin resulted in a significant decrease in MMP-1 production compared to control. Notably, for both UVA and UVB exposed EpiDerm^{TM} treated with 4nmol/cm^2 quercetin, extracellular production of MMP-1 decreased to the level seen in non-UVR exposed skin mimics (dark control).

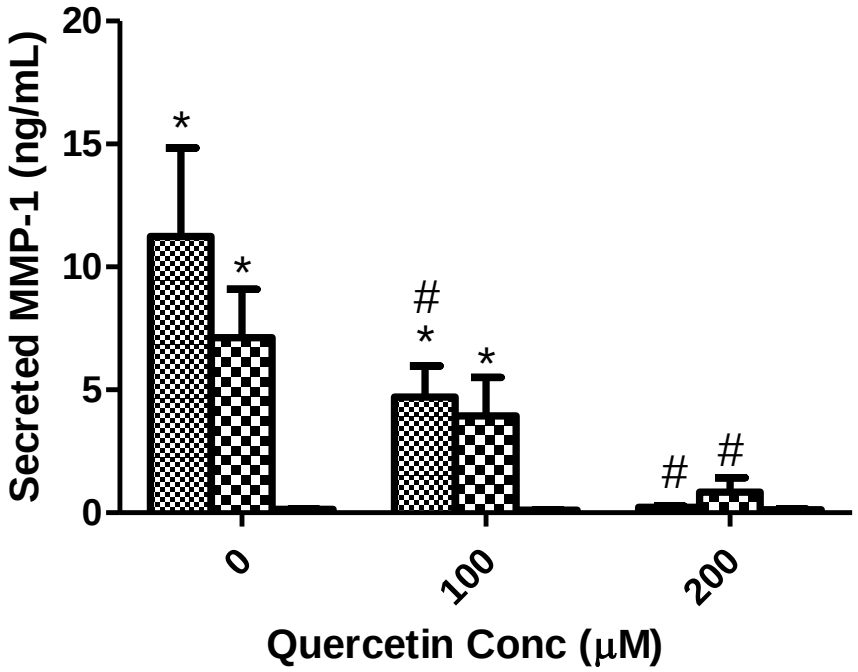

Figure 5.2: Prevention of MMP-1 production by quercetin in EpiDerm™ skin mimics exposed to either 10 J/cm^2 UVA or 0.9 J/cm^2 UVB (in open culture dishes, UVC removed by filtration) or no UVR (dark). MMP-1 was measured by ELISA. EpiDerm™ was treated with quercetin in acetone, which was allowed to evaporate immediately prior to UVR exposure leaving a thin film of quercetin. Following treatment skin mimics were returned to the incubator. Media was collected for MMP-1 analysis 24 hours later and stored at -80ºC until analysis. = UVA, = UVB Treatment, = Dark Control. * = significantly different from dark control ($p<0.05$), # = significantly different from control ($p<0.05$).

5.4.2. Effect of Quercetin on UVR-mediated production of TNF-α

Figure 5.3 shows the effects of topical treatment of EpiDerm™ with quercetin on the production of TNF-α. For UVR treated EpiDerm™, TNF-α production shows a pattern similar to that seen for MMP-1, with significant decreases in both UVA and UVB-induced TNF-α production at 2nmol/cm^2 and a complete loss of TNF-α production to dark control levels in those skin mimics treated with 4nmol/cm^2 of quercetin. For the UVA exposed samples, reduction to dark control levels of TNF-α was seen at 2nmol/cm^2 of quercetin treatment.

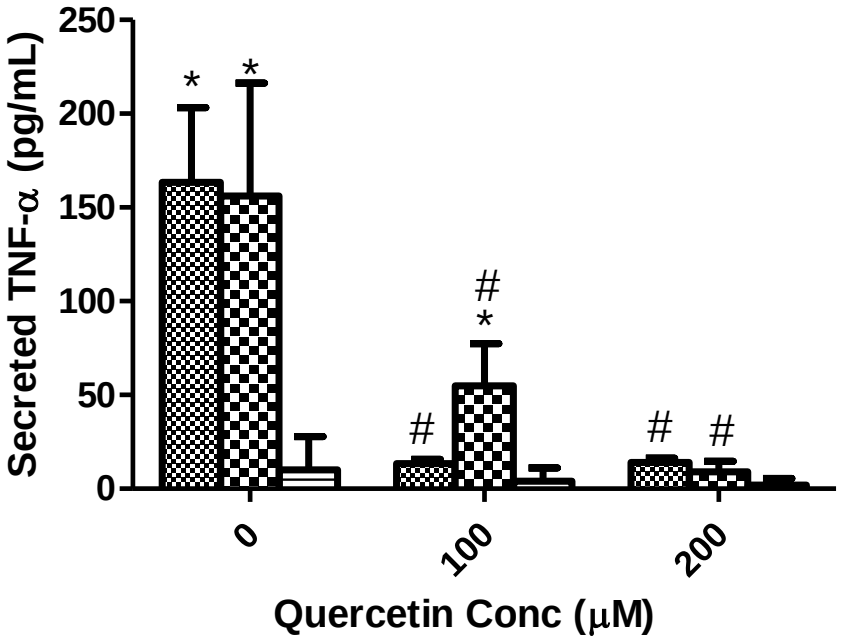

Figure 5.3: Quercetin prevention of TNF-α production in EpiDerm™ skin mimics exposed to either 10 J/cm^2 UVA, 0.9 J/cm^2 UVB (in open culture dishes, UVC removed by filtration) or no UVR (dark). TNF-α was measured by ELISA. Cell cultures were treated with quercetin in acetone, which was allowed to evaporate, immediately prior to UVR exposure leaving a thin film of quercetin. Following treatment skin mimics were returned to the incubator. Media was collected for TNF-α analysis 24 hours later and stored at -80ºC until analysis. ▩ = UVA, ▩ = UVB Treatment, ▭ = Dark Control. * = significantly different from dark control ($p<0.05$), # = significantly different from control ($p<0.05$).

5.4.3. Effect of flavonols on UVB-radiation mediated formation of T<>T

The effect of topical application of a range of flavonols on T<>T formation in reconstructed human skin models is presented in Figure 5.4. The EpiDerm™ was topically treated with flavonol quercetin, kaempferol and galangin in acetone. The acetone was allowed to evaporate, immediately prior to UVR exposure leaving a thin film of flavonol on the surface. Due to the immediate exposure to UVR, the flavonols were anticipated to act as physical block agents. The analysis was performed in duplicate on three different days, to determine the prevention of T<>T formation in flavonol treated EpiDerm™ skin mimics exposed to UV-radiation.

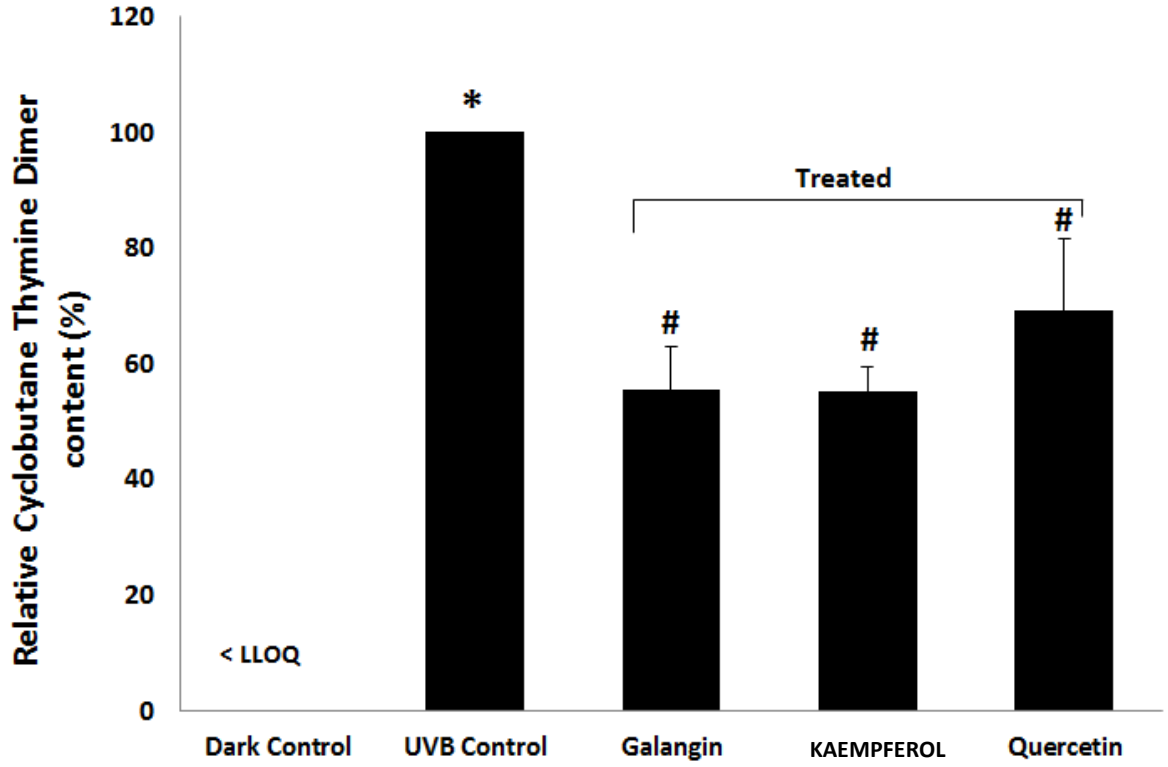

Figure 5.4: The graph represents the mean levels of relative content (%) of cyclobutane thymine dimer (±SD) in EpiDerm^{TM} skin mimics exposed to 0.05 J/cm^2 UVB and treated with quercetin, kaempferol or galangin (4nmol/cm^2). Dark control represents untreated samples exposed to UV but covered with foil, UVB control represent s UVB exposed, untreated samples. The statistically significant differences ($p<0.05$) between groups are indicated by labels containing different symbols. The results containing labels with the same symbols are not significantly different.

UVB exposed samples treated with 4nmol/cm^2 of flavonol resulted in a significant decrease in T<>T formation compared to UVB exposed control. The levels of T<>T formation in UVB exposed control and flavonol treated skin samples was significantly different from non-UVR exposed skin mimics (dark control). Although, the levels of T<>T formation in galangin, kaempferol and quercetin treated samples are not significantly different, however it shows galangin and kaempferol to be comparable but provide better protection than quercetin. The results indicate that quercetin, kaempferol and galangin applied topically act as sunblock agents

and protect the skin mimics against direct DNA damage. The same study was also performed experiment for UVA exposed EpiDerm^{TM}, however the levels of T<>T formation in both control and flavonol treated samples were below our lower limit of quantification.

5.5. Discussion

A number of studies have suggested that flavonoids such as quercetin may be effective photoprotective agents. We decided to investigate the use of EpiDerm™ as a model system to test topical photoprotectants and employed three biomarkers of UVR induced damage, MMP-1 secretion, which is a marker of ROS mediated damage and photoaging effects, TNF-α, a marker of photo-immunosuppression and T<>T which is biomarker of direct photodamage to DNA.

In an effort to establish an appropriate dose range of quercetin for these experiments, a pilot study was carried out using a HaCaT cell culture system. We initially assessed the ability of quercetin to prevent UVA and UVB induced production and/or release of MMP-1 and TNF-α in cultured keratinocyte mono-layers. Keratinocyte cultures were dosed with quercetin in the cell media for 24 hours, the media was removed followed by UVA or UVB. Pre-treatment of HaCaT cells with quercetin in media 24 hours prior to UVR exposure resulted in a significant decrease in the amount of MMP-1, however no significant decrease in TNF-α production was found (supplementary data). In contrast with EpiDerm^{TM}, we did not see inhibition of TNF- α production in HaCaT cells, the most possible reason is rapid degradation of quercetin in DMEM but still active in the skin mimics because of the use of a non-aqueous vehicle (acetone).

5.5.1. Effect of Quercetin on UVR Mediated MMP-1 Production

The EpiDerm^{TM} skin models were treated topically with quercetin immediately prior to UVA and UVB exposure. Due to the immediate exposure to UVR, quercetin could have only undergone minimal absorption by the skin and as a result would largely act as a physical screen or as a surface / intracellular antioxidant. The topical treatment of EpiDerm^{TM} with quercetin resulted in significant decreases in MMP-1 secretion.

The quercetin-mediated concentration-dependent decrease in MMP-1 secretion seen in the EpiDerm^{TM} study could result from either inhibition of MMP-1 secretion via antioxidant

activity or direct photo-absorption. MMP-1 induction by UVA and UVB radiation has been shown to be caused by the formation of ROS at the cell surface[4,20-22]. As a result, both the absorbed and surface quercetin would be able to prevent initiation of MMP-1 secretion by preventing the formation of ROS at the surface of the cell, as was seen in this study. Our previous studies on UVR induced decomposition of quercetin [50] as well as other oxidation studies [54] suggest that $^1O_2$ may interact with quercetin and this scavenging of $^1O_2$ may contribute to the quercetin-mediated reduction in MMP-1 production [23].

Quercetin can act as a direct UVR screen, absorbing UVR and dissipating energy before ROS can be generated (note: quercetin was used at concentrations below those known to generate ROS in the presence of UVR). This absorptive effect should be localized to the surface of the skin in the EpiDerm™ samples. However, the absorbance spectrum of quercetin has a λ_{max} in the UVA region (365 nm, $\varepsilon = 28{,}400\ M^{-1}cm^{-1}$) and a low extinction coefficient in the UVB region, so it seems unlikely that the photoprotective effect would be equally strong against both UVB and UVA radiation, as is seen in this study.

5.5.2. Effect of Quercetin on UVR Mediated TNF-α Production

Interestingly, we observed a dose-dependent decrease in TNF-α secretion in the EpiDerm™ study, a result that was not predicted by the HaCaT pilot study as no significant decrease in TNF-α secretion was seen in the HaCaT cells. The most possible explain this observation, is the instability of quercetin in DMEM which resulted in decreased level of protection in HaCaT cells as compared to the skin mimics.

TNF-α is known to be formed as a result of the formation of thymine dimers by a UVR-induced photo-reaction [34,35]. This is a direct photo-reaction caused by absorption of light by DNA, primarily thymine (λ_{max} = 264 nm), and does not go through a ROS intermediate. DNA damage caused by reaction with ROS results in the formation of DNA lesions distinct from thymine dimers which have not been shown to result in TNF-α production [34,35]. This causative relationship between thymine dimer formation and TNF-α production further supports the conclusion that in the case of the decreased TNF-α secretion seen in the EpiDerm™ samples, direct UVR absorption is the major protective mechanism of quercetin. A strong absorbance

band of quercetin (λ_{max} = 256 nm, ε = 28,300 $M^{-1}cm^{-1}$) is near that of thymine, while the major decomposition products previously identified for quercetin show little absorbance in the UVC region, instead having absorbance maxima near 300 nm [50,54].

The decomposition products of quercetin in DMEM which predominate in the HaCaT cells are anticipated to have a diminished ability to absorb UVR relative to quercetin. In addition, the topical treatment immediately prior to UVA and UVB exposure should provide a greater level of protection than the pre-exposure of the HaCaT cells as the cell media containing quercetin is removed from the cell cultures prior to UVR exposure. This leaves only the quercetin which has been absorbed by the cells and remaining near the cell surface available to offer photoprotection by light absorption. A decrease in the effectiveness of the photo-protection offered by quercetin would be expected in the pre-treated HaCaT cells as opposed to the topically treated EpiDerm™ cells, which is in agreement with our results.

5.5.3. Flavonols act as topical sunscreen agents by decreasing UVR mediated T<>T formation

Over the years, several studies have reported photoprotective properties of range of flavonols including myricetin, quercetin and kaempferol. In our previous study, we established that the general pattern of flavonol photostability follows the trend galangin > kaempferol > quercetin demonstrated that the number of B-ring hydroxyl groups is inversely related to flavonol stability in UVA radiation. We hypothesised that the ability of flavonols to protect from UVR induced damage would be inversely proportional to hydroxyl group substitution on the B-ring. Analytical method based on HPLC-APCI-MS/MS technology was used to determine the sunscreen abilities of flavonols, by measuring the decrease in T<>T formation in UV irradiated reconstructed human skin model.

Our results showed that quercetin applied topically to the reconstructed human skin model is effective in preventing the production of MMP-1, TNF-α and T<>T. In addition kaempferol and galangin are all effective at decreasing T<>T formation. These results, together with our previous findings on the photostability [50] and ability to inhibit UVR induced lipid

oxidation[49] indicate that kaempferol and galangin may prove to be effective components of a topically applied sunscreen.

Our data from the EpiDerm™ study suggests that the flavonols can act as sunscreen agents by direct absorption of UV-radiation. The decrease in T<>T formation indicates that quercetin, kaempferol and galangin reduce direct DNA damage caused by UVB radiation. In addition to MMP-1 and TNF-α experiments, the decrease in the levels of T<>T further supports the potential topical sunscreen protectant ability of flavonols. The results indicate that the flavonols quercetin, kaempferol and galangin act as physical sunblock by absorbing UVB-radiation. However, this method was not so sensitive to measure UVA radiation induced damage in EpiDerm™ samples.

Using the reconstructed human skin model, we have demonstrated that topically applied quercetin decreases three markers of UVR-induced skin damage in a concentration-dependent manner. These markers were selected to be indicators of UVR-induced ROS (MMP-1) and direct UVR absorption by DNA (TNF-α and T<>T). Use of HaCaT cells as a pilot study for the EpiDerm™ experiments resulted in a quercetin-mediated decrease of MMP-1, but no effect on TNF-α, which we attribute to the instability of quercetin in cell media such as DMEM. Our previous flavonol stability study indicated that myricetin was the unstable flavonol as compared to quercetin, kaempferol and galangin [56], so did not use myricetin in EpiDerm™ study. Our findings suggest that the more stable flavonols kaempferol and galangin are equally effective as quercetin, so they may be the most promising candidates. While we observed different markers of biological damage than Bowden's group, our results agree with studies on topical quercetin formulations which suggest the importance of quercetin stability in the prevention of UVR-induced skin damage[55].

Acknowledgments: This work has been supported by the Natural Sciences and Engineering Research Council and the College of Pharmacy and Nutrition Research Trust, B.M.F. is a recipient of an Rx&D award, and S.M is a recipient of a University of Saskatchewan GTA.

Abbreviations: basal cell carcinomas: BCC; cyclobutane pyrimidine dimers: CPD; dimethyl sulfoxide; DMSO; Dulbecco's Modified Eagle Medium: DMEM; Enzyme-linked immunosorbent assay: ELISA; ethylenediaminetetraacetic acid: EDTA; foetal bovine serum: FBS; High Performance Liquid Chromatography: HPLC; interleukin: IL; matrix metalloprotease 1: MMP-1; non-melanomic skin carcinomas: NMSC; phosphate buffered saline : PBS; reactive oxygen species: ROS; squamous cell carcinomas; SCC; thymine dimer: T<>T; tumor necrosis factor-α:TNF-α; ultraviolet radiation: UVR.

5.6. References

1 D. E. Godar, UV doses worldwide, Photochem. Photobiol. 81 (2005) 736-749.

2 D. Goltzman, Vitamin D action : Lessons learned from genetic mouse models, Ann. N. Y. Acad. Sci. 1192 (2010) 145-152.

3 K. M. Dixon, V. B. Sequeira, A. J. Camp, and R. S. Mason, Vitamin D-fence, Photochem. Photobiol. Sci. 9 (2010) 564-570.

4 J. Taira, K. Mimura, T. Yoneya, A. Hagi, A. Murakami, and K. Makino, Hydroxyl radical formation by UV-irradiated epidermal cells, J. Biochem (Tokyo) 111 (1992) 693-695.

5 J. Nishi, R. Ogura, M. Sugiyama, T. Hidaka, and M. Kohno, Involvement of active oxygen in lipid peroxide radical reaction of epidermal homogenate following ultraviolet light exposure, J. Invest Dermatol. 97 (1991) 115-119.

6 J. Longstreth, F. R. de Gruijl, M. L. Kripke, S. Abseck, F. Arnold, H. I. Slaper, G. Velders, Y. Takizawa, and J. C. van der Leun, Health risks, J. Photochem. Photobiol. B: Biol. 46 (1998) 20-39.

7 S. E. Ullrich, The role of epidermal cytokines in the generation of cutaneous immune reactions and ultraviolet radiation-induced immune suppression, Photochem. Photobiol. 62 (1995) 389-401.

8 R. B. Setlow, E. Grist, K. Thompson, and A. D. Woodhead, Wavelengths effective in induction of malignant melanoma, Proc. Natl. Acad. Sci. U. S A 90 (1993) 6666-6670.

9 N. Ramakrishnan and D. S. Pradhan, Occurrence of pyrimidine-rich tracts in ascites tumor DNA and the formation of UV-induced thymine dimers, Photochem. Photobiol. 29 (1979) 539-542.

10 Z. Kuluncsics, D. Perdiz, E. Brulay, B. Muel, and E. Sage, Wavelength dependence of ultraviolet-induced DNA damage distribution: involvement of direct or indirect mechanisms and possible artefacts, J. Photochem. Photobiol. B: Biol. 49 (1999) 71-80.

11 K. Scharffetter-Kochanek, M. Wlaschek, P. Brenneisen, M. Schauen, R. Blaudschun, and J. Wenk, UV-induced reactive oxygen species in photocarcinogenesis and photoaging, Biol. Chem. 378 (1997) 1247-1257.

12 M. Wlaschek, K. Bolsen, G. Herrmann, A. Schwarz, F. Wilmroth, P. C. Heinrich, G. Goerz, and K. Scharffetter-Kochanek, UVA-induced autocrine stimulation of fibroblast-derived-collagenase by IL-6: a possible mechanism in dermal photodamage?, J. Invest Dermatol. 101 (1993) 164-168.

13 M. Berneburg, H. Plettenberg, and J. Krutmann, Photoaging of human skin, Photodermatol. Photoimmunol. Photomed. 16 (2000) 239-244.

14 C. S. Sander, H. Chang, S. Salzmann, C. S. Muller, S. Ekanayake-Mudiyanselage, P. Elsner, and J. J. Thiele, Photoaging is associated with protein oxidation in human skin in vivo, J. Invest Dermatol. 118 (2002) 618-625.

15 M. H. Shin, G. E. Rhie, Y. K. Kim, C. H. Park, K. H. Cho, K. H. Kim, H. C. Eun, and J. H. Chung, H_2O_2 accumulation by catalase reduction changes MAP kinase signaling in aged human skin in vivo, J. Invest Dermatol. 125 (2005) 221-229.

16 G. J. Fisher, S. C. Datta, H. S. Talwar, Z. Q. Wang, J. Varani, S. Kang, and J. J. Voorhees, Molecular basis of sun-induced premature skin ageing and retinoid antagonism, Nature 379 (1996) 335-339.

17 S. Kang, G. J. Fisher, and J. J. Voorhees, Photoaging and topical tretinoin: therapy, pathogenesis, and prevention, Arch. Dermatol. 133 (1997) 1280-1284.

18 G. J. Fisher, Z. Q. Wang, S. C. Datta, J. Varani, S. Kang, and J. J. Voorhees, Pathophysiology of premature skin aging induced by ultraviolet light, N. Engl. J Med. 337 (1997) 1419-1428.

19 K. Scharffetter, M. Wlaschek, A. Hogg, K. Bolsen, A. Schothorst, G. Goerz, T. Krieg, and G. Plewig, UVA irradiation induces collagenase in human dermal fibroblasts in vitro and in vivo, Arch. Dermatol. Res. 283 (1991) 506-511.

20 M. Budai, A. Reynaud-Angelin, Z. Szabo, S. Toth, G. Ronto, E. Sage, and P. Grof, Effect of UVA radiation on membrane fluidity and radical decay in human fibroblasts as detected by spin labeled stearic acids, J. Photochem. Photobiol. B: Biol. 77 (2004) 27-38.

21 K. Scharffetter-Kochanek, M. Wlaschek, K. Briviba, and H. Sies, Singlet oxygen induces collagenase expression in human skin fibroblasts, FEBS Lett. 331 (1993) 304-306.

22 G. Herrmann, M. Wlaschek, K. Bolsen, K. Prenzel, G. Goerz, and K. Scharffetter-Kochanek, Photosensitization of uroporphyrin augments the ultraviolet A-induced synthesis of matrix metalloproteinases in human dermal fibroblasts, J. Invest Dermatol. 107 (1996) 398-403.

23 M. Wlaschek, K. Briviba, G. P. Stricklin, H. Sies, and K. Scharffetter-Kochanek, Singlet oxygen may mediate the ultraviolet A-induced synthesis of interstitial collagenase, J. Invest Dermatol. 104 (1995) 194-198.

24 M. Wlaschek, G. Heinen, A. Poswig, A. Schwarz, T. Krieg, and K. Scharffetter-Kochanek, UVA-induced autocrine stimulation of fibroblast-derived collagenase/MMP-1 by interrelated loops of interleukin-1 and interleukin-6, Photochem. Photobiol. 59 (1994) 550-556.

25 P. McLoone, G. M. Woods, and M. Norval, Decrease in langerhans cells and increase in lymph node dendritic cells following chronic exposure of mice to suberythemal doses of solar simulated radiation, Photochem. Photobiol. 81 (2005) 1168-1173.

26 N. Schade, C. Esser, and J. Krutmann, Ultraviolet B radiation-induced immunosuppression: molecular mechanisms and cellular alterations, Photochem. Photobiol. Sci. 4 (2005) 699-708.

27 J. M. Rivas and S. E. Ullrich, Systemic suppression of delayed-type hypersensitivity by supernatants from UV-irradiated keratinocytes. An essential role for keratinocyte-derived IL-10, J Immunol. 149 (1992) 3865-3871.

28 J. M. Rivas and S. E. Ullrich, The role of IL-4, IL-10, and TNF-alpha in the immune suppression induced by ultraviolet radiation, J Leukoc. Biol 56 (1994) 769-775.

29 N. Nishimura, C. Tohyama, M. Satoh, H. Nishimura, and V. E. Reeve, Defective immune response and severe skin damage following UVB irradiation in interleukin-6-deficient mice, Immunology 97 (1999) 77-83.

30 H. J. Niggli and P. A. Cerutti, Cyclobutane-type pyrimidine photodimer formation and excision in human skin fibroblasts after irradiation with 313-nm ultraviolet light, Biochemistry 22 (1983) 1390-1395.

31 S. Courdavault, C. Baudouin, S. Sauvaigo, S. Mouret, S. Candeias, M. Charveron, A. Favier, J. Cadet, and T. Douki, Unrepaired cyclobutane pyrimidine dimers do not prevent proliferation of UV-B-irradiated cultured human fibroblasts, Photochem. Photobiol. 79 (2004) 145-151.

32 C. Kielbassa, L. Roza, and B. Epe, Wavelength dependence of oxidative DNA damage induced by UV and visible light, Carcinogenesis 18 (1997) 811-816.

33 J. L. Ravanat, T. Douki, and J. Cadet, Direct and indirect effects of UV radiation on DNA and its components, J. Photochem. Photobiol. B: Biol. 63 (2001) 88-102.

34 D. B. Yarosh, S. Boumakis, A. B. Brown, M. T. Canning, J. W. Galvin, D. M. Both, E. Kraus, A. O'Conner, and D. A. Brown, Measurement of UVB-Induced DNA damage and its consequences in models of immunosuppression, Methods 28 (2002) 55-62.

35 J. M. Kuchel, R. S. Barnetson, and G. M. Halliday, Cyclobutane pyrimidine dimer formation is a molecular trigger for solar-simulated ultraviolet radiation-induced suppression of memory immunity in humans, Photochem. Photobiol. Sci. 4 (2005) 577-582.

36 J. G. Einspahr, S. P. Stratton, G. T. Bowden, and D. S. Alberts, Chemoprevention of human skin cancer, Crit Rev. Oncol. Hematol. 41 (2002) 269-285.

37 R. A. Schwartz, Skin Cancer - Recognition and Management, Blackwell Publishing, Oxford 2008.

38 F. Afaq, V. M. Adhami, and H. Mukhtar, Photochemoprevention of ultraviolet B signaling and photocarcinogenesis, Mutat. Res. 571 (2005) 153-173.

39 E. S. Krol, K. A. Kramer-Stickland, and D. C. Liebler, Photoprotective actions of topically applied vitamin E, Drug Metab. Rev. 32 (2000) 413-420.

40 H. Wei, R. Saladi, Y. Lu, Y. Wang, S. R. Palep, J. Moore, R. Phelps, E. Shyong, and M. G. Lebwohl, Isoflavone genistein: photoprotection and clinical implications in dermatology, J. Nutr. 133 (2003) 3811S-3819S.

41 D. F. Birt, D. Mitchell, B. Gold, P. Pour, and H. C. Pinch, Inhibition of ultraviolet light induced skin carcinogenesis in SKH-1 mice by apigenin, a plant flavonoid, Anticancer Res. 17 (1997) 85-91.

42 A. I. Scott, Interpretation of the Ultraviolet Spectra of Natural Products, The MacMillan Company, New York 1964.

43 K. E. Wilson, M. I. Wilson, and B. M. Greenberg, Identification of the flavonoid glycosides that accumulate in Brassica napus L. cv. Topas specifically in response to ultraviolet B radiation, Photochem. Photobiol. 67 (1998) 547-553.

44 K. G. Ryan, K. R. Markham, S. J. Bloor, J. M. Bradley, K. A. Mitchell, and B. R. Jordan, UVB radiation induced increase in quercetin: Kaempferol ratio in wild-type and transgenic lines of Petunia, Photochem. Photobiol. 68 (1998) 323-330.

45 A. Solovchenko and M. Schmitz-Eiberger, Significance of skin flavonoids for UV-B-protection in apple fruits, J. Exp. Bot. 54 (2003) 1977-1984.

46 H. Lim and H. P. Kim, Inhibition of mammalian collagenase, matrix metalloproteinase-1, by naturally-occurring flavonoids, Planta Med. 73 (2007) 1267-1274.

47 P. A. Steerenberg, J. Garssen, P. Dortant, d. van, V, L. Geerse, A. P. Verlaan, W. Goettsch, Y. Sontag, M. Norval, N. K. Gibbs, H. B. Bueno-de-Mesquita, and H. Van Loveren, Quercetin prevents UV-induced local immunosuppression, but does not affect UV-induced tumor growth in SKH-1 hairless mice, Photochem. Photobiol. 65 (1997) 736-744.

48 P. A. Steerenberg, J. Garssen, P. M. Dortant, d. van, V, E. Geerse, A. P. Verlaan, W. G. Goettsch, Y. Sontag, H. B. Bueno-de-Mesquita, and H. Van Loveren, The effect of oral quercetin on UVB-induced tumor growth and local immunosuppression in SKH-1, Cancer Lett. 114 (1997) 187-189.

49 B. M. Fahlman and E. S. Krol, Inhibition of UVA and UVB radiation-induced lipid oxidation by quercetin, J. Agric. Food Chem. 57 (2009) 5301-5305.

50 B. M. Fahlman and E. S. Krol, UVA and UVB radiation-induced oxidation products of quercetin, J. Photochem. Photobiol. B: Biol. 97 (2009) 123-131.

51 S. V. Jovanovic, S. Steenken, M. Tosic, B. Marjanovic, and M. G. Simic, Flavonoids As Antioxidants, J. Am. Chem. Soc. 116 (1994) 4846-4851.

52 F. T. Vicentini, T. He, Y. Shao, M. J. Fonseca, W. A. Verri, Jr., G. J. Fisher, and Y. Xu, Quercetin inhibits UV irradiation-induced inflammatory cytokine production in primary human keratinocytes by suppressing NF-kappaB pathway, J. Dermatol. Sci. (2011) doi:10.1016/j.jdermsci.2011.01.002.

53 E. R. Olson, T. Melton, Z. Dong, and G. T. Bowden, Stabilization of quercetin paradoxically reduces its proapoptotic effect on UVB-irradiated human keratinocytes, Cancer Prev. Res. (Phila Pa) 1 (2008) 362-368.

54 A. Zhou and O. A. Sadik, Comparative analysis of quercetin oxidation by electrochemical, enzymatic, autoxidation, and free radical generation techniques: a mechanistic study, J. Agric. Food Chem. 56 (2008) 12081-12091.

55 R. Casagrande, S. R. Georgetti, W. A. Verri, Jr., M. F. Borin, R. F. Lopez, and M. J. Fonseca, In vitro evaluation of quercetin cutaneous absorption from topical formulations and its functional stability by antioxidant activity, Int. J. Pharm. 328 (2007) 183-190.

56 S. Maini, H.L. Hodgson, E.S. Krol, The UVA and Aqueous Stability of Flavonoids Is Dependent on B-Ring Substitution, J Agric Food Chem; dx.doi.org/10.1021/jf3016128 (2012).

5.7. Supplementary data

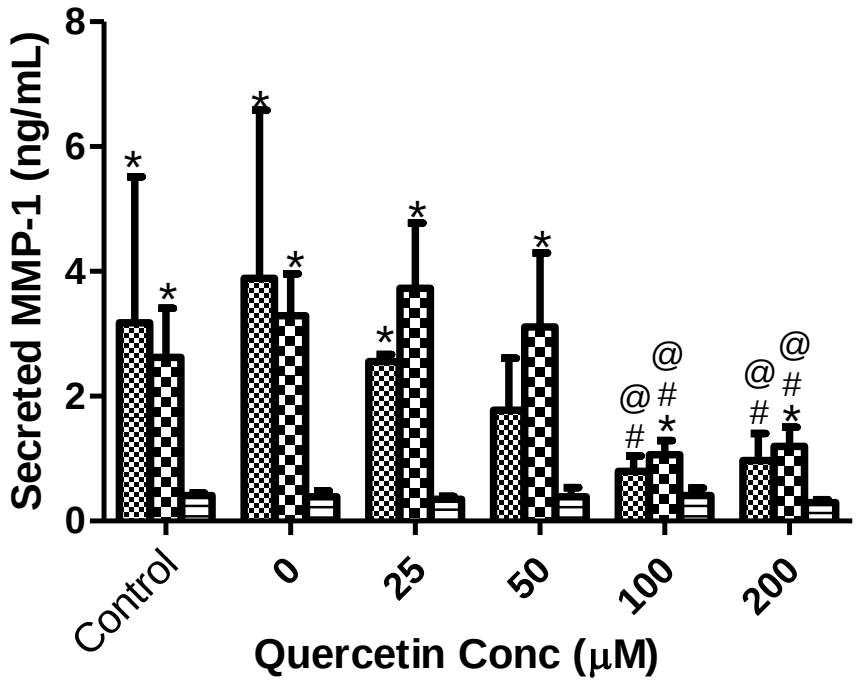

Figure 5.5: Quercetin prevention of MMP-1 production by HaCaT cell cultures exposed to either 100kJ/m^2 UVA, 9000J/m^2 UVB (in open culture dishes, UVC removed by filtration) or no UVR (dark) by ELISA. Cell cultures were treated with quercetin in DMSO (<2% by volume) added to media 24 hours prior to exposure. For UVR exposure, media was replaced with phosphate buffered saline and then following treatment saline was replaced with DMEM and cells were returned to the incubator. Media was collected for pro-MMP-1 analysis 24 hours later and stored at -80ºC until analysis. = UVA, = UVB Treatment, = Dark Control. * = significantly different from dark control ($p<0.05$), # = significantly different from control ($p<0.05$), @ = significantly different from 0μM (vehicle control) ($p<0.05$).

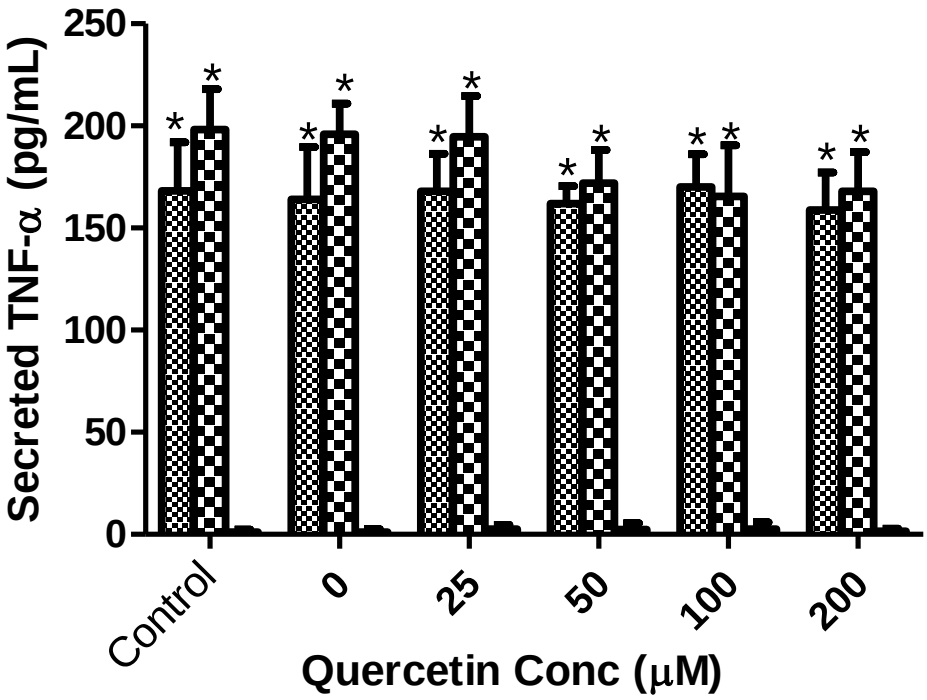

Figure 5.6: Quercetin prevention of TNF-α production by HaCaT cell cultures exposed to either 100kJ/m^2 UVA, 9000J/m^2 UVB (in open culture dishes, UVC removed by filtration) or no UVR (dark) by ELISA. Cell cultures were treated with quercetin in DMSO (<2% by volume) added to media 24 hours prior to exposure. For UVR exposure, media was replaced with phosphate buffered saline and then following treatment saline was replaced with DMEM and cells were returned to the incubator. Media was collected for TNF-α analysis 24 hours later and stored at -80ºC until analysis. = UVA, = UVB Treatment, = Dark Control. * = significantly different from dark control ($p<0.05$).

6. Objective 3 & 4

To determine the effect of B-ring substitution on the UV and aqueous stability of flavonols (galangin, kaempferol, quercetin and myricetin)

To determine the UV and aqueous decomposition products of flavonols (galangin, kaempferol, quercetin and myricetin)

The UVA and aqueous stability of flavonoids is dependent on B-ring substitution.

Authors: Sabia Maini, Heather L. Hodgson and Ed S. Krol*

Published in Journal of Agricultural and Food Chemistry

Accepted: June 20, 2012

dx.doi.org/10.1021/jf3016128 | J. Agric. Food Chem. 2012, 60, 6966−6976

NOTE:

In this paper the role of Sabia Maini includes- Stability of flavonols to UVA, DMEM and DPBS using HPLC-PDA, identification of breakdown products of flavonols using HPLC-ESI-MS/MS. In this paper the role of Heather Hodgson includes- Stability of flavonols to UVA using HPLC-PDA.

dx.doi.org/10.1021/jf3016128

7. Objective 5

To determine the UV-induced decomposition of flavonol 3-hydroxyflavone in polar and non-polar solvents

7.1. Introduction

Flavonol quercetin has shown the potential as topical sunscreen agent [1]; however the ability to act as sunscreen is directly dependent on the stability to UV radiation [2]. Our study on relationship between flavonol stability and increasing B-ring substitution, suggests that the future investigation of potential photoprotective properties of flavonols are needed to develop a trend of stability. Understanding the mechanism of UV-radiation induced decomposition of 3-OH-F may provide an insight into the photoprotective properties of flavonols without A-ring substitution.

The stability of 3-OH-F is likely to be dependent on its anti-oxidant ability. The ability to donate electrons is an important mechanism in deprotonation and higher the ability deprotonate would enhance the antioxidant ability of flavonols [4]. The graph (figure 7.1) shows the correlation between the antioxidant ability of flavones and the number of hydroxyl group substitutions. The study indicates that the antioxidant ability of 3-OH-F is less than quercetin.

3-OH-F exhibits properties like antioxidant by free radical scavenging and a DNA-protectant against induced oxidative stress [3]. 3-OH-F when exposed to UV radiation decomposes into different products in polar and non-polar solvents [3]. In order to investigate the UV photodecomposition of 3-OH-F, we exposed 3-OH-F to UV-radiation in methanol and in cyclohexane.

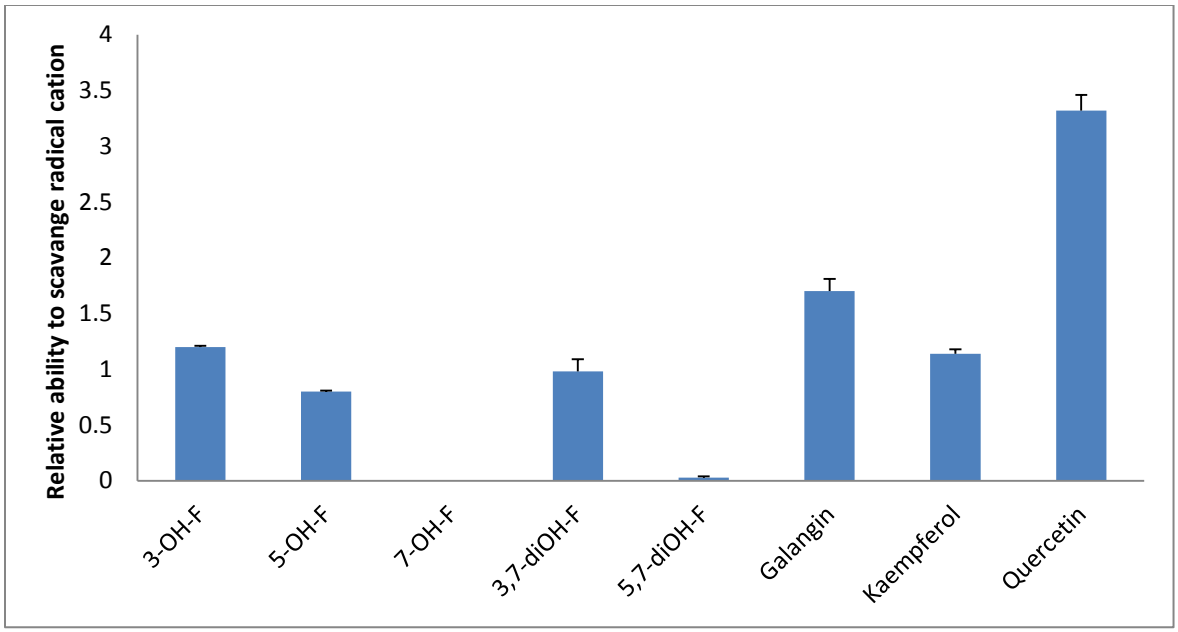

Figure 7.1: The graph represents the relationship between the hydroxyl group substitution on flavones and their relative ability to scavenge radical cation (adapted from reference [4]).

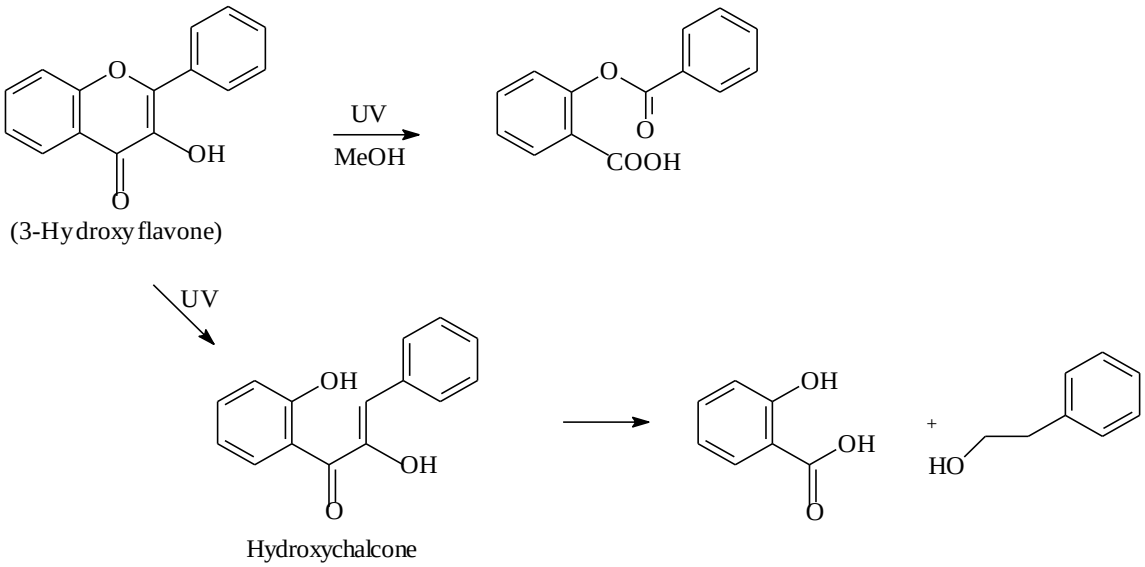

Figure 7.2: The proposed pathway of photodegradation of 3-OH-F in methanol)

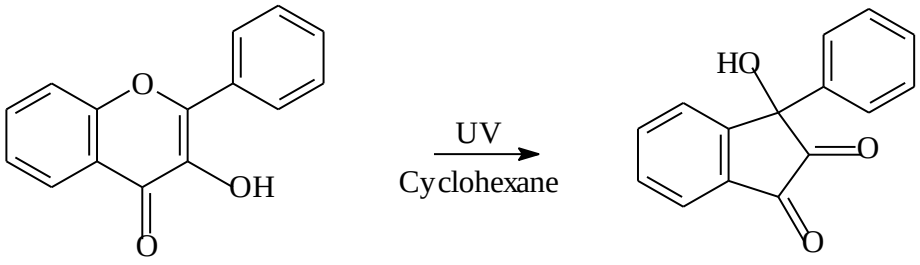

(3-Hydroxyflavone)

Figure 7.3: The proposed pathway of photodegradation of 3-OH-F in cyclohexane

7.2. Materials and methods

7.2.1. General

3-Hydroxyflavone was purchased from Sigma (St. Louis, MO). HPLC grade methanol was purchased from Fisher Scientific Canada (Ottawa, ON). Water was purified using a Millipore Super Q water system with one carbon cartridge followed by two ion exchange cartridges (Bedford, MA). UVA irradiations were carried using two F20T12/BL/HO UVA lamps (National Biological Corp., Beachwood, OH) filtered to remove UVC with an intensity of 740 $\mu W \bullet cm^{-2}$ at 365 nm as measured with a UVP UVX-36 sensor.

7.2.2. HPLC-UV-PDA

High Performance Liquid Chromatography – Ultraviolet Photodiode Array analysis was performed on an Alliance system using a Waters 2996 photodiode array detector. Aliquots of 100 µL were injected onto a 250 x 4.6 mm Allsphere ODS-2 column, 5 µ particle size (Alltech, Calgary AB). Data was processed using Empower software (Waters, Milford MA). Elution was carried out in gradient mode using two components: A = 0.1% formic acid in water, B = 0.1% formic acid in methanol. HPLC analysis was performed using the gradient follow: 0 to 10 min, linear gradient from 90% A to 40% A; 10 to 25 min, isocratic 40% A; 25 to 28 min, linear gradient from 40% A to 90% A; 28 to 30 min, isocratic 90% A.

7.2.3. UV-exposure

<u>For 3-OH-F in methanol:</u> 50ml of 100uM solution of 3-OH-F in methanol was exposed to UV radiation for 6hr. The samples collected after regular interval of time were analyzed via HPLC and NMR.

<u>For 3-OH-F in cyclohexane:</u> 50ml of 100uM solution of 3-OH-F in cyclohexane was exposed to UV radiation for 4hr. The samples collected were kept on vacuum evaporator, in order to evaporate cyclohexane. Dissolved the solute in methanol and analyzed via HPLC and NMR.

7.2.4. Semi preparative HPLC

Photoproducts of 3-OH-F in methanol and in cyclohexane were collected via semi preparative HPLC. The separation and isolation of photoproducts of 3-OH-F in methanol and in cyclohexane was performed by using semi preparative LC with Allsphere ODS-2 5µ column (10mm by 300mm). The solvent system consisted of gradient flow of water and methanol with 0.1% formic acid at a flow rate of 3ml/min. Aliquots of 150µL were injected onto column and photoproducts were collected using a fraction collector. The column was maintained at room temperature (22ºC) and washed with (50:50) water: methanol after every use. The solvent from fraction collected parts was evaporated using freeze drier, in order to collect the product for analysis via LC-MS and NMR.

7.3. Results and Discussion

Our study shows that the 3-OH-F is less photostable as compared to quercetin; whether this is also the case for stability in DMEM, is yet unknown. From our stability study, we determined that flavonols slowly decompose in the presence of UV-radiation. Based on the photostability study of flavonols, we propose that 3-OH-F can decompose to form three major photoproducts in methanol and indanedione in cyclohexane **(figure 7.2 and 7.3).**

When 3-OH-F in methanol when exposed to UV-radiation, it produced two identifiable peaks by HPLC (Figure 7.4a, 7.4b) one at Rt = 12.3min and the other at 16.5min. The peak at 12.3min is broad and may be a mixture of more than one product. For UV exposure of 1hr, 3-OH-F readily decomposes into a peak with Rt = 12.3min, however after 6hr of UV exposure the Rt = 16.5min peak was the major product with maximum absorbance of 256nm. Based on this result, it was anticipated that 3-OH-F readily decomposes when exposed to UV radiation in methanol, resulting in a transient intermediate or intermediates, that converts into a stable photoproduct in 6hr as analyzed via HPLC. A time-course (Figure 7.4c) for 3-OH-F in methanol exposed to UV radiation for 7hr was plotted showing the loss of 3-OH-F in 2h and transient nature of 12min peak.

This was not the case with 3-OH-F in cyclohexane when exposed to UV radiation for 4hr. The HPLC result (Figure 7.5a) was found to form a single major peak in 3hr with Rt = 15.4min with maximum absorbance of 250.1nm. The graph (Figure 7.5b) was plotted for 3-OH-F in cyclohexane exposed to UV radiation for 4hr.

3-OH-F readily decomposes when exposed to UV-radiation in methanol, resulting in a transient intermediate or intermediates that convert into a stable photoproduct in 6hr. Conversely, 3-OH-F exposed to UVR in cyclohexane is partially converted into a unique product in 3hr with a distinct UV profile from that observed in the methanol exposure.

Attempts to isolate and purify the two photoproducts via semi preparative HPLC resulted in only one product which was identified by NMR. We attempted to isolate the photoproducts of 3-OH-F in methanol and in cyclohexane via semi preparative HPLC. Interestingly it was found that

upon re-injection of the two photoproducts they now had identical retention times (Rt = 17.1min) and maximum absorbance (248.9 nm). H^1 NMR of the two products suggestd they were the same compound or compounds although we unable to determine the structure. We determined that 3-OH-F exposed to UV-radiation decomposes into different products in polar and non-polar solvents. In addition, we determined that the 3-OH-F cyclohexane photoproduct is unstable under acidic conditions and decomposes to yield the 3-OH-F methanol photoproduct.

(A)

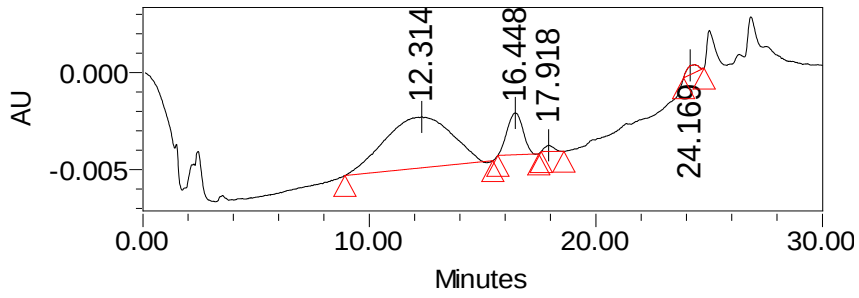

(B)

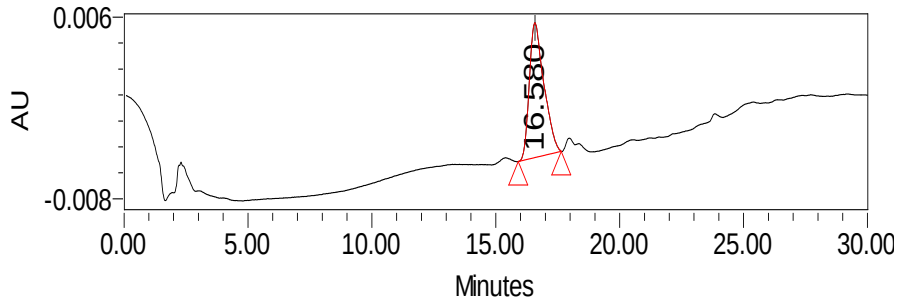

(C)

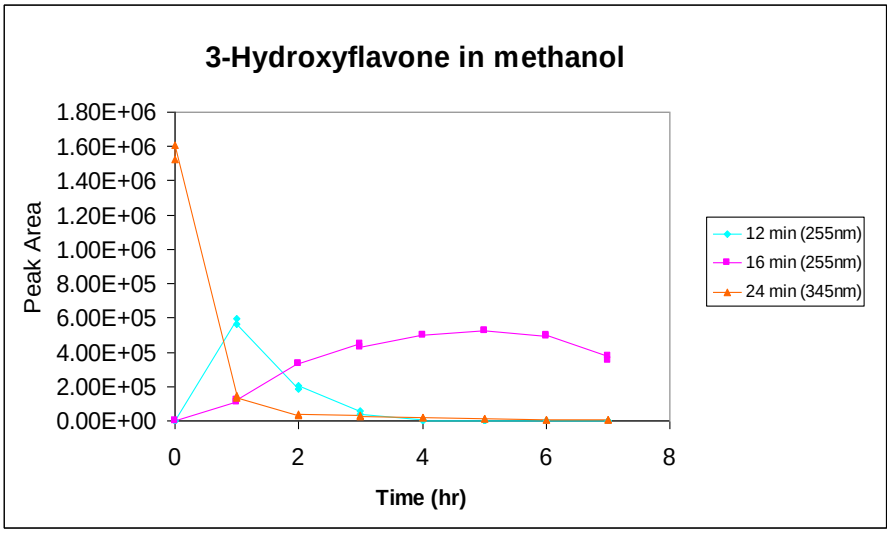

Figure 7.4: (A) HPLC results of 100uM 3-OH-F in methanol after 1hr exposure to UV radiation at 255nm. (B) HPLC results of 100uM 3-OH-F in methanol after 6hr exposure to UV radiation at 255nm. (C) Plotted the graph for HPLC results of 3-OH-F in methanol exposed to UV radiation for 7hr

(A)

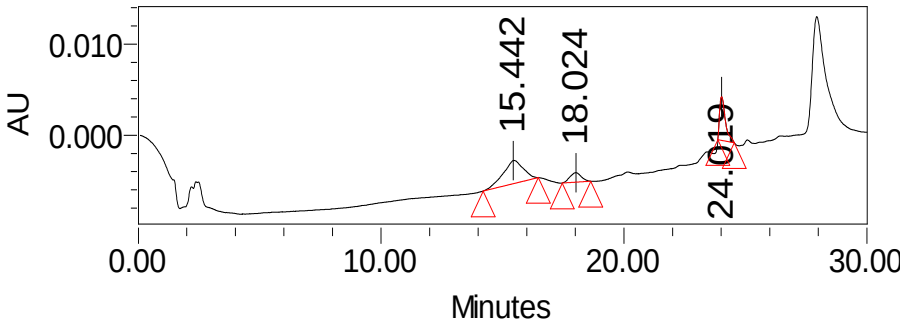

(B)

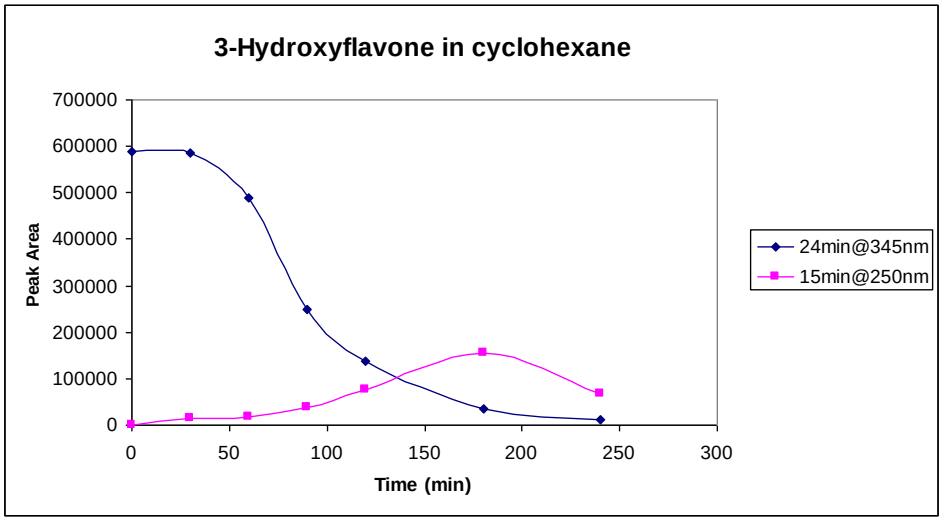

Figure 7.5: (A) HPLC results of 100uM 3-OH-F in cyclohexane after 3hr of exposure to UV radiation. Peak at Rt=15.4 min identified as consistent. (B) The graphical representation of HPLC results of 100uM 3-OH-F in cyclohexane after 4hr of exposure to UV radiation

3-OH-F does not appear to be a good model for flavonol decomposition study. 3-OH-F stability goes against the trend for decreasing OH group substitution on the B-ring is related to increased stability of flavonol. 3-OH-F does not appear to result in the same products as observed for A-ring substituted flavonols.

7.4. References

[1] E.R. Olson, T. Melton, S.E. Dickinson, Z. Dong, D.S. Alberts, G.T. Bowden, Quercetin potentiates UVB-induced c-Fos expression: Implications for its use as a chemopreventive agent, Cancer Prev. Res. 3 (2010) 876-884.

[2] Fahlman BM, Krol ES (2009) UVA and UVB radiation-induced oxidation products of quercetin. J. Photochem. Photobiol. B: Biol. 97:123

[3] Tommasini S, Calabrò ML, Donato P et al (2004) Comparative photodegradation studies on 3-hydroxyflavone: Influence of different media, pH and light sources. J Pharm Biomed Anal 35:389

[4] K. Lemańska, H. Szymusiak, B. Tyrakowska, R. Zieliński, A.E.M.F. Soffers, I.M.C.M. Rietjens, The influence of pH on antioxidant properties and the mechanism of antioxidant action of hydroxyflavones, Free Radic. Biol. Med. 31 (2001) 869-881.

8. Summary of findings

The overall goal of this research project was to investigate the photoprotective properties of plant flavonols as topically-applied sunscreen agents. In order to achieve our goal, specific objectives were set. First, to quantify direct DNA damage caused by exposure to UVR, we developed a specific and selective analytical method to quantify T<>T. Second, the ability of flavonols to act as topical sunscreen agents was determined by the decrease in T<>T formation in flavonol treated EpiDerm™ skin mimics. Third, the stability of flavonols to UVA and aqueous media was determined by using HPLC-UV analysis and was found to be dependent on B-ring substitution. Fourth, the decomposition products of flavonols to UV radiation were determined by qualitative analysis using HPLC-MS/MS technology. Fifth, stability of 3-OH-F a prototype flavonol to UVA was found to give different products in polar and non-polar solvents. The summary of the finding from each objective is listed below:

8.1. Develop and validate an analytical method for detection and quantification of cyclobutane thymine dimer

Liquid chromatography combined with mass spectrometry appears to be an efficient technique for quantitative analysis of UV-induced DNA adducts. APCI proves to be an effective ionization technique for coupling liquid chromatograph to a mass spectrometer. As per FDA guidelines, we have developed and validated an efficient analytical technique for quantification of DNA lesion involving two thymine residues. The major advantages of our method over previous techniques are improved selectivity and relatively simple and swift sample preparation. The use of HaCat cells as a pilot study for the EpiDerm™ experiments resulted in a galangin dependent decrease of T<>T. The application of this assay allows accurately to measure the amount of T<>T produced *in vitro* after exposure to UV radiation.

8.2. To determine the topical sunscreen properties of flavonols in UVA/B exposure reconstructed human skin models (EpiDerm™)

The reconstructed human skin models were exposed to UVR immediately after topical treatment with range of flavonol. Here the flavonols are anticipated to act as physical sun block agents.

The results indicate that the topical application of naturally-occurring flavonols significantly decreased the formation of T<>T (a biomarker of UVR-induced skin damage). Our results are in agreement with flavonols providing a photoprotective effect through absorption of UVB. One limitation to our method is that it is not sensitive enough to quantify UVA-radiation induced skin damage, however in spite of this shortcoming we were still able to use this assay to accurately measure the amount of T<>T produced *in vitro* after exposure to UVB radiation.

8.3. To determine the effect of B-ring substitution on the UVA and aqueous stability of flavonols (galangin, kaempferol, quercetin and myricetin)

To determine the ability of flavonols to act as topical skin photoprotectants, their stability to UVA and aqueous media was an important consideration. We used an HPLC-UV method to measure the loss of starting material as % remaining flavonol in DMEM and after UVA exposure over time. Our study suggests that stability of flavonols is dependent on B-ring substitution. The general pattern of flavonol stability (galangin > kaempferol > quercetin > myricetin) demonstrated that the number of B-ring hydroxyl groups is inversely related to flavonol UVA and aqueous stability including DMEM except DPBS. Our stability study suggests that kaempferol and galangin, have greater stability to UVA and DMEM, and may prove to be attractive alternatives to study flavonols as photoprotectants.

8.4. To determine the UVA and DMEM induced decomposition products of flavonols (galangin, kaempferol, quercetin and myricetin)

In order to confirm the decomposition pathway of flavonols, we identified their decomposition products of using HPLC-ESI-MS/MS. We used HPLC-ESI-MS/MS with enhanced resolution and product ion mode to identity the breakdown products of flavonols in UVA and DMEM. Our study suggests that the major decomposition products of flavonols were consistent with the presence of a C-ring carbocation intermediate and the B-ring hydroxyl groups contribute by stabilization of the C-ring carbocation and *para*-quinone methide intermediates.

8.5. To determine the UV-induced decomposition of the flavonol 3-hydroxyflavone in polar and non-polar solvents

3-OH-F in methanol when exposed to UV-radiation produced two decomposition products by HPLC. On the other hand, 3-OH-F in cyclohexane produced a single major product. We anticipated that, 3-OH-F in methanol readily decomposes when exposed to UV-radiation, resulting in a transient intermediate that converts into a stable photoproduct. Our study indicates that 3-OH-F exposed to UV-radiation decomposes into different products in polar and non-polar solvents. Efforts were done to separate the decomposition products by using semi preparative HPLC. Interestingly it was found that 3-OH-F cyclohexane photoproduct decomposes to the 3-OH-F methanol photoproduct.

9. Conclusion

The primary goal of this research project was to determine the topical sunscreen ability of range of flavonols as possible sun protectant agents. In order to determine the sun protection ability of flavonols, our secondary goal was development and validation of an analytical method to quantify the DNA damage. The topical application of flavonol protect the skin mimics from UVB-radiation induced T<>T formation. Due to the maximal UV absorbance bands of flavonols at 256nm and 368nm of sunlight, flavonols are likely to provide protection from UVA radiation induced T<>T formation, though further studies are needed. Majorly our study has two conclusions, first that the galangin, kaempferol and quercetin can provide photoprotection against UVR induced DNA damage; second that photostability is an important consideration and our studies demonstrate that kaempferol and galangin, not quercetin as initially thought, may be the better candidates. Galangin appears to be the best candidate for future UV photoprotection studies.

10. Future Research directions

The future research direction of this research project could be in the following areas:

i. **Formulation :**

Our study suggests that both photoprotective and photostability characteristics of flavonols make them good candidates for topical sunscreen use. Galangin has shown to be an effective photoprotectant, but the method of application of flavonol involved the use of acetone as a vehicle. In order to use flavonols are sunscreen agents, suitable formulation has to be developed, by using an inert cream for topical application of flavonols. And it might be also interesting to compare photoprotective and photostability properties of flavonols with the sunscreen product currently on the market.

ii. **Quantification of 8-oxoGua:**

DNA base guanine is most prone to oxidative damage from both UVA and UVB radiation. HPLC-MS/MS technology can be used to develop an analytical method to measure 8-oxoGua, an oxidative DNA damage. It can prove to be an effective analytical method to measure the oxidative DNA damage.

iii. **3-OH-F stability study:**

To determine the decomposition products of 3-OH-F, and to investigate the mechanism of decomposition of 3-OH-F in polar and non-polar solvents. And to investigate the effect of 5-OH and 7-OH group substitution on the photostability of flavonols compared to 3-OH-F.